NASA Contractor Report 179525
AiResearch 86-60365

Improved Silicon Nitride for Advanced Heat Engines

Hun C. Yeh
AiResearch Casting Company
Torrance, California

and

Ho T. Fang
Garrett Turbine Engine Company
Phoenix, Arizona

February 1987

Prepared for the
Lewis Research Center
Under Contract NAS3-24385

Date for general release February 1989

National Aeronautics and
Space Administration

FOREWORD

Fabrication and processing of the ceramic specimens was conducted by the AiResearch Casting Company (ACC) at Torrance, California. Under subcontract, the Garrett Turbine Engine Company (GTEC), Phoenix, Arizona, was responsible for statistical design of experiments, modulus of rupture (MOR) determination, and fractography and statistical analysis.

The co-principal investigators were Dr. Hun C. Yeh of ACC and Mr. Ho T. Fang of GTEC. Mr. Edwin Hodge of ACC served as overall program manager and Dr. Jay R. Smyth served as program manager at GTEC. Mr. Marc R. Freedman of NASA Lewis Research Center is project manager. The significant contributions of Mike E. Rorabough and Leonard Donahue of ACC, and An Ling Lu and Jim Wimmer of GTEC, are gratefully acknowledged.

TABLE OF CONTENTS

	Page
EXECUTIVE SUMMARY	1
Task I	1
Task II	1
Task VII	2
INTRODUCTION	3
TECHNICAL PROGRESS	6
Task II - MOR Bar Matrix Study	6
Powder characterization	6
Matrix II-1 (Starck H-1 Si_3N_4)	13
Matrix II-2 (Denka 9FW Si_3N_4)	20
Task II modifications	45
Subtask (A) high Weibull/reproducibility	45
Subtask (B) high-temperature materials	48
Subtask (C) net shape component fabrication evaluation	50
Task VII - Advanced Materials and Processing	60
Matrix 6 - raw materials, molding, and thermal processing	61
Matrix 8 - sintering	76
Matrix 9 - iron contamination from processing	86
Matrix 10 - binder composition	90
Matrix 11 - sinter/HIP, additive, binder, and milling time	90
Additional investigations on binders	94
CONCLUSION	103
APPENDIX A: Task II New Goal Plan	104
APPENDIX B: Glossary	110

EXECUTIVE SUMMARY

The objective of the program is to establish the technology base required to fabricate silicon nitride components having the strength, reliability, and reproducibility necessary for heat engine applications.

The program consists of seven major tasks. The Task I technical effort on baseline characterization was completed in the first nine months of the program. Current efforts are in Tasks II and VII. The following is a summary of the technical efforts conducted in the first two years (September 1984 through September 1986).

Task I

The major objective of Task I was the complete characterization of ACC baseline silicon nitride (92% GTE SN 502 Si_3N_4 + 6% Y_2O_3 + 2% Al_2O_3) test bars fabricated by injection molding. The characterization methods included chemical analysis, oxygen content determination, electrophoresis, particle size distribution (PSD) analysis, surface area determination, and analyses of degree of agglomeration and maximum particle size of elutriated powder. These analyses were conducted on as-received powder as well as on sized powder. MOR test bars were injection molded and processed through sintering at 0.68 MPa (100 psi) of nitrogen. The as-sintered test bars were evaluated by X-ray phase analysis, room and elevated temperature MOR strength, Weibull slope, stress rupture, strength after oxidation, fracture origins, microstructure, and density from quantities of samples sufficiently large to generate statistically valid results.

A total of 452 test bars were injection molded to provide specimens for the various characterization tests. Of these, 216 were fully processed to provide specimens for the post-processing tests.

A total of 108 test bars were strength tested at room temperature, 1066°, 1232°, and 1399°C (1950°, 2250°, and 2550°F). The mean strength at room temperature for 66 bars was 540 MPa (79.3 ksi), with a Weibull slope of 7.9. These are baseline properties that are to be improved by 20 percent in strength and 100 percent in Weibull slope. The mean strengths at 1066°, 1232°, and 1399°F were 420, 320, and 140 MPa (61.1, 47.1, and 21.7 ksi), respectively.

Static oxidation test data showed that test bars exposed for 200 hours to air in the temperature range of 388° to 1296°C (730° to 2365°F) exhibited a slight degradation in room temperature strength.

Task II

Task II, the MOR bar matrix study, which was initiated at the completion of Task I, consists of a series of statistically designed experiments to establish the optimum materials and processing parameters

so that the initial program goal (20 percent improvement in MOR and 100 percent in Weibull slope over the baseline) of improving test bar properties will be achieved. Two statistically designed half-replicate of 2^5 factorial experiments (Matrixes II-1 and II-2) were designed based primarily on information obtained from Tasks I and VII. Starck H-1 Si_3N_4 powder was used for Matrix II-1, and Denka 9FW Si_3N_4 powder was used for Matrix II-2; except for the Si_3N_4 powder used, the matrixes were identical. Five processing variables--sintering, powder bed, mixing, binder, and sintering aids--were evaluated at two levels.

Sufficient material was processed through sintering to make the 1500 test bars required to complete Matrix II-1. The test bars did not achieve satisfactory density or MOR; consequently, only a limited amount of characterization was conducted.

Satisfactory test bar densities were obtained for Matrix II-2, and detailed characterization and statistical analysis of the results were conducted. This matrix identified a processing treatment condition "ab," which produced test bars with an average room temperature MOR of 97 ksi and a Weibull slope of 13.2. Because these results came close to satisfying the program goals, the program was redirected to include the following more aggressive goals: (1) reproducibility experiment to confirm the achievement of strength and Weibull slope that met the program goals, (2) a new effort aimed at increasing the high temperature strength, and (3) accelerating the transition of test bar studies to net-shape components. Work is in progress in all three areas.

Task VII

Task VII, advanced materials and processing, is being conducted continuously throughout the program, both to perform screening experiments on advanced materials and processing and to identify critical variables affecting strength and reliability. During this reporting period, Matrixes 6 through 11 were completed. These matrix experiments investigated the effect of various processing parameters, including milling, mixing, injection molding, dewaxing, and sintering. In Matrix 6, GTE SN 502 powder produced specimens with the highest room temperature MOR using the processing conditions in this matrix. Matrix 11 was a screening experiment to evaluate the effects of the sinter/HIP cycle including post-sinter cooling.

INTRODUCTION

This document, submitted by AiResearch Casting Company (ACC), a division of The Garrett Corporation, is the second annual technical report for the Improved Silicon Nitride For Advanced Heat Engines Program. The program is being conducted for the National Aeronautics and Space Administration (NASA) under contract No. NAS3-24385. Garrett Turbine Engine Company (GTEC) is the major subcontractor on this program, responsible for statistical design of experiments, modulus of rupture (MOR) determination, fractography, and statistical analysis. This report covers the period October 1, 1985 through September 30, 1986.

The objective of this program is to develop the technology base required to fabricate silicon nitride components having the strength, reliability, and reproducibility necessary for heat engine applications.

The master program schedule is presented in figure 1. The program consists of two phases of process development to be completed in 60 months. Phase I includes fabrication, evaluation, and optimization of test bars. Phase I is divided into four tasks. The objectives of these tasks are:

Task I - Characterize the baseline sintered silicon nitride.

Task II - The original objective was to use statistically designed matrix experiments to achieve material and process improvements as demonstrated by a 20-percent increase in strength and a 100-percent increase in Weibull slope. Because of the near-program-goal results achieved in the first iteration in the early part of the second year, the program was redirected to focus on more aggressive goals, including improved high temperature strength and net shape fabrication evaluation.

Task III - Characterize the improved material and process.

Task VII - Perform screening experiments on advanced materials and processing for input to Task II statistically designed experiments.

Phase II includes the fabrication and evaluation of a large complex shape of potential use in a gas turbine engine application. Phase II is divided into four tasks, the objectives of which are:

Task IV - Evaluate the improved process (from Task III) in the fabrication of a large shape and identify critical process variables requiring further improvement due to the scale-up in size.

ORIGINAL PAGE IS
OF POOR QUALITY

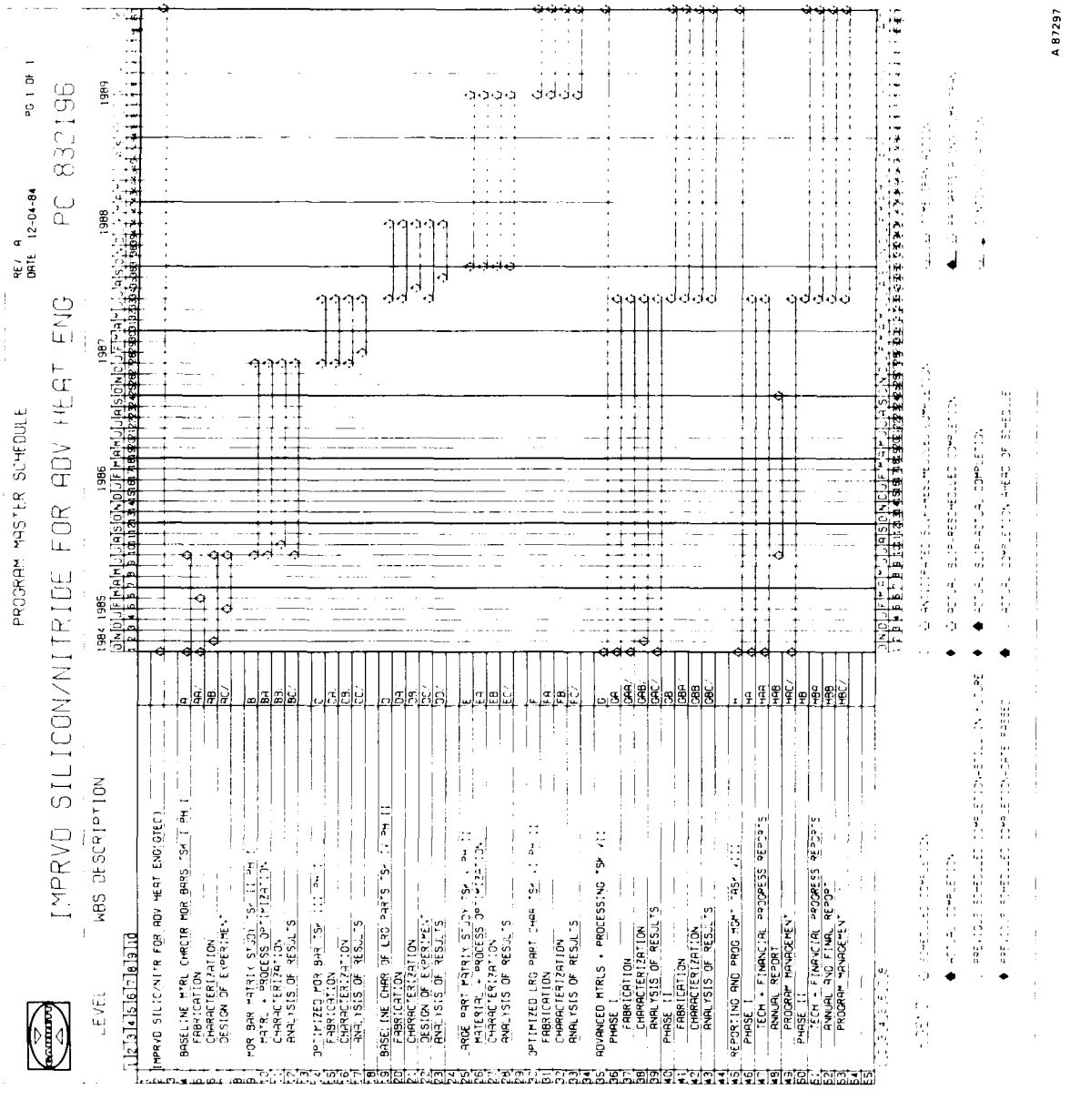

Figure 1.--Master Program Schedule.

Task V - Use statistically designed matrix experiments to achieve material and process improvements.

Task VI - Characterize the improved material and process.

Task VII - Continue screening experiments, especially those related to the requirements of the large size.

More than 40 variables have been identified for study. Major efforts in the study consist of statistically designed experiments, processing of test bars, characterization of MOR, fractography and density, and statistical analysis of results. Critical variables are identified in these experiments. Interactions between variables are identified and studied using statistically designed experiments.

During the first year of this five-year program, Task I of Phase I was completed as scheduled. It was reported in its entirety in the first annual report. Tasks II and VII were both initiated in the first year. Progress made in the first year for both tasks was also included in the first annual report.

During the second year (this reporting period), major efforts were devoted to Task II and the continuation of Task VII. The first iteration of Task II was completed on schedule. Two statistically designed half-replicated, fractional factorial (2^5) experiments were conducted. The program was subsequently redirected to aim at more aggressive goals.

TECHNICAL PROGRESS

Task II - MOR Bar Matrix Study

Two statistically designed fractional factorial experiments were conducted to evaluate a series of materials and processing conditions. A minimum of 1600 bars was needed to complete the requirements of these two matrixes. Two raw materials (Starck H-1 Si_3N_4 and Denka 9FW Si_3N_4) were evaluated, one material in each matrix. The design for both matrixes (Matrixes II-1 and II-2) was the same with five variables evaluated in each matrix. The experimental design was discussed in the last annual report and is repeated here in figure 2, showing the five variables and the sixteen treatments (shaded areas) selected for each matrix. Figure 3 shows the process flow chart for both Matrix II-1 and II-2.

Matrixes II-1 and II-2 were originally planned as the first of three iterations designed to achieve the program goals. However, at the end of the first iteration, the Task II program goal was considered by NASA to be nearly accomplished. The best group of test specimens from Matrix II-2 achieved an average room temperature flexure strength of 97 ksi with a Weibull slope of 13.2. (Program goals: MOR $\geq$95.2 ksi, Weibull slope $\geq$15.8.) The specimens were made from Denka 9FW powder with 6% Y_2O_3 + 2% Al_2O_3 additives and processed with the "ab" treatment condition, which incorporated a 4-hr sintering period in a powder bed. The Matrix II-1 specimens made from the Starck H-1 powder did not achieve satisfactory density and MOR under the same processing conditions.

Due to the near-program-goal results obtained in Matrix II-2, a more aggressive go-forward plan was submitted by ACC/GTEC and approved by NASA (Appendix A). This included: (1) a reproducibility experiment to confirm the achievement of strength and high Weibull slope which met the program goals, (2) a new effort aimed at increasing the high temperature strength, and (3) accelerating the transition of test specimen studies to net-shape components. An existing T-25 turbocharger rotor tool was used to initiate the net-shape effort. These three efforts are designated as subtasks (A), (B), and (C), respectively. This section will discuss the results of Matrixes II-1 and II-2 and the progress made in subtasks (A), (B), and (C).

Powder characterization.--Powders from Matrixes II-1 (Starck H-1) and II-2 (Denka 9FW) have been fully characterized according to the plan that included chemical, oxygen, particle size distribution (PSD), and surface area analyses. Particle shape was characterized by SEM also. For convenience of comparison, the powder characterization results for both matrixes are presented in parallel in the following text.

Table 1 gives the results of the chemical analysis by emission spectroscopy on as-received Si_3N_4, as well as the milled powders. Both as-received Si_3N_4 powders contain higher levels of calcium, iron, and

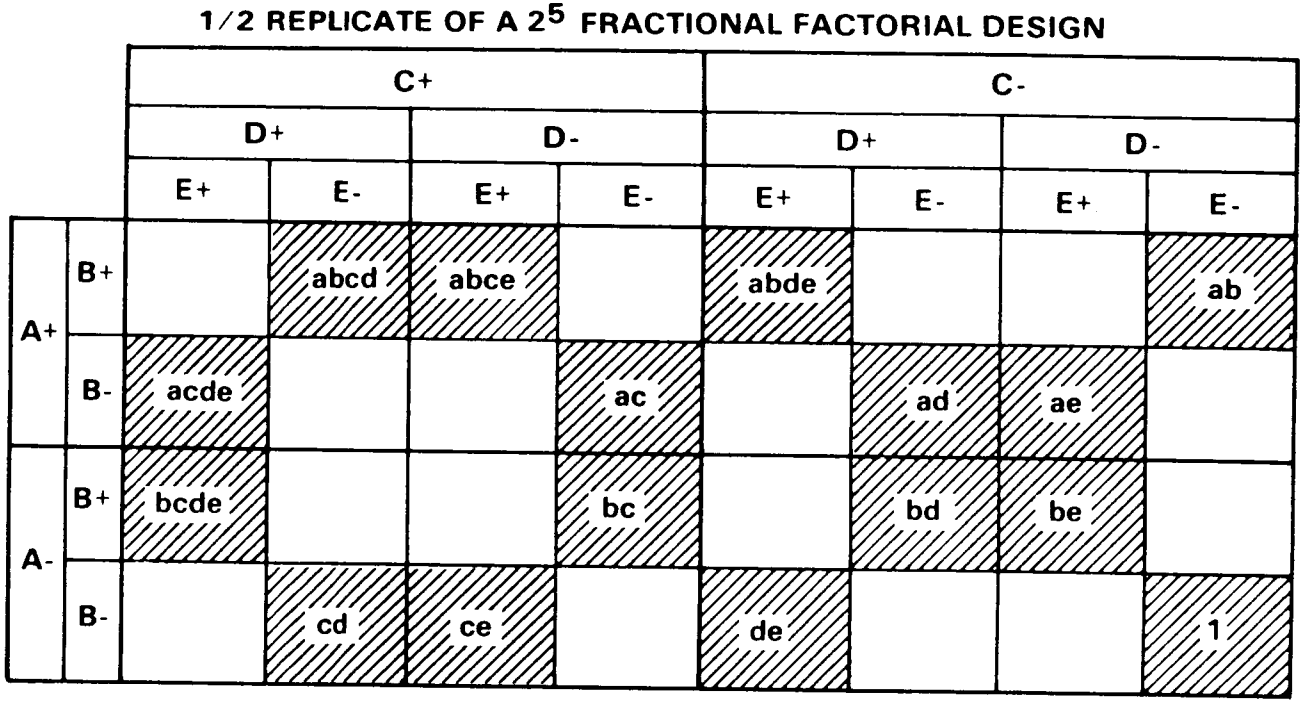

Figure 2.--Experimental Design.

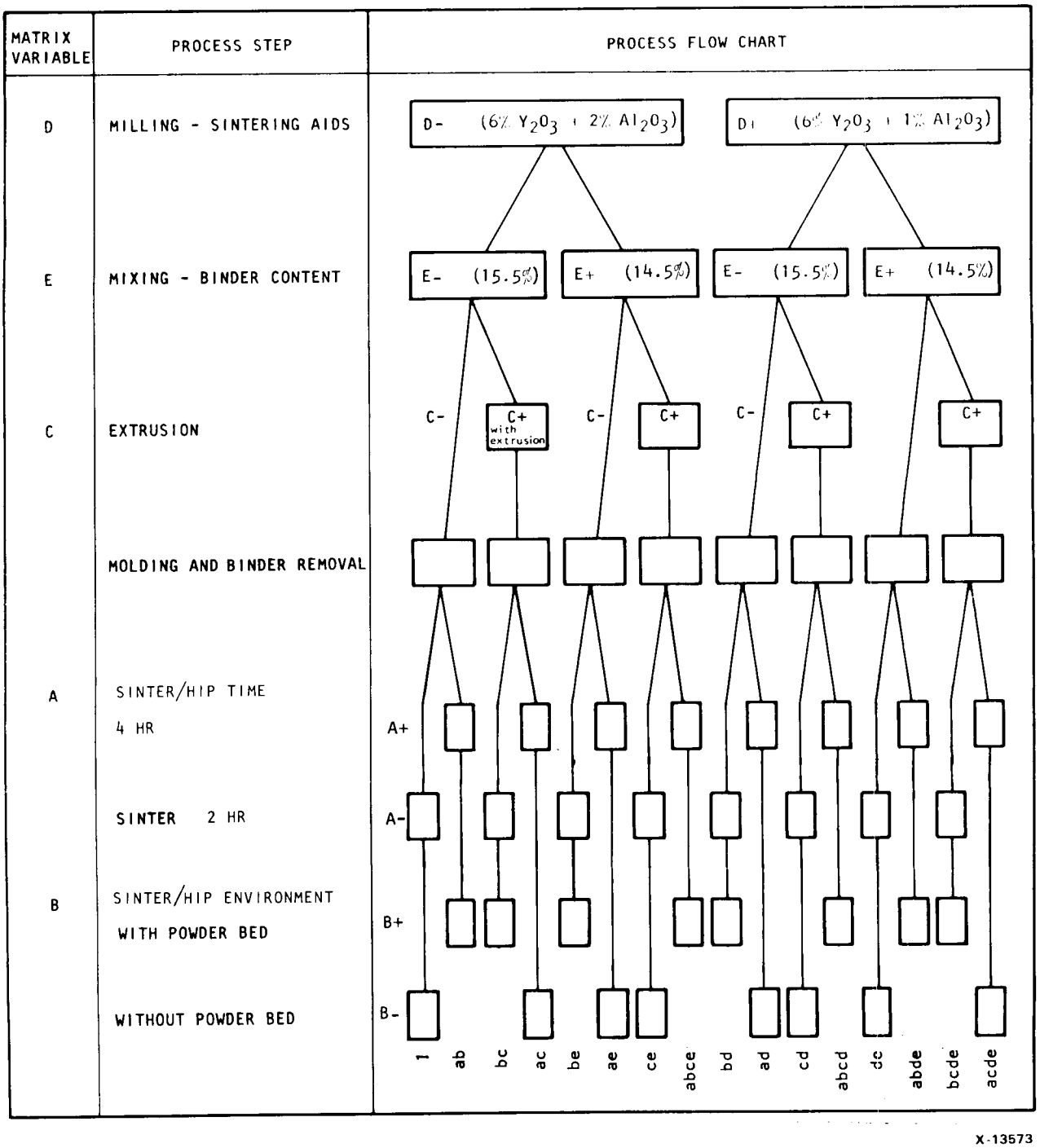

Figure 3.--Process Flowchart for Task II, Matrixes 1 and 2.

TABLE 1

POWDER COMPOSITION, CHEMICAL, AND OXYGEN ANALYSIS[1] (WEIGHT PERCENT)

Element	Matrix II-1 (Starck H-1)			Matrix II-2 (Denka 9FW)		
	AR[2] Si_3N_4	Milled (6+1)[3]	Milled (6+2)[4]	AR[2] Si_3N_4	Milled (6+1)[3]	Milled (6+2)[4]
Aluminum	0.03	0.7	L-M[5]	0.07	0.8	L-M
Calcium	0.002	0.01	0.007	0.09	0.2	0.2
Chromium	--	--	--	0.01	0.01	0.01
Iron	0.02	0.01	0.01	0.02	0.02	0.01
Lithium	<0.001	<0.001	<0.001	<0.001	<0.001	<0.001
Magnesium	0.004	0.007	0.007	0.003	0.007	0.007
Manganese	--	--	--	0.002	0.001	0.001
Sodium	<0.001	<0.001	<0.001	<0.001	<0.001	<0.001
Silicon	H[5]	H	H	H	H	H
Titanium	0.002	0.002	0.002	0.006	0.002	0.007
Vanadium	--	--	--	0.001	--	--
Yttrium	--	M	M	--	M	M
Potassium	<0.001	<0.001	<0.001	<0.001	<0.001	<0.001
Oxygen	1.52	3.39	3.86	0.98	3.00	3.67

NOTES:

1. Ledoux & Company spectrographic analysis, IRT oxygen analysis by neutron activation.
2. As-received powder
3. 93 percent Si_3N_4, 6 percent Y_2O_3, and 1 percent Al_2O_3
4. 92 percent Si_3N_4, 6 percent Y_2O_3, and 2 percent Al_2O_3
5. L, M, H, = low 0.1 - 1 percent, medium 1 to 10 percent, and high 10 to 100 percent, respectively

magnesium than the Task I baseline powder (GTE SN 502); however, the Task II powders are free of molybdenum, a SN 502 impurity.

Oxygen analysis data are also included in Table 1. Both as-received Si_3N_4 powders have a lower oxygen content than the Task I baseline powder--1.52 percent for Starck H-1 and 0.98 percent for Denka 9FW, compared with 2.18 percent for the baseline. Good agreement was seen in higher oxygen levels in milled powder corresponding to the addition of oxide sintering aids.

Particle size distributions for powders from both matrixes are shown in figures 4 and 5. Milled Starck H-1 is comparable to the GTE SN 502 baseline. Milled Denka 9FW powder is much finer than either of the above materials. Figure 5 shows that the as-received Denka 9FW is slightly finer than the milled powder. This shift in particle size distribution is evidently the result of the larger particle size of the sintering aids.

Surface area data are presented in table 2. In both material systems, little change occurs in the surface area during the milling process. All milled powders have surface areas greater than the Task I baseline powder (7.2 m^2/g).

TABLE 2

SURFACE AREAS

Powder	Surface Area, m^2/g
AR Starck H-1	10.78
Milled H-1 6+2 (M94-54C)	11.78
Milled H-1 6+1 (M94-56A)	11.32
AR Denka 9FW	11.81
Milled 9FW 6+2 (M94-110)	11.97
Milled 9FW 6+1 (M94-111A)	12.15

Scanning electron micrographs illustrate the general shape of Task II powders. Figure 6 shows the AR Starck H-1, and figure 7 shows the AR Denka 9FW. The powders appeared to be similar in size and shape; both showed angular equiaxed grains with average grain size of about 0.5 micron and containing a few large grains about 5 microns in diameter. In the nondispersed form, the Denka 9FW powder appear as spherical

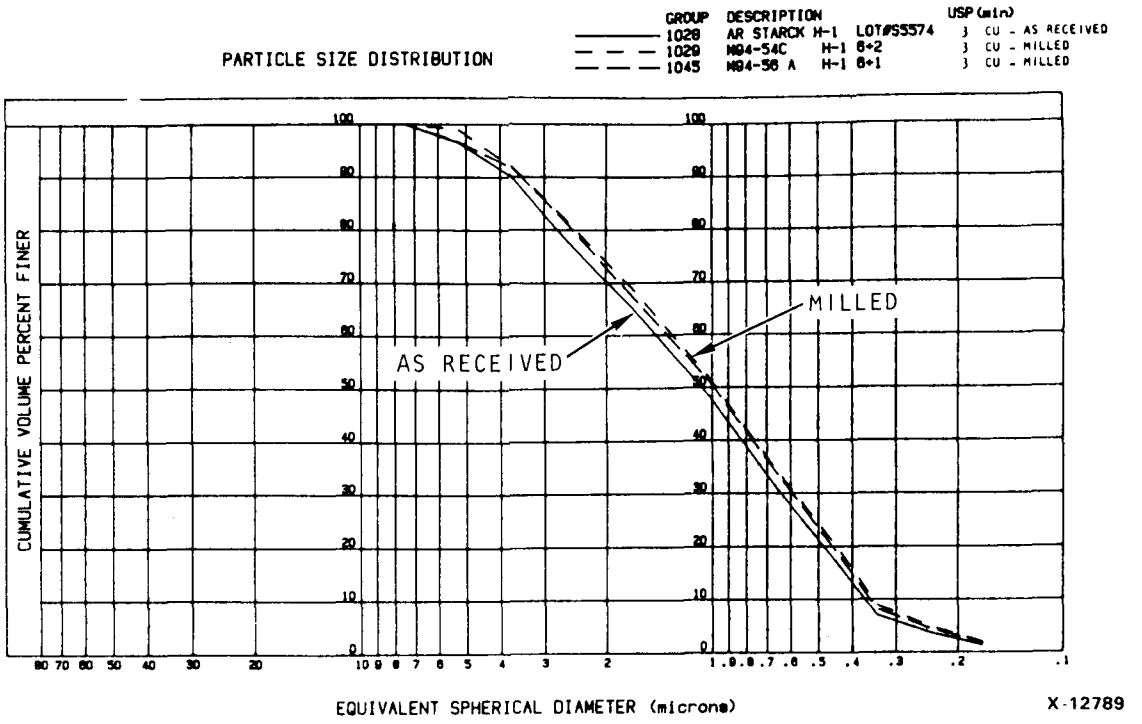

Figure 4.--Particle Size Distribution Data for As-Received and Milled Starck H-1 Powders (Matrix II-1).

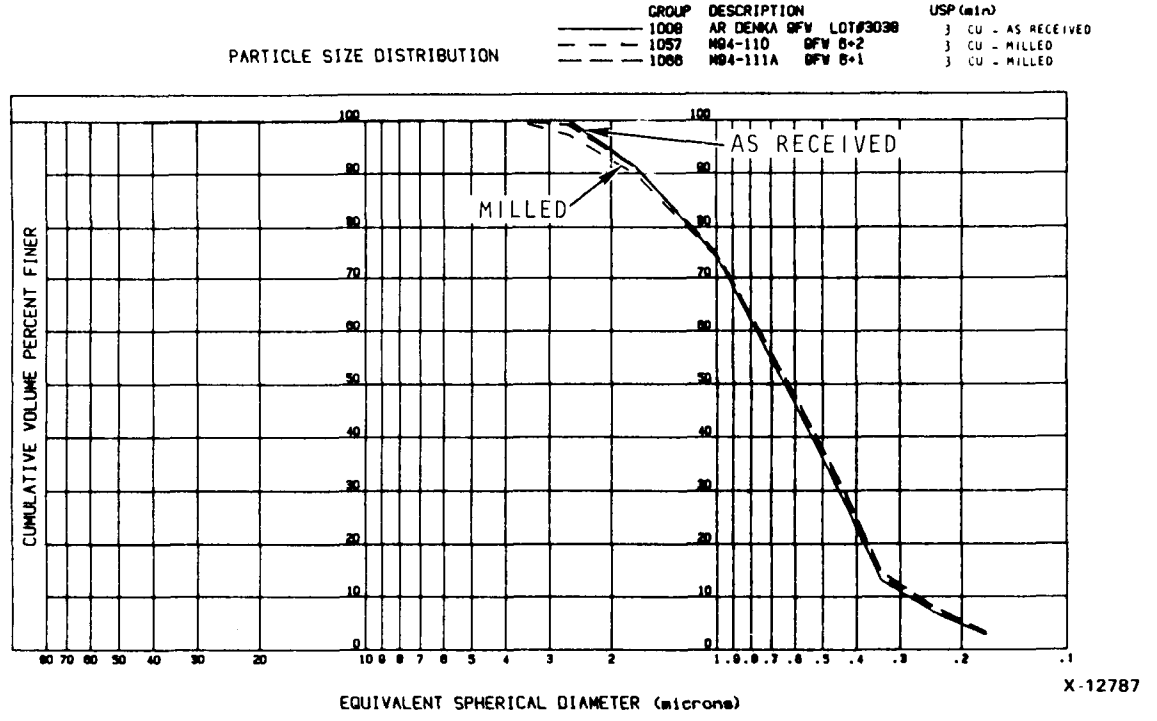

Figure 5.--Particle Size Distribution Data for As-Received and Milled Denka 9FW Powders (Matrix II-2).

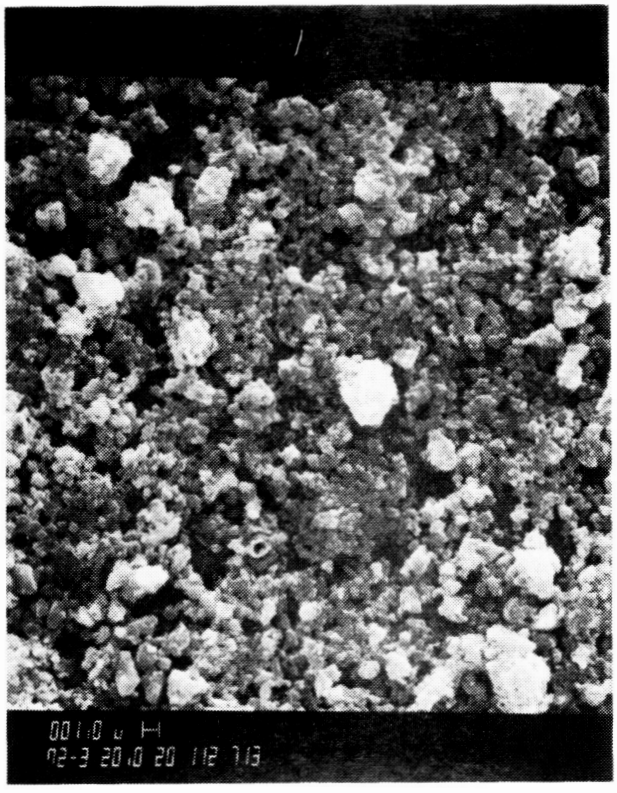

Figure 6.--SEM Micrograph of As-Received Starck H-1 Powder.

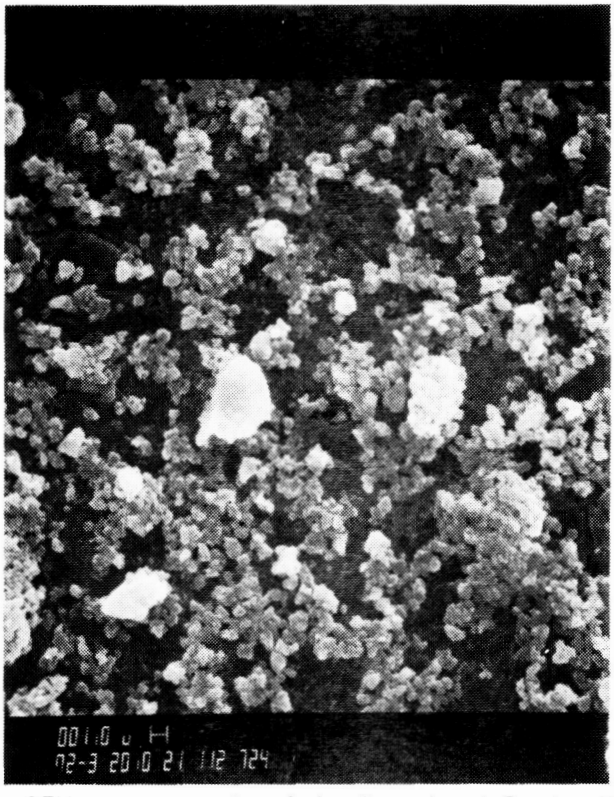

F-48892

Figure 7.--SEM Micrograph of As-Received Denka 9FW Powder.

agglomerates between 20 to 60 microns in diameter and the Starck H-1 powders were 20- to 200-micron irregular agglomerates.

Matrix II-1 (Starck H-1 Si_3N_4).

Processing: Milling, mixing, and molding were completed for Matrix II-1 using Starck H-1 Si_3N_4 powder. Eight injection molding batches were prepared and their viscosity characteristics compared in a torque rheometer. The torque data are presented in table 3 and in figure 8 (for the mixed batch prior to extrusion).

TABLE 3

TORQUE AT 65°C (150°F) FOR MATRIX II-I INJECTION MOLDING BATCHES

	Torque, m·g			
	D- (6% Y_2O_3 + 2% Al_2O_3)		D+ (6% Y_2O_3 + 1% Al_2O_3)	
	E- 15.5% Binder	E+ 14.5% Binder	E- 15.5% Binder	E+ 14.5% Binder
C-	1450	1500	1386	1544
C+ (Extruded)	1100	1452	762	1290

NOTES:

1. Values are from single mixer runs.
2. Mixer cooling rate was 1°C (1.8°F) per minute.
3. m·g = meter·gram

Torque data were obtained from a new cycle that was introduced for the purpose of characterizing premixed powder and binder. The cooling rate of this cycle was 1°C (1.8°F) per minute. Another cycle, with a cooling rate of 2°C (3.6°F) per minute, had been used for mixing in most of the previous experiments of Task VII. The new cycle provides for better temperature control.

The data in table 3 are consistent in showing that by reducing the binder content the torque is increased. The data also indicate that passing the mix through a high-shear, twin-screw extruder reduces the torque. The reason for the exceptionally low value at condition (C+D+E-) is not known.

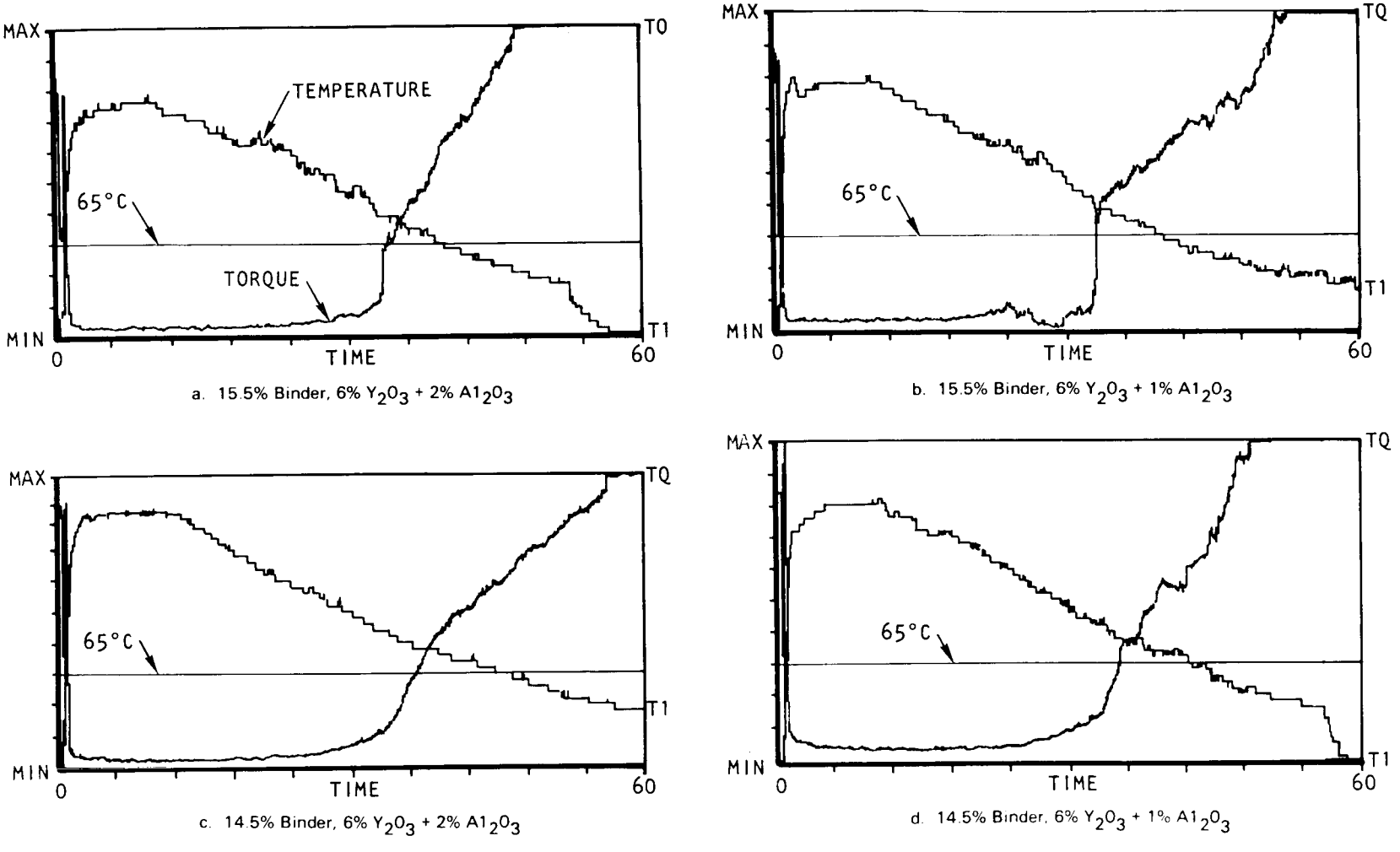

Figure 8.--Torque Characterization Curves, Matrix II-1, Not Extruded; Torque and Temperature Are Plotted as a Function of Time with Scale Minimum Values of 0 m·g and 50°C (122°F) and Maximum Values of 2500 m·g and 100°C (212°F).

For the powders milled in Matrix II-1, figure 8 illustrates a significant difference in torque behavior between 15.5 percent and 14.5 percent binder content. Figures 8a and 8b show the two powder compositions that were mixed with 15.5 percent binder. Both torque curves show a sudden increase at about 68°C (154°F). The same material, mixed with 14.5 percent binder, shows a more uniform torque increase.

Injection molding of 1592 bars in a four-cavity die was accomplished, thereby completing the molding requirements for Matrix II-1. A summary of the injected bars is provided in table 4. Each of the 8 groups of bars was subjected to 2 different densification conditions to provide the 16 treatments identified for this matrix.

X-ray radiography on all as-injected test bars was evaluated. Bars with internal voids were identified, and the yield for each of eight groups is presented in table 5. These data indicate additional mixing, using a twin-screw extruder, provided a better yield at the injection molding stage of processing. Improved x-ray radiography inspection quality using extruded materials is likely to result from improved uniformity of the mix.

Bars selected for dewax are identified in table 6. Most bars that included x-ray voids were deleted from the sample prior to dewax. A 3-day cycle was used instead of the baseline 7-day cycle, and the number of bars was increased to 213 in the dewax load. These changes were demonstrated satisfactory in Task VII Matrixes 3, 6, and 7 and represented an 80-percent reduction in time and energy for dewax when compared with the baseline process. No detrimental effects were observed in any of the prior work.

Densification by sinter/HIP was completed. Four runs were required, each containing up to 160 test bars. Runs 1 and 2 satisfied the parameter requirements of the A- sintering condition, and runs 3 and 4 satisfied the requirements of the A+ conditions. Each run contained both bars covered and bars not covered with a powder bed (B+ and B-) to assure that effects of the powder bed covering could be distinguished from potential variations between runs.

Characterization of density and room temperature MOR: Density and MOR values achieved in Matrix II-1 (Starck H-1) were much lower than those obtained in Matrix II-2 (Denka 9FW, to be presented in a subsequent section). Only a portion of the data is presented, from sinter/HIP run No. 36, to demonstrate that different process parameters control density and strength.

Density values from measurements on all 160 test bars in the run are summarized in table 7. The data show that higher densities resulted from the use of a powder bed in both compositions. The data also show that reduced binder content consistently resulted in higher densities, especially for the 6 + 2 composition in a powder bed. Finally, within layers

TABLE 4

MATRIX II-1 TEST BAR INJECTION SUMMARY

Bar Serial Numbers	Process Code[1]	Molding Temperature, °C (°F)
1541-1744	1 ab	82 (180)
1957-2132	bc ac	82 (180)
1753-1956	be ae	88 (190)
2343-2542	ce abce	88 (190)
2543-2742	bd ad	82 (180)
2743-2942	cd abcd	82 (180)
2133-2342[2]	de abde	88 (190)
2943-3142	bcde acde	88 (190)

NOTES:

1. Statistical design treatment codes defined in figure 2.

2. Serial numbers 2325-2334 were not used.

TABLE 5

X-RAY RADIOGRAPHY YIELD OF AS-INJECTED BARS, STARCK H-1 Si_3N_4

Mixing Procedure	Yield in Percent			
	D- (6% Y_2O_3 + 2% Al_2O_3)		D+ (6% Y_2O_3 + 1% Al_2O_3)	
	E- 15.5% Binder	E+ 14.5% Binder	E- 15.5% Binder	E+ 14.5% Binder
C-	77	77	69	76
C+ (Extruded)	87	92	68	92

TABLE 6

BAR SELECTION FOR DEWAXING

Bar Serial Number Matrix II-1	Process Code*
1616-1651, 1653-1656	1
1657-1696	ab
2017-2056	bc
2057-2084, 2093-2104	ac
1813-1852	be
1853-1868, 1877-1900	ae
2415-2444, 2450-2459	ce
2464-2503	abce
2693, 2606-2611, 2622-2654	bd
2675-2714	ad
2775-2798, 2831-2846	cd
2867-2906	abcd
2193-2232	de
2233-2272	abde
3003-3007, 3010-3035, 3038-3046 3047-3086	bcde

*Statistical design treatment codes as defined in figure 2.

TABLE 7

MATRIX II-1 DENSITY BY SETTER LAYER, g/cc

Setter Layer	Powder Bed	Composition 6 + 2						Composition 6 + 1					
		E- 15.5%			E+ 14.5%			E- 15.5%			E+ 14.5%		
		Average	Max.	Min.	Average	Max.	Min.	Average	Max.	Min.	Average	Max.	Min.
6 (Top)	No	2.97	3.02	2.87	3.00	3.05	2.93	2.66	2.70	2.62	2.69	2.72	2.66
5	No	2.97	3.00	2.91	3.01	3.07	2.93	2.66	2.69	2.62	2.69	2.72	2.66
4	No	2.94	2.96	2.92	2.98	3.01	2.95	2.67	2.79	2.62	2.68	2.70	2.64
3	PB-2	3.09	3.12	3.05	3.18	3.21	3.16	2.83	2.86	2.80	2.86	2.90	2.83
2	PB-2	3.10	3.19	3.00	3.18	3.19	3.16	2.86	2.87	2.85	2.89	2.92	2.86
1 (Bottom)	PB-2	3.01	3.04	2.99	3.10	3.14	3.06	2.80	2.83	2.74	2.83	2.85	2.79

1 to 3 (all samples in powder bed) layer 1 yielded distinctly lower density bars.

Individual density values covered a broad range, as indicated by maximum and minimum values presented for the six or seven bars in each layer for each composition. This scatter was not anticipated, as sample selection procedures ensured maximum sample uniformity within a group. Each group of six or seven bars generally represented consecutive injection moldings (four bars per molding), and bars from each group were processed through dewax together (e.g., composition 6 + 2, 15.5 percent, layer 6 consisted of bars 1854 through 1859).

In table 8, room-temperature MOR data are summarized for 60 bars made with the 6 + 2 composition. It is obvious that the parameters that yielded high densities--powder bed, lower binder content, and lower layer--were not the primary factors in achieving the strength results shown.

In both the density and MOR summaries presented here, the C variable, extrusion, is not identified. This and earlier work indicate that extrusion is a minor factor in achieving high density. Extrusion was shown to have a detrimental effect on strength due to inclusions introduced in processing in Matrix II-2. In table 8, the three high MOR values, 73 to 80 ksi, represent extruded materials. However, the effect due to extrusion cannot be separated from the effect due to powder bed or binder content.

TABLE 8

MATRIX II-1 TEST BAR MOR AVERAGE VS SETTER LAYER

Percent Binder		15.5%	14.5%
Powder Bed	Setter Layer	$\bar{x}$, ksi	$\bar{x}$, ksi
No	6	80*	65
No	5	73*	65
No	4	77*	57
PB_2	3	62	57*
PB_2	2	59	52*
PB_2	Bottom	36	70*

*Extruded

It should be mentioned that extrusion is probably beneficial to material property since the high shear mixing action improves material homogeneity. It is also possible that the extruder tends to shed stainless steel particles into certain materials mix during extrusion, as shown in the Matrix II-2 (Denka 9FW) results to be discussed in a subsequent section. These stainless steel inclusions were found to be detrimental to strength because they act as stress concentration defects.

The density and MOR results showed that the Starck H-1 specimens were not fully densified with the processing conditions used in this matrix. The average room temperature MOR was 60.4 ksi and the highest strength specimen was only 84.6 ksi. Most of the specimens also had low sintered densities of less than 3.00 g/cc. Only one treatment condition, abce, produced some specimens with density above 3.10 g/cc. The elevated temperature strengths of the specimens were also low, averaging 30.6 ksi and ranging from 16.4 to 44.0 ksi.

Since the low MOR and densities indicated that the processing conditions used in this matrix were not suitable for the Starck H-1 powder, only a partial fractographic evaluation was carried out for these specimens. Among the 120 specimens examined, 75 percent failed from surface flaws and 25 percent from internal flaws. Only six specimens (5 percent) failed due to inclusions, a much smaller proportion than found in Matrix II-2 (Denka 9FW specimens).

At elevated temperature (2250°F) most of the specimens deformed during testing. Fifteen specimens bent so seriously that they bottomed out in the testing fixture. Slow crack growth was also observed in nearly every failed test specimen.

Statistical analysis: Because of the unsatisfactory results discussed above, no detailed statistical analysis was carried out for this matrix.

Matrix II-2 (Denka 9FW Si_3N_4).

Processing: Milling, mixing, and molding were completed for Matrix II-2 using Denka 9FW Si_3N_4 powder. Eight batches were prepared and then characterized in the torque rheometer at 65°C. The data are presented in table 9.

Torque of the extruded mixes is consistently 36 to 50 percent lower than the as-mixed material. All torque-vs-temperature curves show a smooth transition from high temperature and low viscosity to low temperature and high viscosity. Finally, torque values are lower than those presented for Matrix II-1 (see table 3).

TABLE 9

TORQUE AT 65°C (150°F) FOR MATRIX II-2 INJECTION MOLDING BATCHES

Mixing Procedure	Torque, m·g			
	D- (6% Y_2O_3 + 2% Al_2O_3)		D+ (6% Y_2O_3 + 1% Al_2O_3)	
	E- 15.5% Binder	E+ 14.5% Binder	E- 15.5% Binder	E+ 14.5% Binder
C-	876	1304	948	1175
C+ (Extruded)	439	796	500	748

Notes:

1. Values are from single mixer runs.
2. Mixer cooling rate was 1°C (1.8°F) per minute.
3. m·g = meter·gram

Injection molding of 1412 bars was completed to fulfill the requirements of Matrix II-2 and provide additional bars for optimization experiments. This also includes the initial bars injected in each group to obtain optimum molding parameters as determined by visual quality.

X-ray radiography was completed on as-injected test bars. The yield of bars free from internal voids is presented in table 10. The quality of bars in Matrix II-2 is better than in Matrix II-1. This is probably a result of the flow behavior of the Matrix II-2 material as seen in lower torque values and more uniform torque increases during cooling.

Table 11 identifies test bars selected for dewax. Bars observed to contain voids by x-ray were deleted.

Binder removal was completed on bars required for Matrix II-2. Visual and radiographic inspection were completed on all bars. All test bar fabrication parameters defined in Task II yielded satisfactory dewax results. Defects observed in the as-injected bars appeared unchanged and new defects were not apparent.

Densification by sinter/HIP was completed for all bars (627 bars total) in Matrix II-2. Four runs were required, each containing up to 160 test bars. Runs 1 and 2 satisfied the parameter requirements of the A- sintering condition, and runs 3 and 4 satisfied the requirements of the A+ conditions. Each run contained both bars covered and bars not

TABLE 10

X-RAY RADIOGRAPHY YIELD OF AS-INJECTED BARS

Mixing Procedure	Yield in Percent			
	D- (6% Y_2O_3 + 2% Al_2O_3)		D+ (6% Y_2O_3 + 1% Al_2O_3)	
	E- 15.5% Binder	E+ 14.5% Binder	E- 15.5% Binder	E+ 14.5% Binder
	Matrix II-1, Starck H-1 Si_3N_4, 200 Bars Injected for Each Condition			
C-	77	77	69	76
C+ (Extruded)	87	92	68	92
	Matrix II-2, Denka 9FW Si_3N_4, 160 Bars Injected for Each Condition			
C-	95	95	95	95
C+ (Extruded)	96	96	98	96

covered with a powder bed (B+ and B-) to assure that effects of the powder bed could be distinguished from potential variations between runs.

A summary of the densification results is given in table 12. Data were taken on 8 bars from each group of 20. Data from all 20 bars were taken on 6 groups to compare with the sampled data. Little difference in average density (0.00 to 0.02 g/cc) was seen.

A visual inspection (using 20X stereoscope) was made on the sintered bars to evaluate the injection molding process as it relates to surface quality. For this analysis, defects judged as critical are knit lines that form a reentrant angle into the surface, cracks, and blisters. Scratches or cracks caused by handling are not included, because they are not inherent to the process. The data in table 13 indicate an overall yield of 73 percent for the 6 + 2 composition, and 85 percent for the 6 + 1 composition. The major reason for rejecting the bars in each test group is also listed.

For the 6 + 2 composition, the major defect was blister formation during sintering, which resulted in a surface protrusion. Nominally, one blister per bar was evident, and for this analysis this was considered sufficient cause to reject the bar. The cause for blister formation needs to be investigated. Air entrapment would probably be in evidence

TABLE 11

BAR SELECTION FOR DEWAXING

Bar Serial Number Matrix II-2	Process Code*
3285-3324	1
3325-3364	ab
3425-3464	bc
3465-3504	ac
3597-3636	be
3637-3676	ae
3741-3780	ce
3781-3820	abce
3925-3964	bd
3965-4004	ad
4077-4116	cd
4117-4156	abcd
4237-4276	de
4281-4320	abde
4421-4460	bcde
4521-4560	acde

*Statistical design treatment codes defined in figure 2.

after dewaxing if it was close to the surface. There was a yield difference in surface quality between the four sinter/HIP runs as follows:

Run No.	Yield
1	72 percent
2	68 percent
3	81 percent
4	94 percent

Characterization: Four-hundred seventy-nine Task II-2 test bars were tested in four-point bending. The overall room-temperature strength of the test bars was high; there were 65 bars with MOR over 100 ksi. The average MOR was 86.5 ksi with a standard deviation of 12.9, and the strength of the bars ranged from 41.9 to 115.0 ksi.

TABLE 12

MATRIX II-2, DENKA 9FW SINTERED DENSITY AND WEIGHT CHANGE DATA*

	Sintering+ Run	D- (6 + 2**)				D+ (6 + 1)			
		E- (15.5%***)		E+ (14.5%)		E- (15.5%)		E+ (14.5%)	
		B-	B+	B-	B+	B-	B+	B-	B+
C- Not Extruded	1	3.04 (0.04) -1.2 (0.1)			3.25 (0.01) -0.9 (0.1)		2.99 (0.01) -0.5 (0.1)	2.97 (0.01) -0.7 (0.1)	
	2	3.03 (0.02) -1.0 (0.1)			3.14 (0.04) -0.4 (0.1)		3.00 (0.04) +0.3 (0.1)	2.94 (0.01) -0.6 (0.1)	
	3		3.13 (0.06) -0.4 (0.2)	3.10 (0.04) -1.2 (0.1)		2.99 (0.02) -0.6 (0.1)			3.02 (0.08) +0.4 (0.2)
	4		3.20 (0.02) -0.2 (0.2)	3.12 (0.10) -0.7 (0.3)		2.95 (0.03) -0.3 (0.3)			2.96 (0.03) +0.4 (0.2)
C+ Extruded	1		3.22 (0.03) -1.0 (0.1)	3.17 (0.04) -1.2 (0.1)		2.97 (0.01) -0.8 (0.1)			3.00 (0.01) -0.4 (0.1)
	2		3.09 (0.05) -0.3 (0.2)	2.99 (0.02) -1.1 (0.1)		2.94 (0.01) -0.6 (0.0)			3.01 (0.03) 0.0 (0.4)
	3	3.01 (0.04) -1.3 (0.1)			3.16 (0.04) -0.4 (0.2)		3.03 (0.06) +0.4 (0.2)	2.99 (0.02) -0.6 (0.1)	
	4	3.13 (0.08) -0.8 (0.3)			3.16 (0.05) -0.3 (0.2)		2.98 (0.02) +0.5 (0.2)	2.94 (0.03) -0.3 (0.2)	

*Each data box contains: Average density, gm/cc (standard deviation)
Average weight change, % (standard deviation)

**Percent Y_2O_3 and Al_2O_3, respectively

***Binder content

+Sintering runs 1 and 2 are A- and runs 3 and 4 are A+

TABLE 13

MATRIX II-2, ACCEPTABLE TEST BAR YIELDS BASED ON SURFACE QUALITY

Sintering			D- 6 + 2				D+ 6 + 1			
			E- 15.5%		E+ 14.5%		E- 15.5%		E+ 14.5%	
	Run	Parameter	B-	B+	B-	B+	B-	B+	B-	B+
C- Non-extruded	1	A-	85[b]			90		85	85[s]	
	2	A-	80[b]			85		45[c]	95	
	3	A+		60[b]	85[b]		100			85[w]
	4	A+		100	90		90			95
C+ Extruded	1	A-		45[b]	20[b]		70[b]			95
	2	A-		35[b,c]	80[b]		80[b,s]			45[c]
	3	A+	70[b]			60		90	100	
	4	A+	85			90		100	100	
Overall Yield			73				85			

A = Sintering cycle parameters
B = No powder bed, powder bed
C = Extrusion, non-extrusion
D = Y_2O_3% + Al_2O_3%
E = Percent binder by weight

Xy X is the percent yield of 20 bars examined
y is the major cause of rejection of the bars

Rejection Codes: b = blisters, c = cracks, s = stones or inhomogeneous areas, w = warp

Sixteen different process treatment conditions were included in this matrix, and six of the eight conditions in the 6 + 2 composition produced test bars with a characteristic strength greater than 90 ksi. Condition ab produced the highest characteristic strength of 101.2 ksi and Weibull slope of 13.2.

Optical fractography results show that there were 115 test specimens (26 percent) with failure from internal flaws and 333 (74 percent) with failure from the surface. The average MOR of test specimens that failed from the surface was 88.0 ksi and the average MOR of specimens that failed from internal flaws was 80.0 ksi. Fractography showed 91 (79.9 percent) of the internal flaws were inclusions while the rest consisted of cracks, pores, and voids.

Nearly all of the inclusions were either dark colored or surrounded by a dark patch. Selected specimens with these inclusions were examined under SEM and analyzed by EDX. Micrographs and EDX plots of the specimens are presented in figures 9 through 11. EDX analysis showed that the inclusions contained mainly iron and small quantities of chromium and nickel. No other element except silicon was detected in the surrounding dark zone. SEM examination did show that fracture mode in the dark zone was predominantly transgranular and this patch of smooth flat surface probably emitted less electrons into the detector and appeared dark due to a surface morphology effect. The change in fracture mode for the dark zones may be due to the formation of a different grain boundary phase with higher iron concentration. The fact that the majority of test specimens with dark inclusions or dark patches were extruded (C+ condition) suggests the extruder was introducing stainless steel particles into the mixture.

Internal and surface voids were also found at the fracture origins of some specimens. Figures 12 and 13 show an example of each type. The void shown in figure 13 probably existed before sintering, judging from the growth of needle-shaped Si_3N_4 grains inside the void (figures 13c-d).

The typical fracture surfaces of the 6 + 2 specimens in this matrix are shown in figures 14a-c. The specimens were processed with treatment conditions "ab," "ae," and "be," respectively. The microstructure consisted of predominantly elongated hexagonal Si_3N_4 grains with a small proportion of fine equiaxed grains typical for sintered Si_3N_4. The larger grains were about 5 by 30 microns (0.0002 x 0.0012 in.).

At 2250°F, most specimens tested exhibited fast fracture features, but the influence of temperature could also be observed. Compared to specimens tested at room temperature, fewer failures due to inclusions were observed and the inclusions did not seriously affect the strength. Fractures at this temperature generally originated from the tensile surface. Internal and surface voids were also observed at some of the origins. Figures 15 and 16 show two examples of the voids.

Statistical analysis of room temperature MOR: The average MOR and Weibull slope of the specimens from the 16 treatment conditions are listed in table 14. The treatment that yielded the highest MOR (97.3 ksi) is condition "ab," which utilized 6% Y_2O_3 + 2% Al_2O_3 sintering aid, 15.5% binder, mixing without extrusion, and longer sintering time in

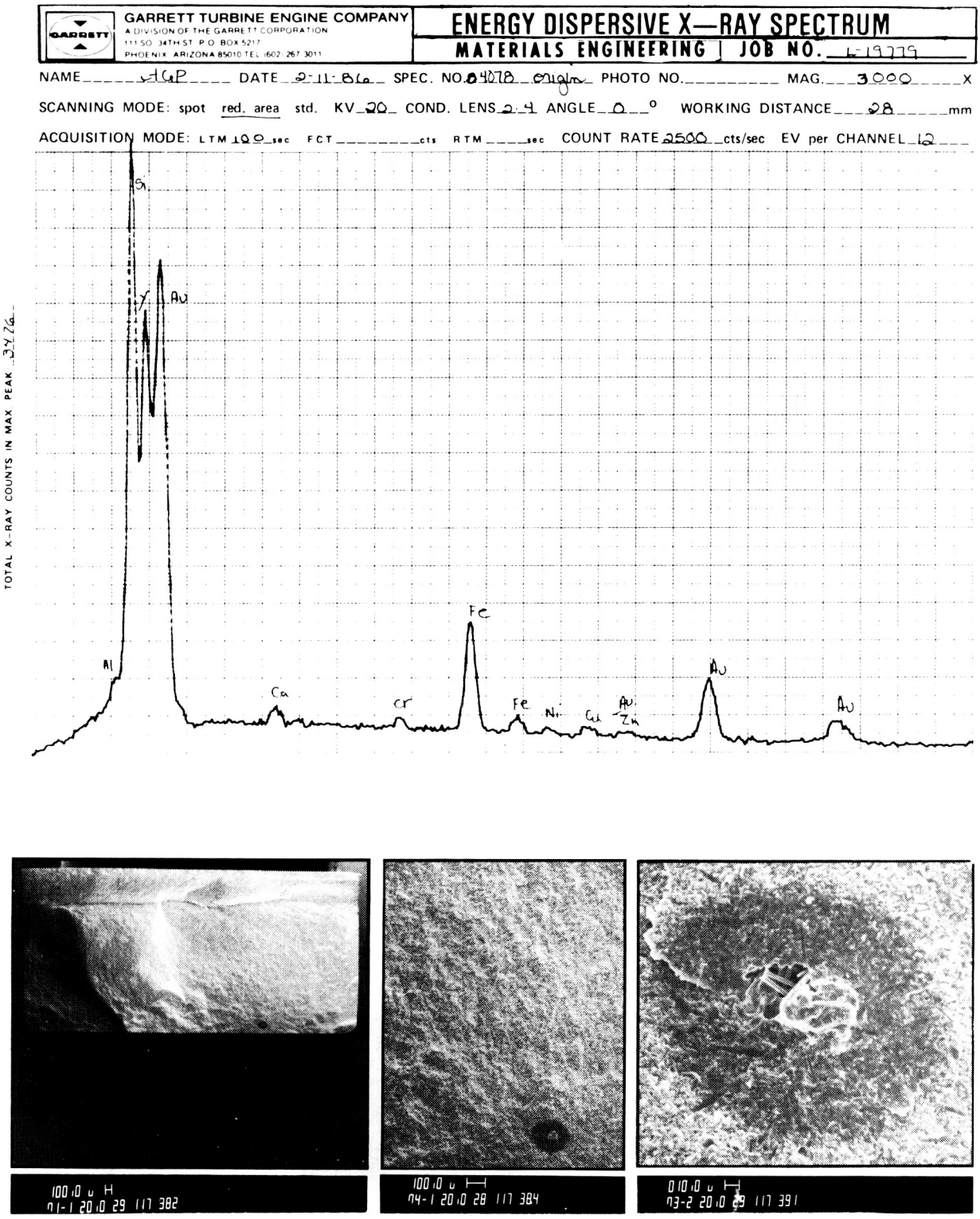

Figure 9.--EDX and SEM Photos of Fractured Bar 4078 Showing Stainless Steel Inclusion and Surrounding Dark Patch.

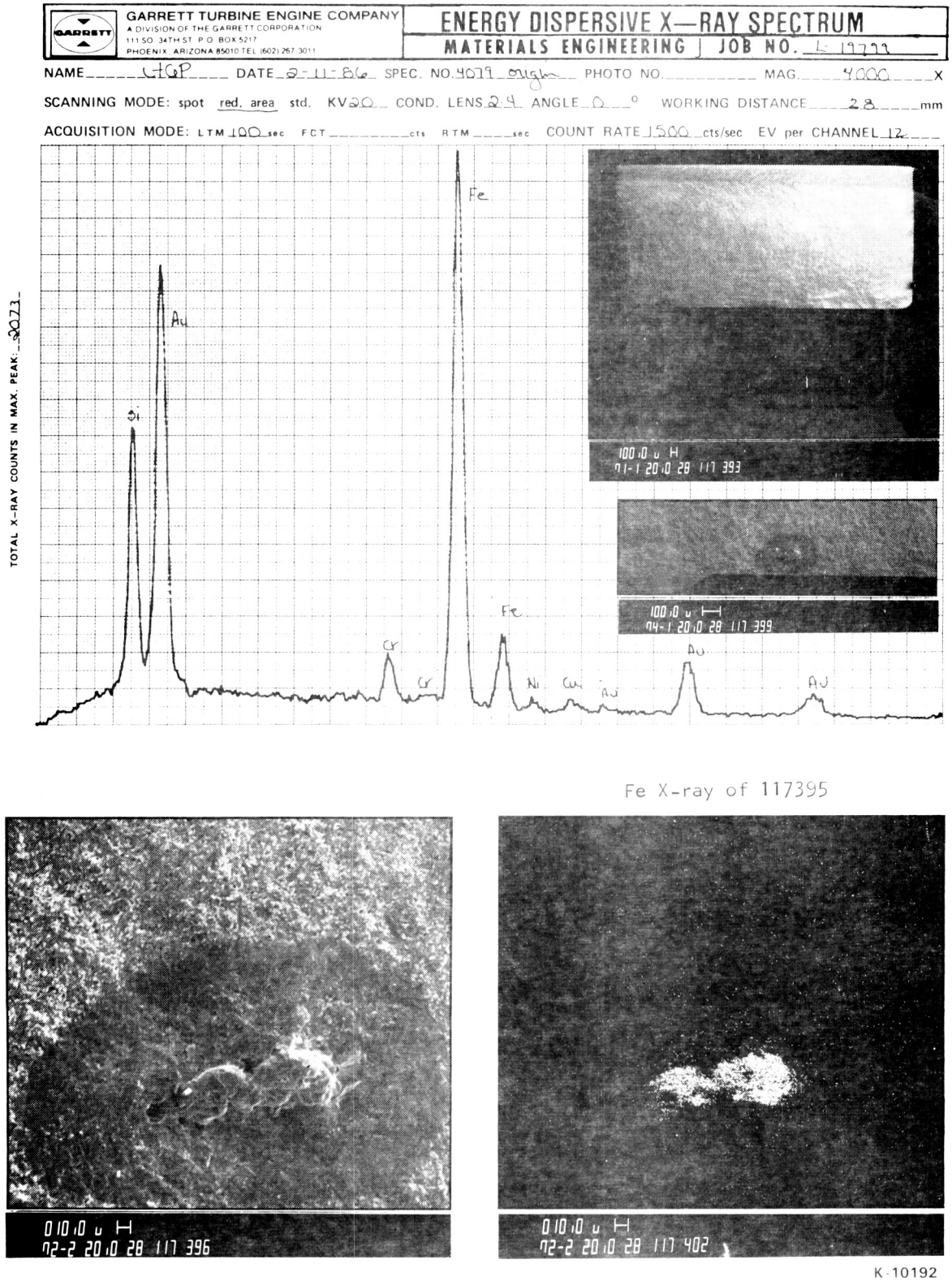

Figure 10.--EDX and SEM Photos of Fractured Bar 4079
Showing Dark Inclusion and Surrounding Patch.

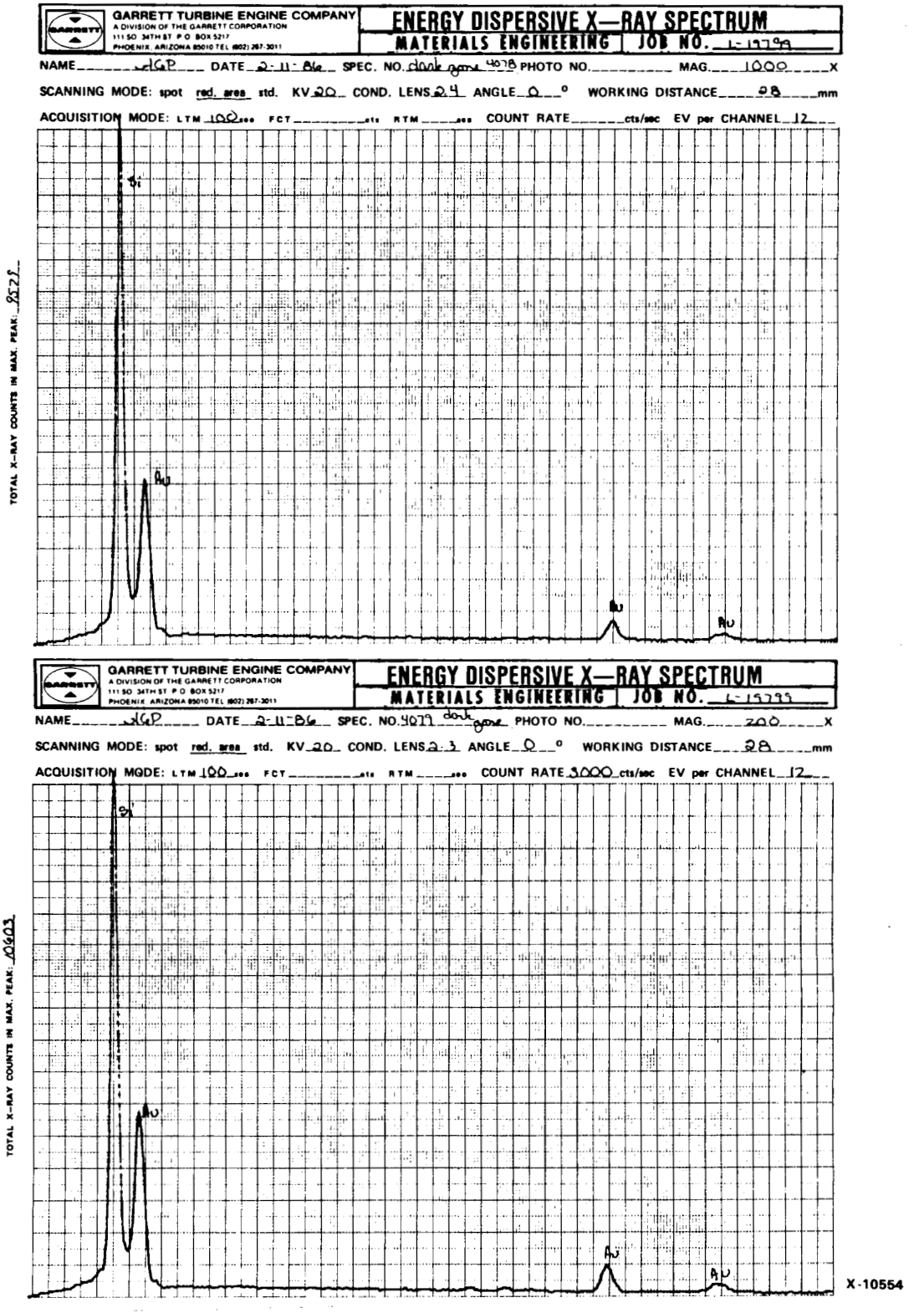

Figure 11.--EDX Plots of the Dark Areas of Bars 4078 and 4079 Showing Only Si (the Au Signal Was From the Sputtered Coating).

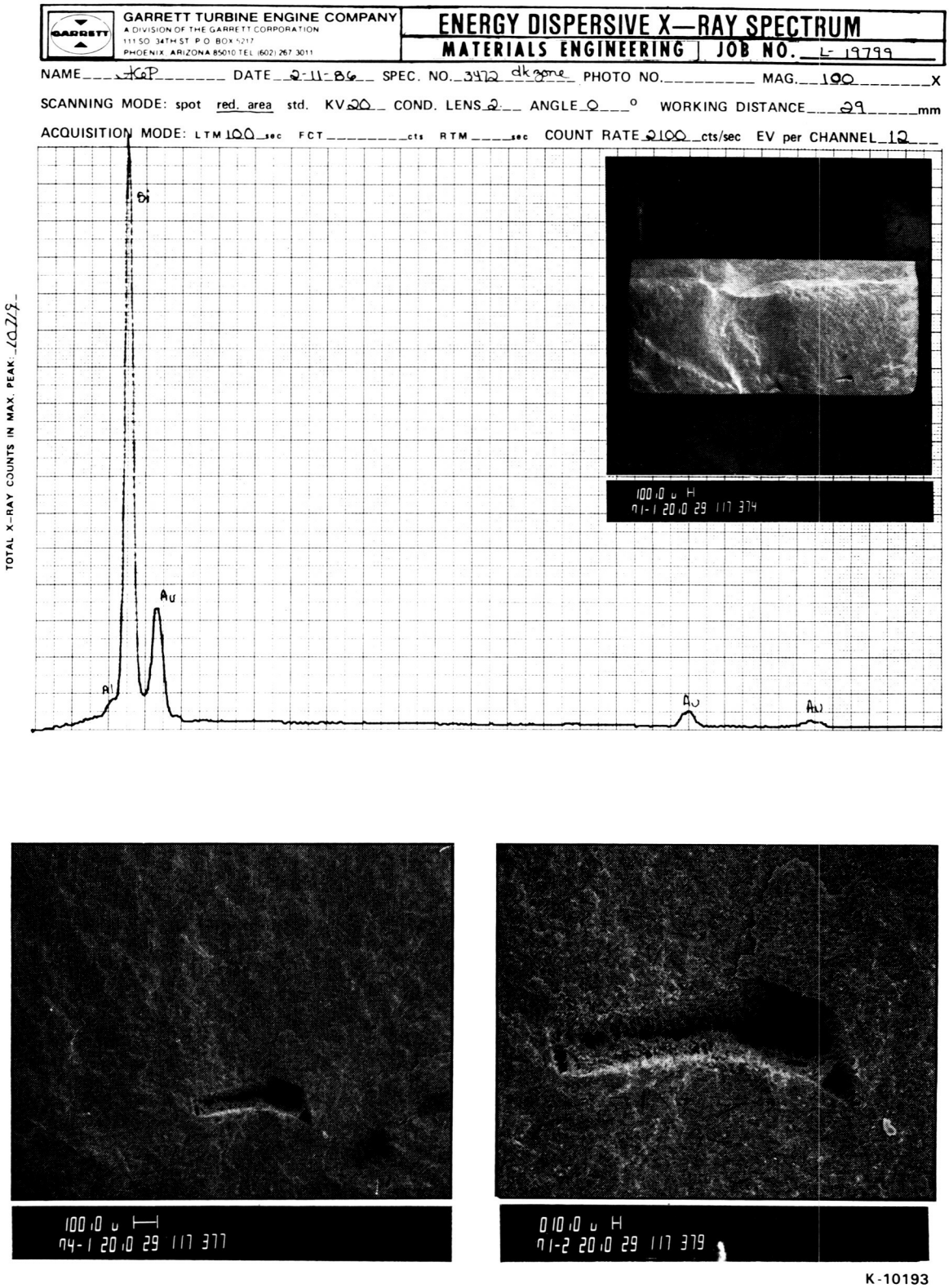

Figure 12.--EDX and SEM Photos of Fractured Bar 3472 Showing an Internal Void Probably Formed During Injection Molding.

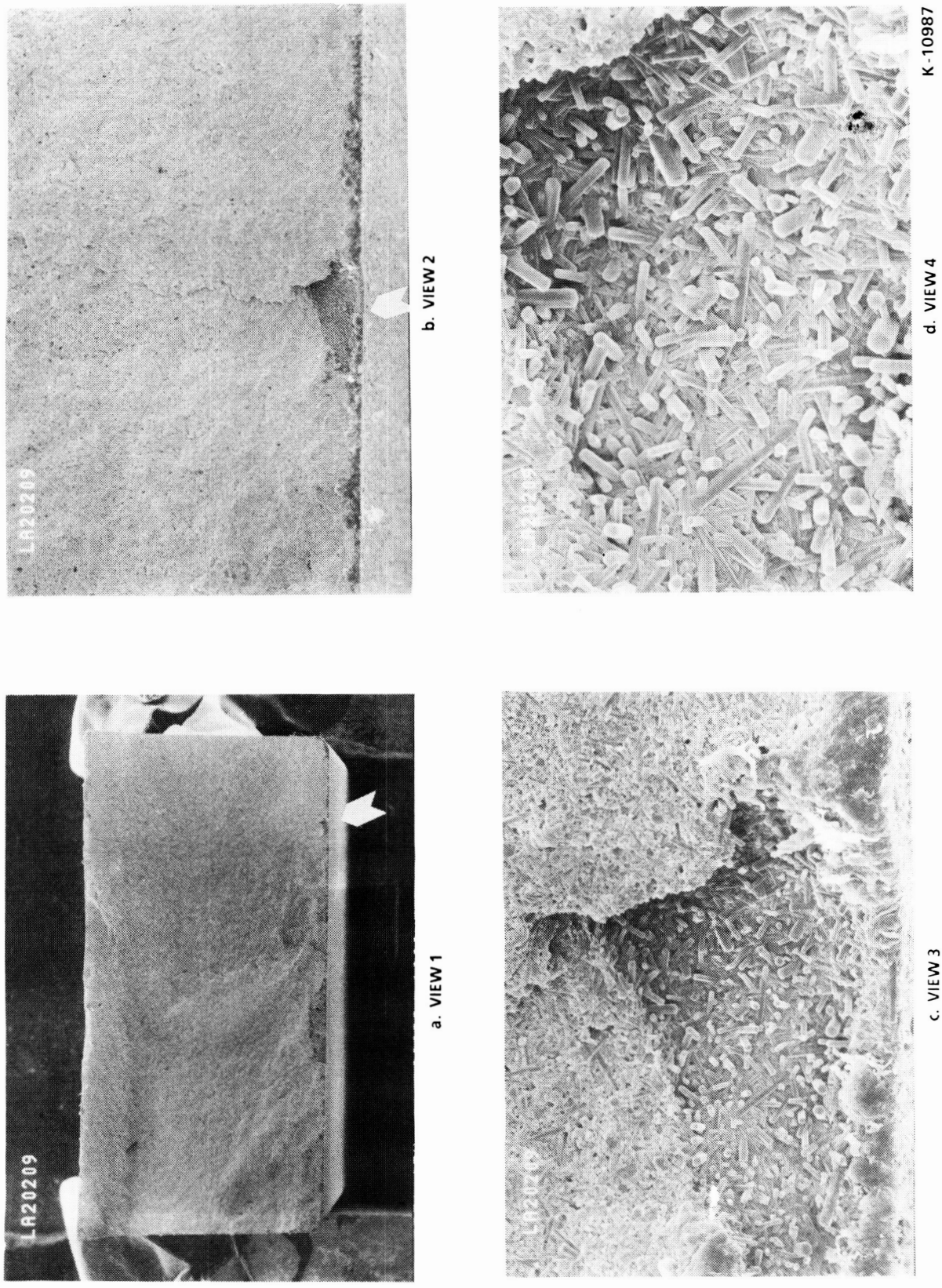

Figure 13.--Void in Specimen 3331, Condition "ab"--MOR = 72.9 ksi;
ρ = 3.07 g/cc (Room Temperature).

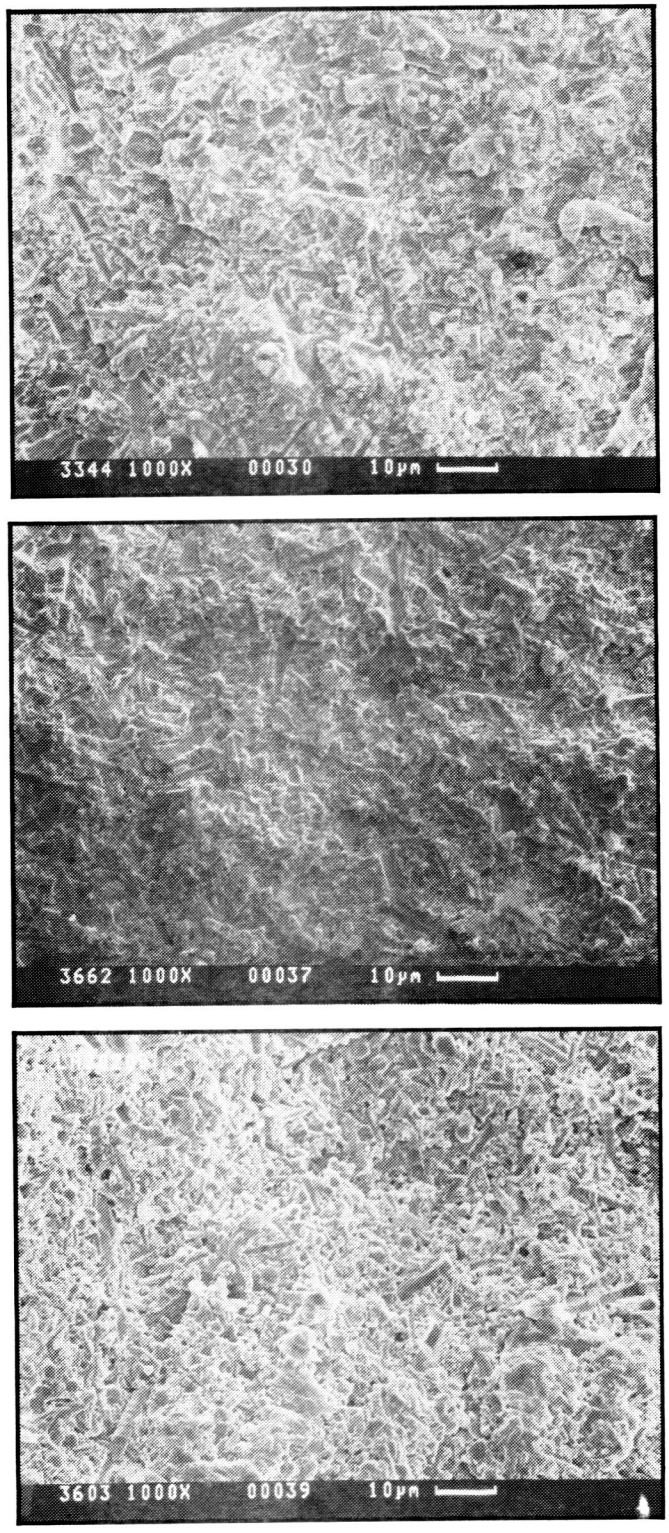

a. NO. 3344, 81.4 KSI CONDITION "AB"

b. NO. 3662, 91.5 KSI CONDITION "AE"

c. NO. 3603, 94.6 KSI CONDITION "BE"

K-11231

Figure 14.--Fracture Surfaces of Specimens from "ab," "ae," and "be" Conditions.

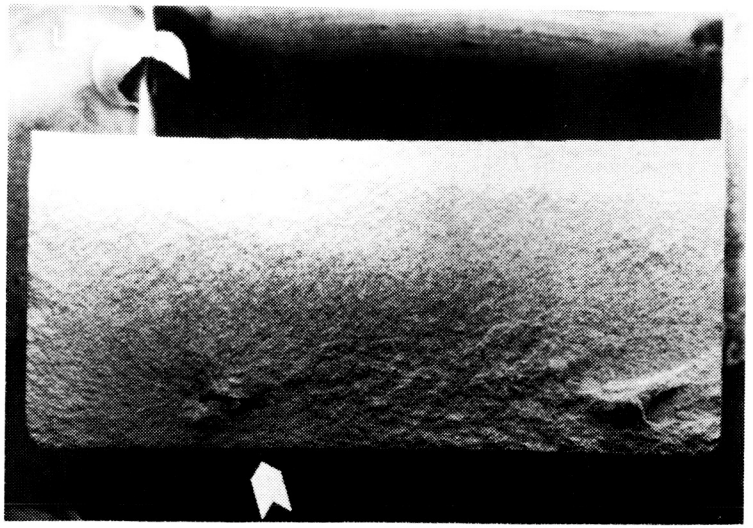

a. VIEW 1

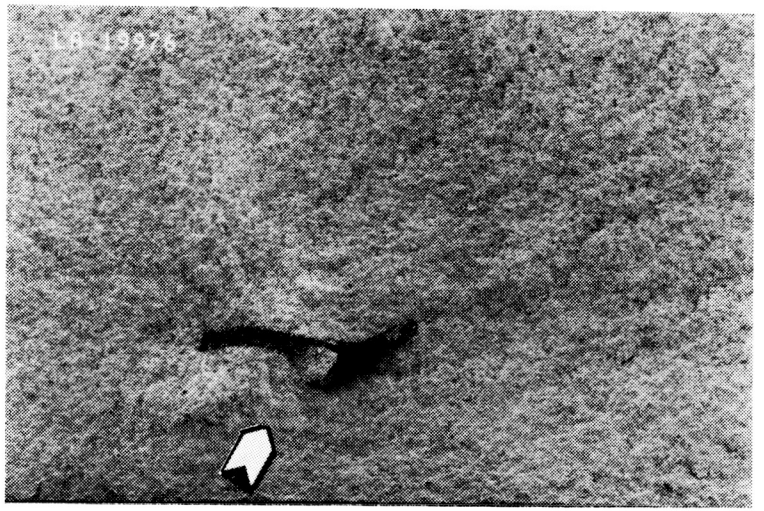

b. VIEW 2

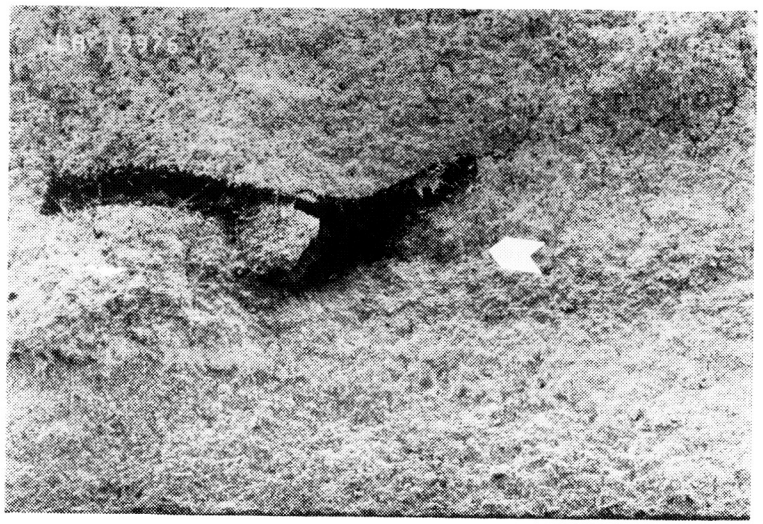

c. VIEW 3

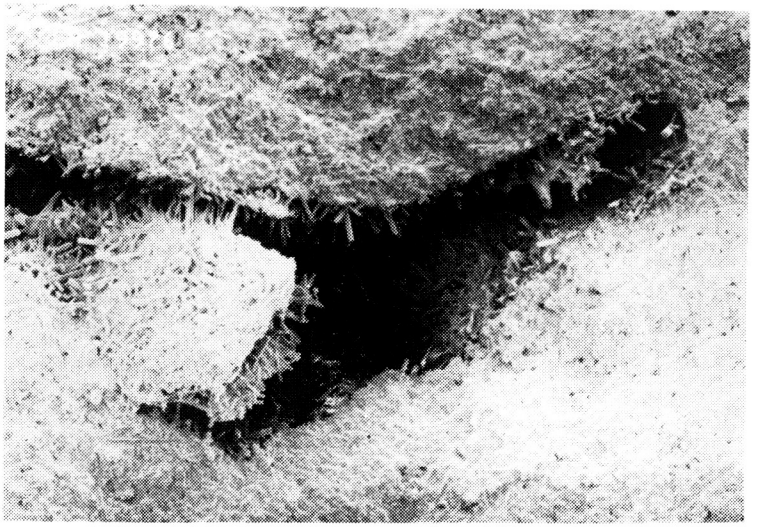

d. VIEW 4

K-10989

Figure 15.--Void in Specimen 3352, Condition "ab"--MOR = 61.5 ksi;
Density Not Measured, Tested at 2250°F.

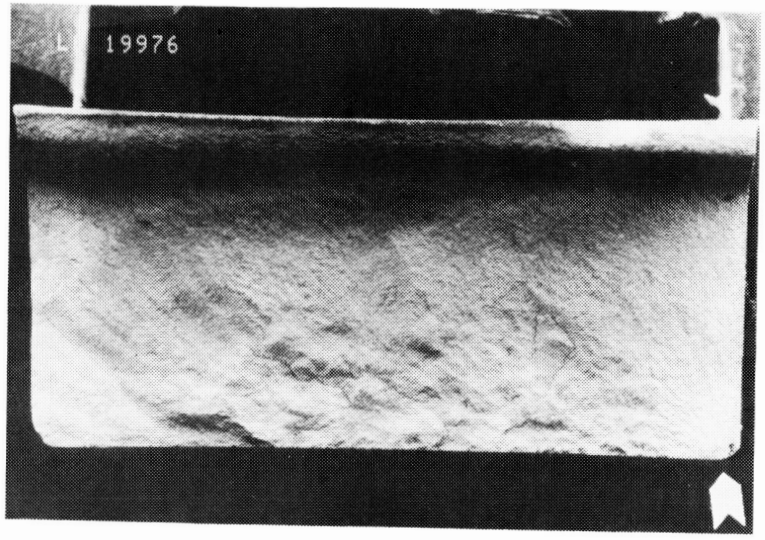

a. VIEW 1

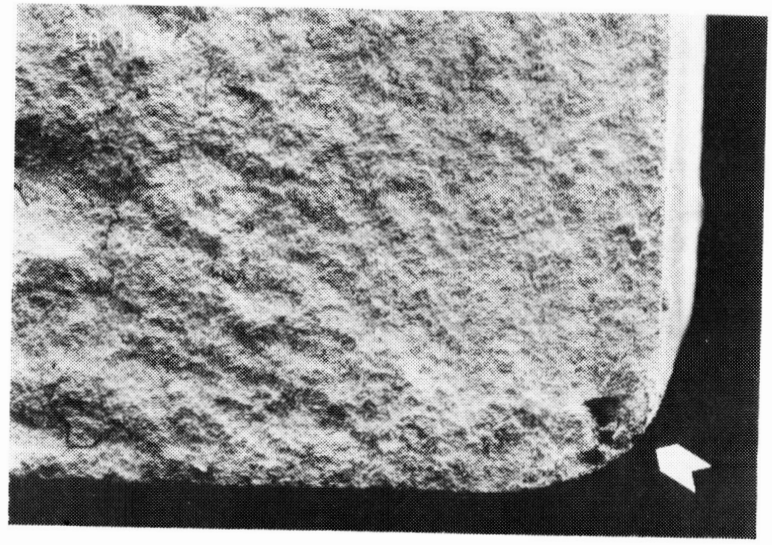

b. VIEW 2

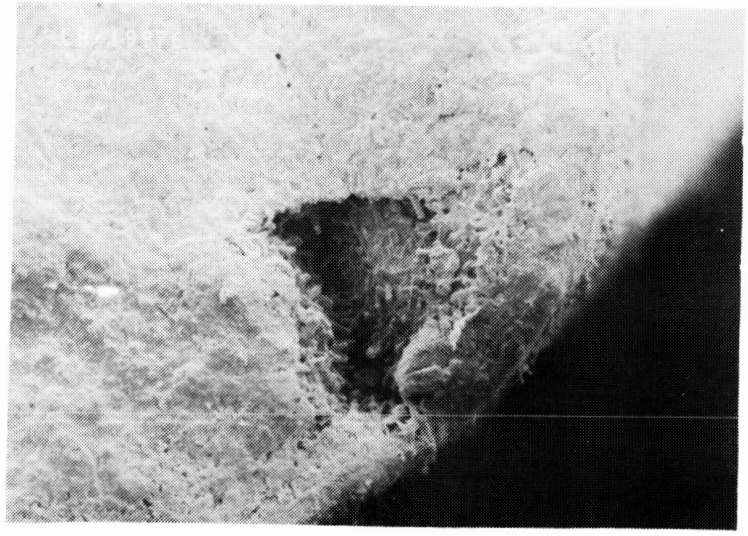

c. VIEW 3

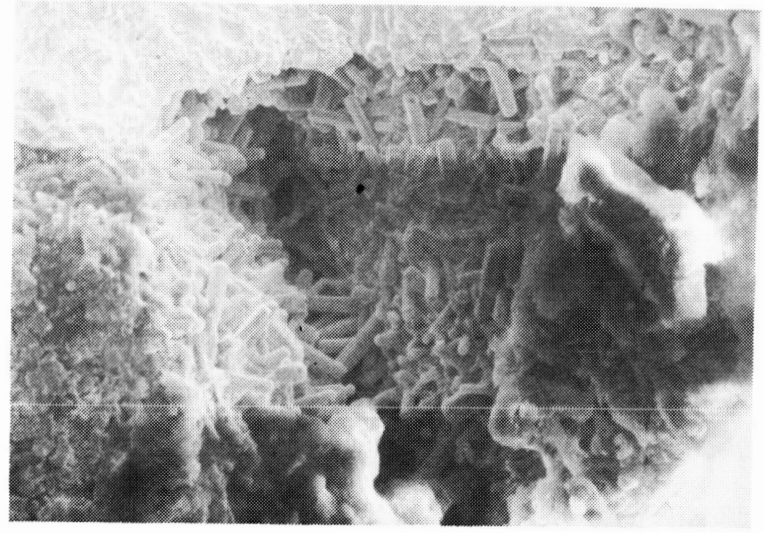

d. VIEW 4

K-10988

Figure 16.--Void at Chamfer Corner of Specimen 3604--MOR = 75.8 ksi;
Density = 3.22 g/cc (Room Temperature).

TABLE 14

MOR AND WEIBULL SLOPES OF TREATMENT CONDITIONS

Condition	All Specimens			Exclude Specimens with Inclusions		
	Mean MOR, ksi	Characteristic MOR, ksi	Weibull Slope	Mean MOR, ksi	Characteristic MOR, ksi	Weibull Slope
1	82.9	89.0	6.6	82.4	88.5	6.6
ab	97.3	101.2	13.2	96.9	100.8	13.2
ac	95.4	99.7	12.4	95.0	99.2	12.0
ad	89.3	93.5	11.3	89.1	93.4	10.9
ae	91.6	96.5	9.6	92.0	97.0	9.6
bc	92.0	98.0	7.5	92.9	99.9	6.4
bd	76.2	79.4	12.4	76.5	79.8	12.5
be	92.2	96.9	10.0	91.3	96.1	9.7
cd	74.7	81.0	5.5	84.0	87.9	11.2
ce	85.7	91.2	7.7	85.4	91.3	7.2
de	82.8	89.4	6.3	84.5	91.1	6.6
abcd	85.0	89.0	11.0	86.8	90.7	11.8
abce	95.4	99.3	12.9	95.5	99.1	14.3
abde	84.9	87.3	19.1	84.8	87.3	19.1
acde	79.0	86.1	5.1	89.7	93.8	11.4
bcde	77.7	81.9	9.5	79.4	83.5	10.1

a powder bed. The treatment that yielded the highest Weibull slope (19.1) is condition "abde" but the average MOR is only 84.9 ksi. The average MOR of the specimens is also plotted in figure 17, in descending order of MOR. The graph also shows the variations in MOR between sintering runs. Detail analysis including the variations will be discussed later.

The analysis of variance was used to determine the factors or multifactor interactions that affected the MOR values. The processing factors that have statistically significant effects (at 95 percent confidence level) were A (sinter/HIP cycle), B (powder bed), and D (sintering aid), and the two-factor interactions B*C, B*D, and C*D. The factor E, binder content, is the only insignificant factor in the determination of MOR. The significant factors and two-factor interactions and their corresponding probabilities are listed in table 15. The change in MOR between different levels of the processing factors and two factor interactions are listed in tables 16 through 19.

In view of the fractographic analysis results concerning the dark inclusions that reduce the MOR, statistical analysis was repeated after eliminating test data of specimens that failed from these inclusions. Overall, the previous statistical analysis results remain the same. The change in average MOR and Weibull slope is negligible except for conditions "cd" and "acde." The MOR and Weibull slope values are listed in table 14. The change in Weibull slope is also presented in figure 18. For condition "cd," there was an increase of 9.3 ksi in average MOR and 6.7 in Weibull slope after eliminating the specimens that failed from inclusions. For condition "acde," the increase was 10.7 ksi and 6.3 in Weibull slope. Both conditions include the 6 + 1 additive composition and extrusion.

The effect of sintering run variations is documented in table 20. Thirty-three specimens were tested in the A- and A+ condition. However, the effect of sintering time is confounded by the effect of sinter/HIP runs. It is impossible to separate the effect of sintering time from the effect due to the differences between runs. At each treatment condition, the mean and standard deviations were calculated for each run. For every treatment combination, the mean MOR of each run and the mean of both runs are plotted in figure 17 to show the variation between runs. The difference between runs was then computed and a t-test was used for testing the significance of the difference at 0.05 level (see table 21). Test results showed that under two treatment conditions (ab and ae) the differences in MOR between runs was significant. The differences range from 7.00 to 9.45 ksi. No consistent pattern of the MOR difference can be found for run 25 and run 26. However, for run 30 and run 32, a pattern was found. In general, bars sintered in run 32 have higher MOR values than bars sintered in run 30.

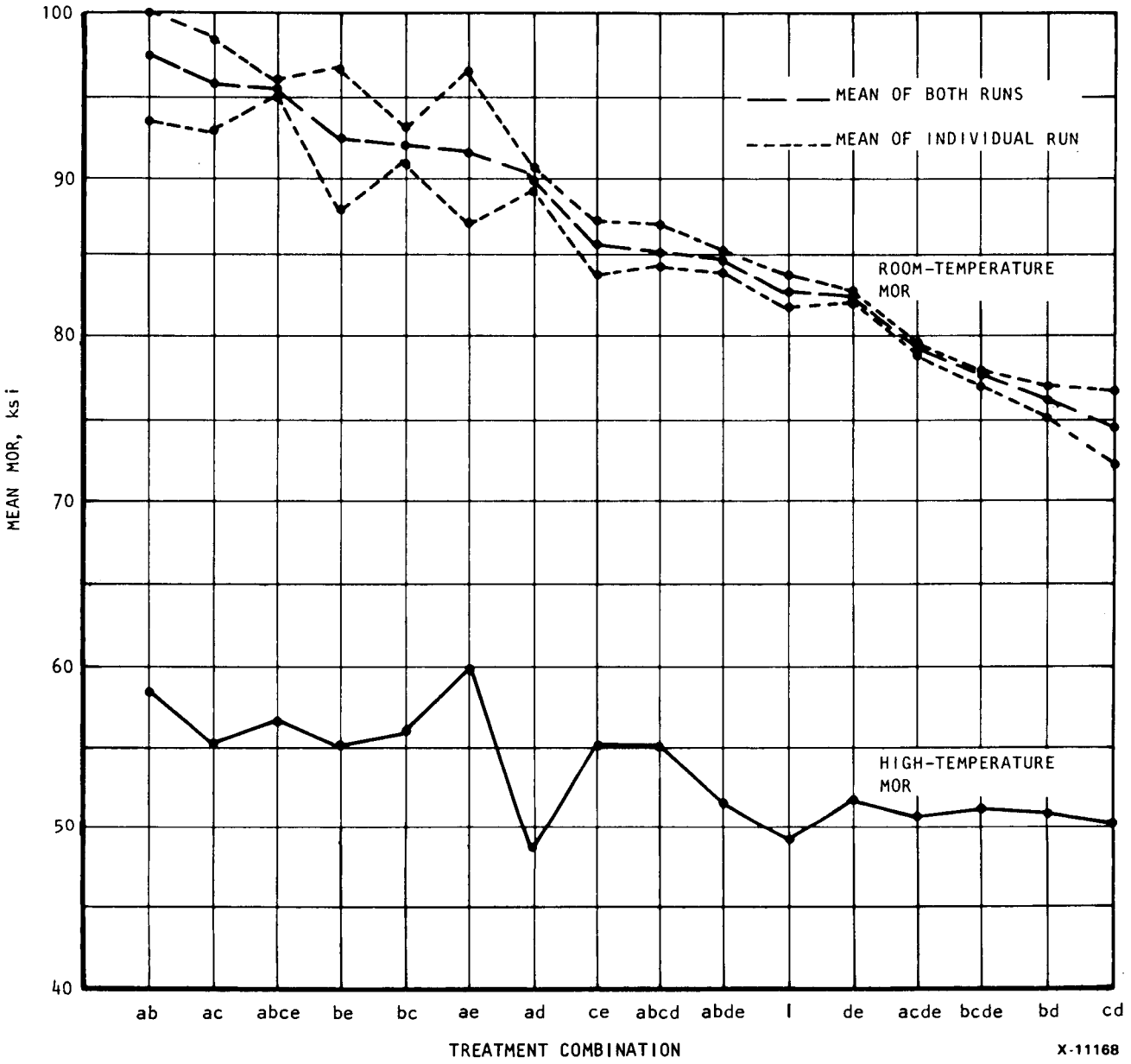

Figure 17.--Comparison of Mean MOR Between Runs.

TABLE 15

SIGNIFICANT FACTORS/INTERACTIONS AND CORRESPONDING PROBABILITY FOR ROOM TEMPERATURE MOR

Significant Factor/Interaction	Probability
A	0.0001*
B	0.0206
D	0.0001
B*C	0.0003
B*D	0.0044
C*D	0.0085

*Significant at 95 percent confidence level, if probability is less than 0.05.

TABLE 16

SUMMARY OF ROOM TEMPERATURE MOR CHANGE AT DIFFERENT LEVELS

Condition	Level	MOR, ksi
Sinter/HIP	A+	90.0
	A-	83.2
Powder bed	B+	87.7
	B-	85.3
Extrusion	C+	85.7
	C-	87.3
Sintering aid	D+	81.3
	D-	91.7
Binder content	E+	82.3
	E-	86.7

TABLE 17

EFFECT OF B*C ON MOR

	(B+) PB2	(B-) No PB
(C+) Extruded	87.7	83.9
(C-) Not Extruded	87.6	86.8

TABLE 18

EFFECT OF B*D ON MOR

	(D+) 6% + 1%	(D-) 6% + 2%
(B+) PB2	81.0	94.3
(B-) No PB	81.6	89.1

TABLE 19

EFFECT OF C*D ON MOR

	(C+) Extruded	(C-) Not extruded
(D+) 6%, 1%	79.2	83.4
(D-) 6%, 2%	92.3	91.1

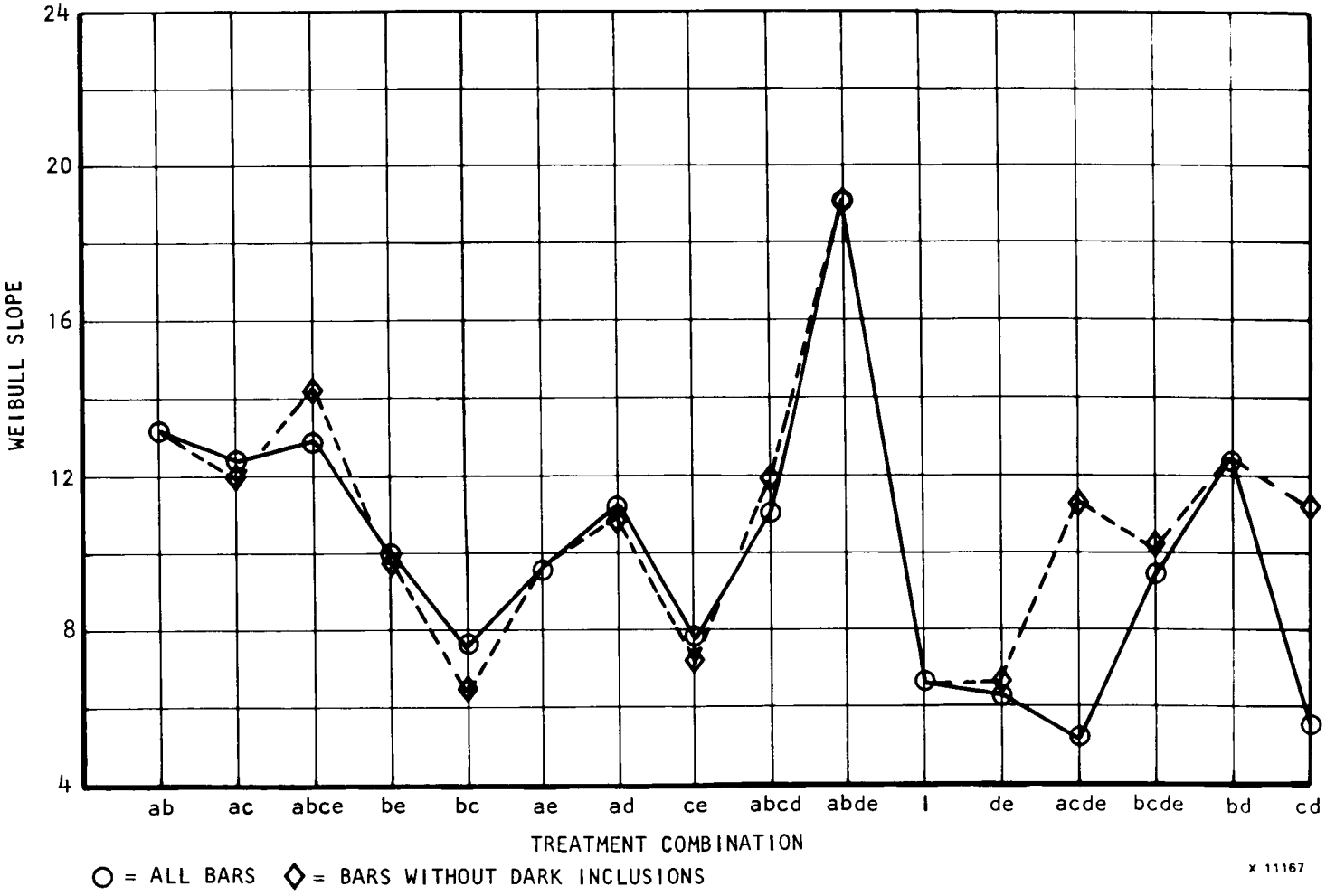

Figure 18.--Comparison of Weibull Slopes.

TABLE 20

MATRIX II-2 SINTER/HIP RUN VARIATION VS PROCESS CONDITIONS (BY MOR VALUE)

Cycle				A-				A+			
Sinter/HIP Run No.				25		26		30		32	
Presinter T, °C				1750		1750		1750		1830	
Sinter T_{max}, °C				1950		1950		1950		1950	
Time at T_{max}				1.11x*		x		2.22x		2.44x	
Percent additional load mass in furnace				50%		--		--		60%	
Powder Bed				B-	B+	B-	B+	B-	B+	B-	B+
D-	6+2	Non-extruded MOR, ksi	C-	1 82	be 97	1 84	be 88	ae 87	ab 95	ae 96	ab 100
	6+2	Extruded MOR, ksi	C+	ce 84	bc 93	ce 87	bc 91	ac 93	abce 95	ac 98	abce 96
D+	6+2	Non-extruded MOR, ksi	C-	de 83	bd 77	de 83	bd 76	ad 88	abde 84	ad 90	abde 86
	6+2	Extruded MOR, ksi	C+	cd 73	bcde 78	cd 77	bcde 78	acde 79	abcd 86	acde 79	abcd 84

*x is time at T_{max} for run 2, two hours.

TABLE 21

MATRIX II-2 DENKA 9FW STUDY OF THE SINTER/HIP RUN EFFECT ON ROOM-TEMPERATURE MOR DATA (RUN 30 VS RUN 32)

Treatment Combination	Mean		Std. Dev.		D
	Run 30	Run 32	Run 30	Run 32	
ae	87.0	96.4	11.1	7.0	9.5*
ad	88.8	90.1	10.5	5.9	1.3
ac	93.1	98.3	7.9	9.2	5.1
acde	79.3	78.9	18.5	15.1	-0.1
ab	93.9	100.9	9.2	6.1	7.0*
abde	84.4	85.5	5.7	4.5	1.1
abce	95.1	95.8	9.5	7.5	0.7
abcd	86.4	83.9	7.8	9.7	-2.5

D = mean MOR (run 32) - mean MOR (run 30)

*An asterisk indicates the difference in mean MOR between runs is significant at $\alpha = 0.05$.

Further analysis was undertaken to check the validity of the best processing condition, including both 6 + 2 and 6 + 1 compositions. Four data sets were formed by combining data from different runs. The first data set consisted of data of run 25 and run 30, the second data set of run 25 and run 32, the third set of run 26 and run 30, and the fourth data set of run 26 and run 32. For each data set, the significant factors on the determination of MOR were identified and the results are summarized in table 22, along with results from previous analyses in which data of all four runs were used. Common significant factors for all analyses are factor A, sintering/HIP cycles, and factor D, sintering aids.

Table 23 shows the mean MOR of each factor at both the "+" and "-" levels for each analysis from all four data sets. These mean values are also presented in figure 19 to show the importance of factors on MOR, based on the statistical results. For each factor, four sets of points are plotted. Each pair of points represent the mean MOR obtained from a set of data, one point represents the "+" level, the other point

TABLE 22

MATRIX II-2 DENKA 9FW--SUMMARY OF ANALYSIS OF VARIANCES AND SIGNIFICANT FACTORS FOUND IN EACH ANALYSIS

Data Source	Significant Factors						
Runs 25 and 30	A	B		D	A*E[1]	B*D	C*D
Runs 25 and 32	A	B	C	D	A*E	B*D	C*E
Runs 26 and 30	A			D	A*E		C*D
Runs 26 and 32	A			D	A*E		C*D
Runs 25, 26, 30, and 32	A	B		D	B*C	B*D	C*D
Common factors for all sets	A, D, A*E						

Note: 1. A*E = B*C*D

TABLE 23

TASK II-2 DENKA 9FW--SUMMARY TABLE
MEAN MOR FOR "+" AND "-" LEVEL OF EACH FACTOR

Factor	Data Set 1 Runs 25, 30	Data Set 2 Runs 25, 32	Data Set 3 Runs 26, 30	Data Set 4 Runs 26, 32
A-	83.3	83.3	83.0	83.0
A+	88.4	91.2	88.4	91.2
B-	83.8	85.7	84.9	86.9
B+	87.8	88.7	86.5	87.5
C-	86.5	89.0	85.4	88.0
C+	85.2	85.5	86.0	86.4
D-	90.6	93.4	89.9	92.7
D+	81.1	81.1	81.5	81.5
E-	85.8	87.2	86.1	87.6
E+	85.8	87.2	85.3	86.7

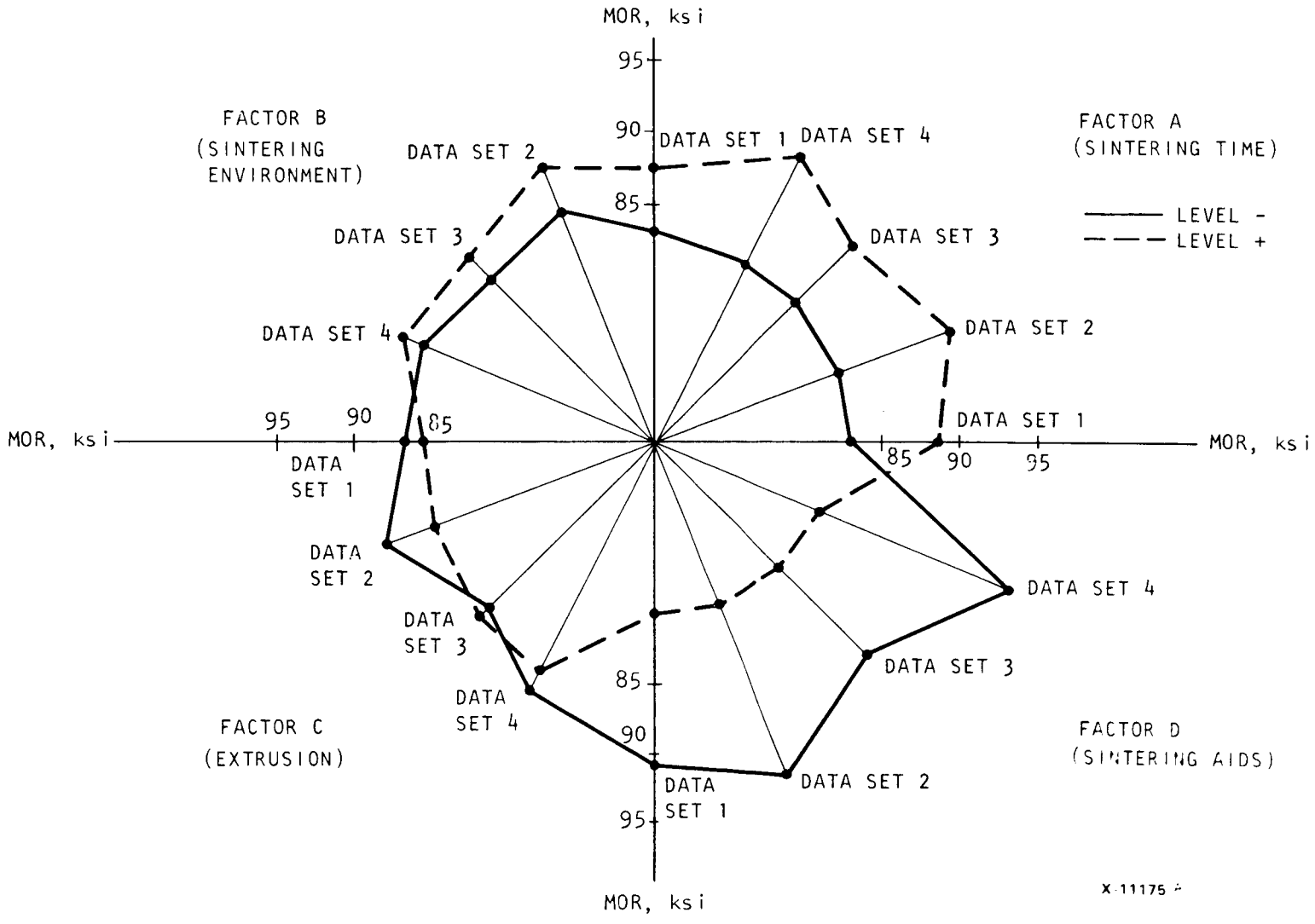

Figure 19.--Matrix II-2 Denka 9FW Comparison of Low-Level vs High-Level Treatment.

represents the "-" level. The distance between the "+" level and the "-" level of every pair of points represents the effect of a factor when its level is changing from one to the other. The distances between the "+" and the "-" level for factors A and D are larger than that for factors B and C, indicating factors A and D are more important. A pattern is also noticed: that the combination of A+, B+, C-, and D- (ab treatment) results in a higher MOR than the combination of A-, B-, C+, and D+ (see figure 20).

Statistical analysis of high temperature MOR: Only 64 high-temperature (2250°F) MOR values were available for statistical analysis. Significant factors found in the analysis are factor D and two-factor interaction B*E (see table 24). It was found that using the 6% Y_2O_3 + 2% Al_2O_3 sintering aid would lead to a higher MOR (2250°F) than the other sintering aid. This is believed to be due mainly to the higher densities achieved in the 6% Y_2O_3 + 2% Al_2O_3 test bars. It was also found that with 15.5 percent binder content, bars processed with powder bed had a higher MOR than those processed without powder bed.

Task II modifications.--The promising results produced in the first iteration by treatments "ab" and "abde" in Matrix II-2 suggested that the program goal (96 ksi and 16 Weibull) could be exceeded in the second iteration without any problem. As a result, ACC/GTEC were directed by NASA to modify the original Task II plan.

A new program plan with more aggressive goals was submitted by ACC/GTEC (Appendix A) and approved by NASA. Statistically designed experiments were developed for Subtask A, High Weibull/Reproducibility; and Subtask B, High Temperature Materials. The following paragraphs discuss the efforts to date on these subtasks.

Subtask (A) high Weibull/reproducibility.--A 2^3 full factional experiment (see table 25) was designed to use processing identical to that of "ab" in Matrix II-2 for the three variables: Arburg versus Battenfeld injection molders, separated material process days using powder from the same lot, and separate but identical sinter/HIP runs.

A minimum of 240 test specimens (30 for each process combination) was required for MOR testing. The process will be considered reproducible if the following criteria are met for the 30 test specimens evaluated from each sintering run:

(a) Average density 3.08 to 3.20 g/cc

(b) Average MOR 93 to 101 ksi

The required number of test bars has been processed through sinter/HIP. In consideration of furnace reliability, the peak sintering temperature was lowered from 1950° to 1900°C. In order to achieve densities equal to or higher than that of the original "ab" test bars, the holding

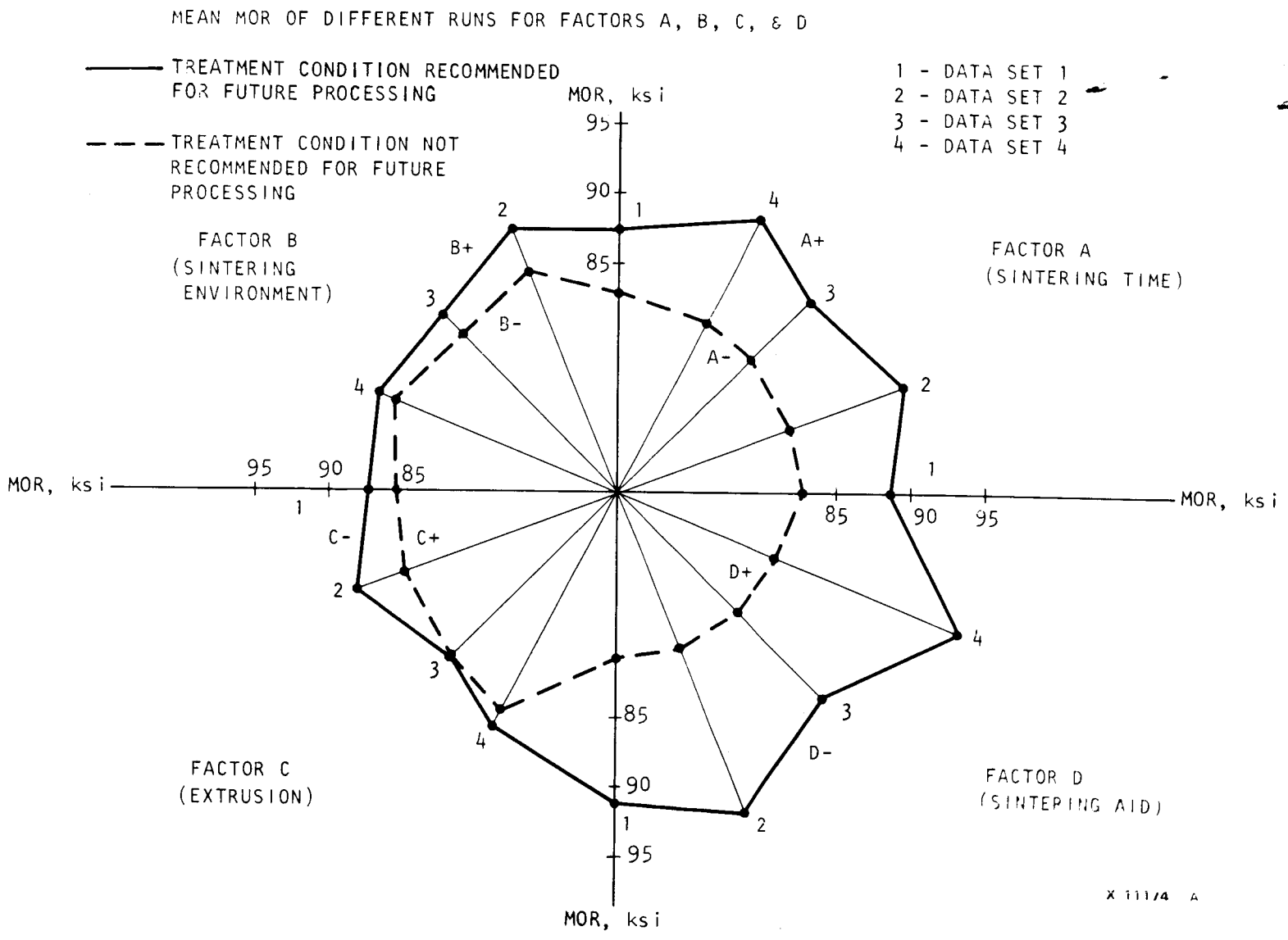

Figure 20.--Matrix II-2 Denka 9FW--Comparison of Recommended Processing Condition vs Not Recommended Ones; Mean MOR of Different Runs for Factors A, B, C, and D.

TABLE 24

HIGH-TEMPERATURE TEST FOR MOR

Significant Factor/Interaction	Probability
D	0.0003
B*E	0.0172

	Effect of Factor D on MOR Sintering Aid (D)	
	(D+) 6% + 1%	(D-) 6% + 2%
Mean MOR	51A ksi	55.8 ksi

Difference = 4.5 ksi

	Effect of B*E on MOR	
	(E+) 14.5%	(E-) 15.5%
PB2 (B+)	53.6 ksi	55.6 ksi
No PB (B-)	54.4 ksi	50.8 ksi

PB = Powder Bed

TABLE 25

FACTORIAL DESIGN FOR REPRODUCIBILITY STUDY

Process Day	Sintering Run	Injection Molder	
		I+	I-
G+	H+	ghi	gh
	H-	gi	g
G-	H+	hi	h
	H-	i	1

G = Material processing day -
First processing day (G+)
Second processing day (G-)
H = Sintering run -
First run (H+)
Second run (H-)
I = Injection molder -
Arburg (I+)
Battenfeld (I-)

time at the peak temperature was increased by 2 hr. The measured densities of the sintered test bars from these two runs (3.25 to 3.28 g/cc) were found to be higher than the earlier "ab" (3.10 to 3.26 g/cc). Characterization and statistical analysis are in progress.

Subtask (B) high-temperature materials.--Ten sintering aid compositions (five binary compositions and five ternary compositions) have been formulated using Y_2O_3, ZrO_2, SrO, CeO_2, and MgO (see table 26).

Six additional compositions (see table 27) have been formulated using Y_2O_3 and Al_2O_3 as the sintering aids. The emphasis in this portion of the program is to optimize the Y_2O_3/Al_2O_3 sintering aid system.

A three-stage screening evaluation will be conducted (see Appendix A). In the first stage, cold isostatically pressed (CIP) samples will be encapsulated in niobium cans then hot isostatically pressed to high density. This is the most effective method to produce high density samples. Samples with high densities (densities ≥95% theoretical) will be evaluated for high-temperature properties. The focus of the second stage is to develop sinter/HIP cycles without encapsulation for those compositions passing the first stage screening. Finally, in the

TABLE 26

HIGH-TEMPERATURE COMPOSITIONS
COMPONENT PERCENT BY WEIGHT

Mix	Si_3N_4	Y_2O_3	SrO*	ZrO_2**	MgO	CeO_2
1	90	8	2			
2	93	4		3		
3	94	5.5			0.5	
4	93	5				2
5	93	6			1	
6	93	3	2	2		
7	93	5	1.5		0.5	
8	93	4.5			0.5	2
9	93	3		3		1
10	93	1		3		3

*Starting material is $SrCO_3$
**Stabilized Zirconia with 12% Y_2O_3

TABLE 27

HIGH-TEMPERATURE COMPOSITIONS
COMPONENT PERCENT BY WEIGHT

Mix	Si_3N_4	Y_2O_3	Al_2O_3
NSHT-11	94	6	0
NSHT-12	94	5	1
NSHT-13	94	4	2
NSHT-14	93	6	1
NSHT-15	93	5.5	1.5
NSHT-16	93	5	2

third stage, the most promising compositions will be fabricated into test bars for the standard room- and high-temperature MOR characterization.

All sixteen billets in the first iteration have been encapsulated in niobium cans (approximately 2 in. dia x 3 in. height) by electron beam welding after being outgased at approximately 1000°C in vacuum. Hot isostatic pressing of these cans was to be carried out at 1900°C at 25 ksi for 4 hr. Due to the malfunctioning of the HIP unit at ACC, HIP'ing of these cans has been delayed.

Subtask (C) net shape component fabrication evaluation.--The 6 + 2 composition was selected for this evaluation. The new Battenfeld molder has a larger capacity than that of the Arburg molder and is equipped with microprocess controls. This new molder is being used in this scale-up study. Standard batches of material ("ab" treatment) were prepared through mixing. An optimized test bar injection molding parameter was established on the new molder. The optimized test bar molding parameters were applied to molding T-25 rotor turbochargers. If defective T-25 rotors result, a systematic variation of molding parameters would be conducted to improve the rotor quality.

The rotors injected with the test bar molding parameters were mostly defective and this was considered as the first iteration. The second and third iterations of injection-molded rotors have been completed. The process parameters for these three iterations are presented in table 28. After each iteration, several test runs with one process parameter modified each time were performed to study the effect of process variations. Based on the results of these test runs, a new set of parameters is then selected for the next iteration of injection molding to achieve quality improvement. Figure 21 shows the nomenclature used for designation of location on the rotor.

After each iteration, a thorough visual inspection of the rotors was performed. Results of the first iteration, as shown in figure 22, indicated that time-dependent injection follow-up allowed material overpacking in the mold, which caused stress crack at the exducer areas. In addition, the material injected for each rotor may have nonuniform viscosity because of the 40°F temperature gradient between the nozzle and Zone 1. This problem may cause various defects, such as knit lines and cracks.

During the second iteration, stroke-dependent injection follow-up was selected, and the Zone 1 temperature was raised to the nozzle temperature. Rotors with fewer exducer cracks were produced. However, other major defects, such as unfilled blade, severe pull-out, and broken blade (see figure 23) still existed.

After five test runs, injection speed, injection pressure, material temperature, amount of mold release, and cooling rate were found to be critical to the quality of the rotors. A new set of process parameters

TABLE 28

INJECTION MOLDING PROCESS PARAMETERS

Process Parameters	Iteration No.		
	1	2	3
Temp (nozzle)	220°F	220°F	200°F
Temp (Zone 1)	180°F	220°F	200°F
Temp (Zone 2)	150°F	173°F	172°F
Temp (Zone 3)	150°F	150°F	150°F
Temp (mold)	98°F	100°F	94°F
Injection pressure	100 psi	100 psi	460 psi
Follow-up pressure	100 psi	100 psi	60 psi
Injection speed	7% on all five speed zones	7% on all five speed zones	100% full speed on all five zones
Time- or stroke-dependent	Time	Stroke	Stroke

NOTE: Nylon sprue and more mold-release lubrication were used for all iterations.

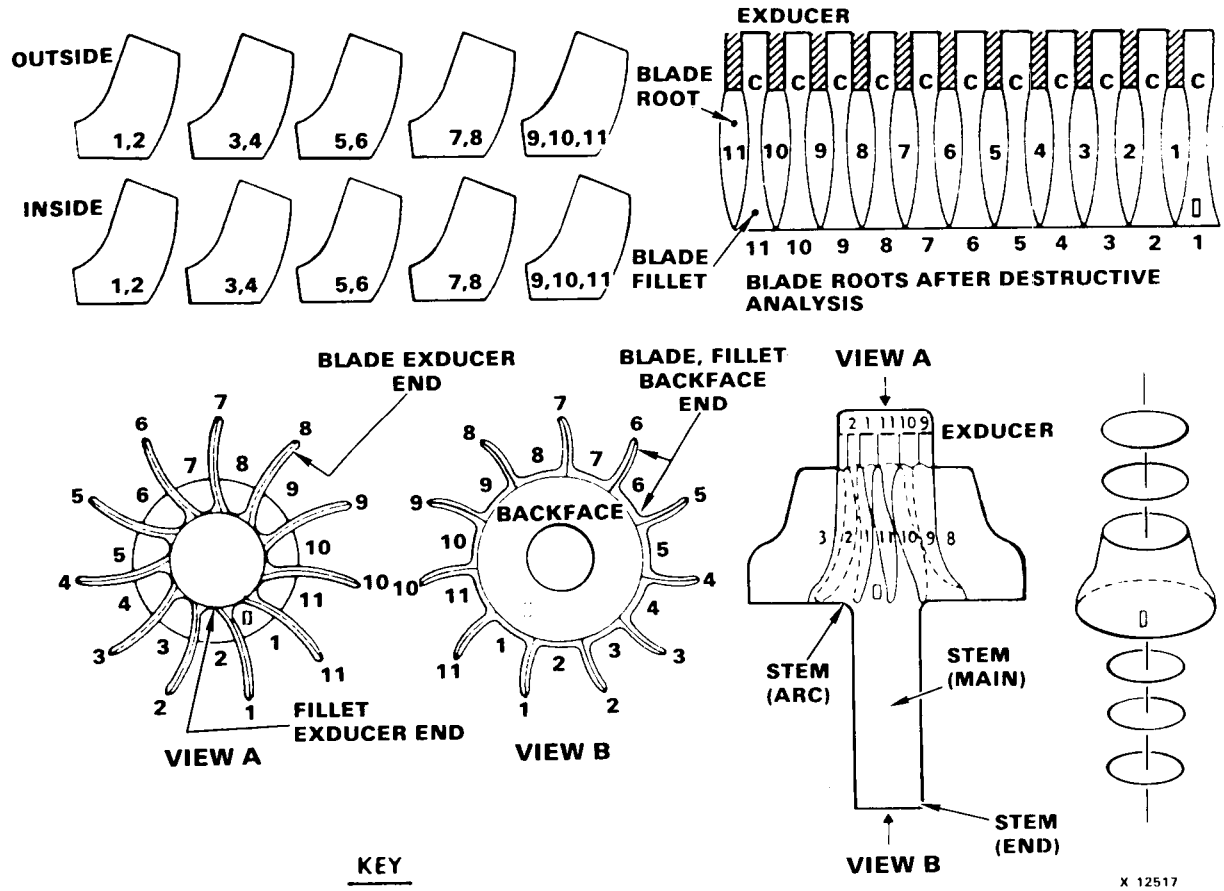

NOTE: The rotor is divided into 11 segments, as shown above, which includes an area along the length of the rotor from the exducer through the end of the stem.

Figure 21.--Nomenclature Used for Designation or Other Number of Location on Rotor.

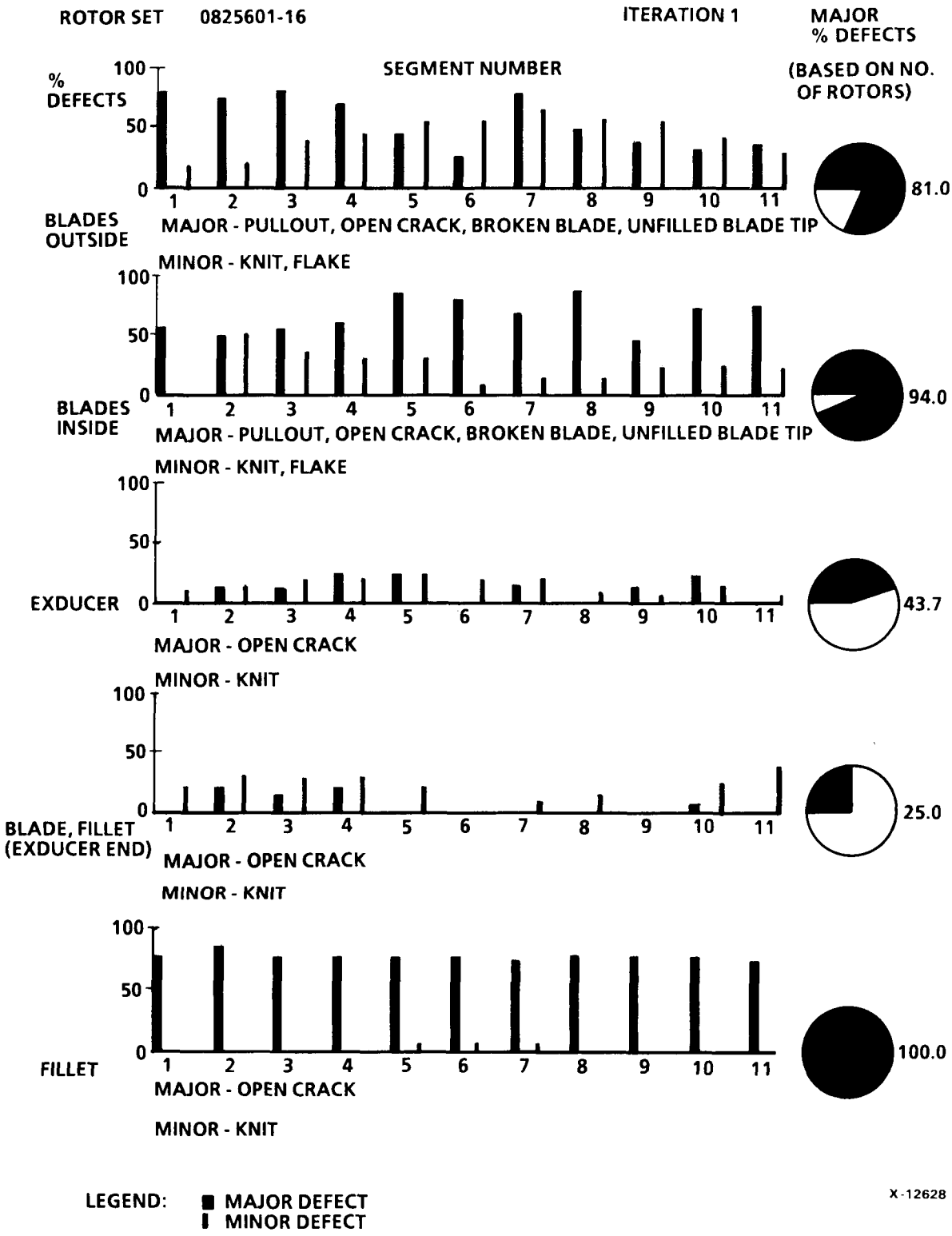

Figure 22.--Summary of Visual Inspection of 16 As-Injected Rotors in Iteration 1.

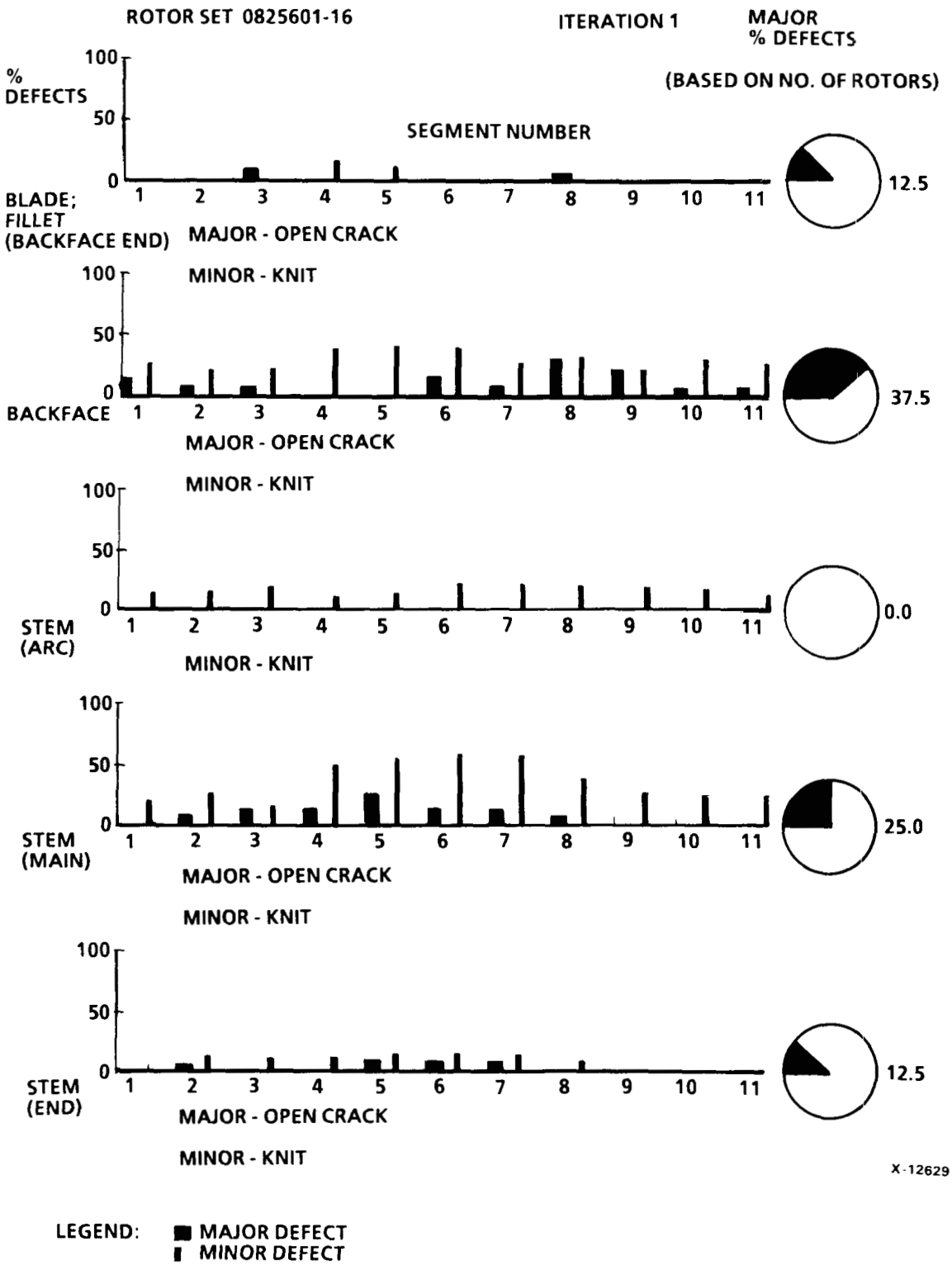

Figure 22.--Continued

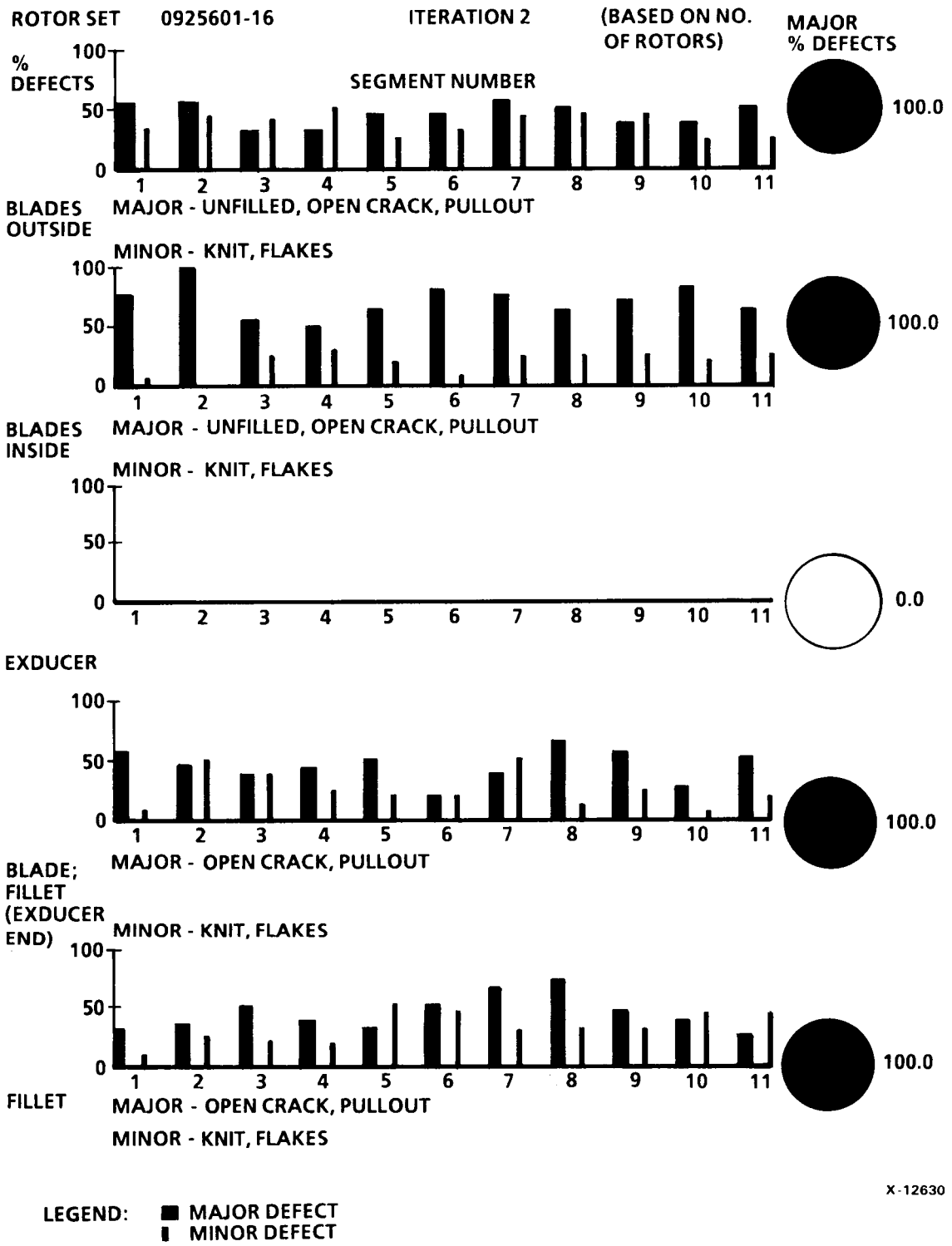

Figure 23.--Summary of Visual Inspection of 16 As-Injected Rotors in Iteration 2.

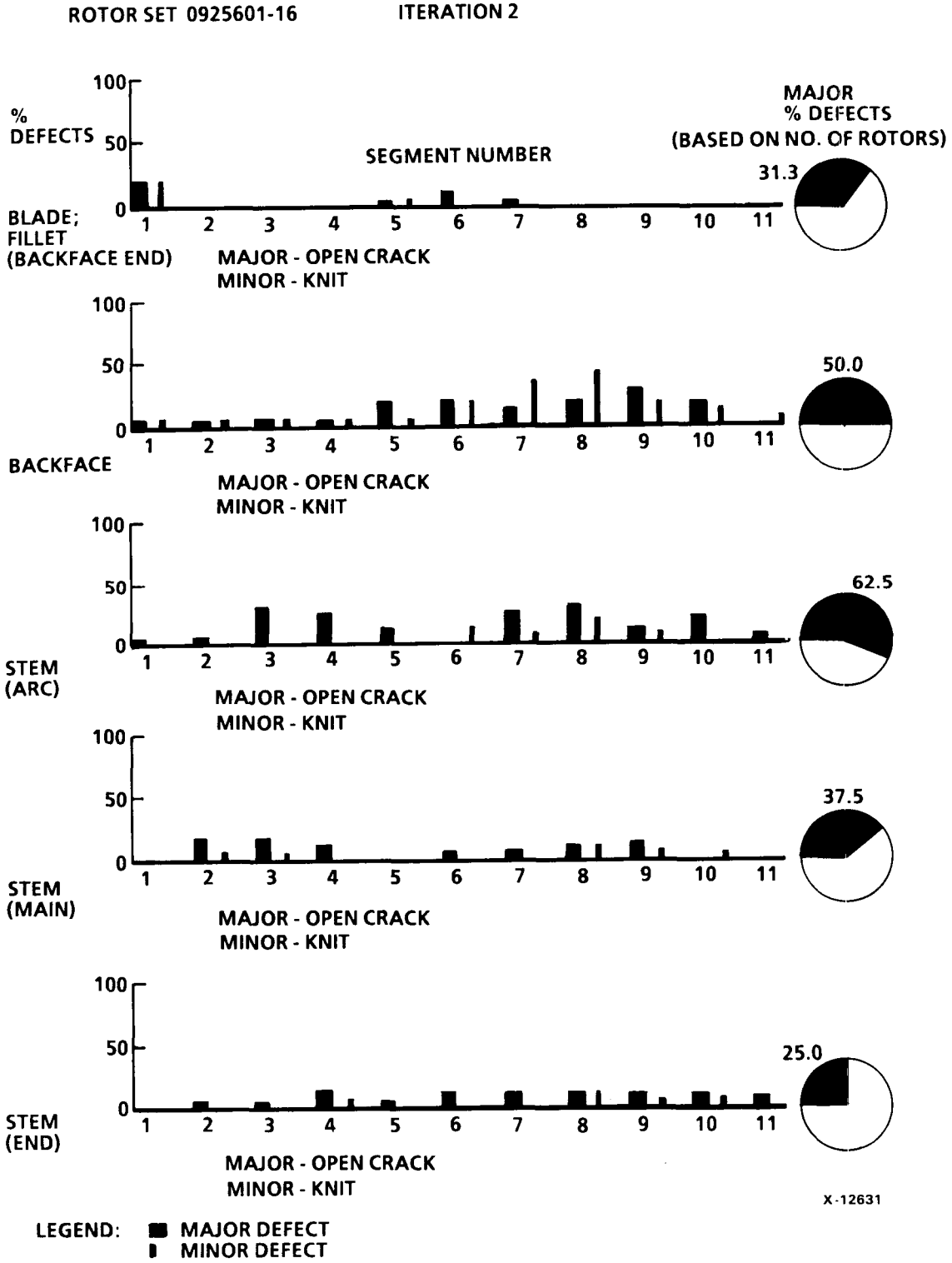

Figure 23.--Continued

for Iteration 3 was established. Higher injection speed (100 percent of maximum machine speed) and pressure (460 psi) were used to obtain better mold filling and to reduce knit line and unfilled blade. The cooling rate was controlled by replacing the metal sprue with a nylon sprue and by adjusting the mold temperature. A lower cooling rate after injection resulted in less thermal stress and cracking. More mold release lubricant was applied to the mold to reduce pull-out. Significant quality improvement in Iteration 3 rotors was achieved. The summary of inspection is presented in figure 24.

Methods of obtaining further improvement are being investigated to address the remaining knit-line defect and the open crack as well as flash and associated broken blade problems.

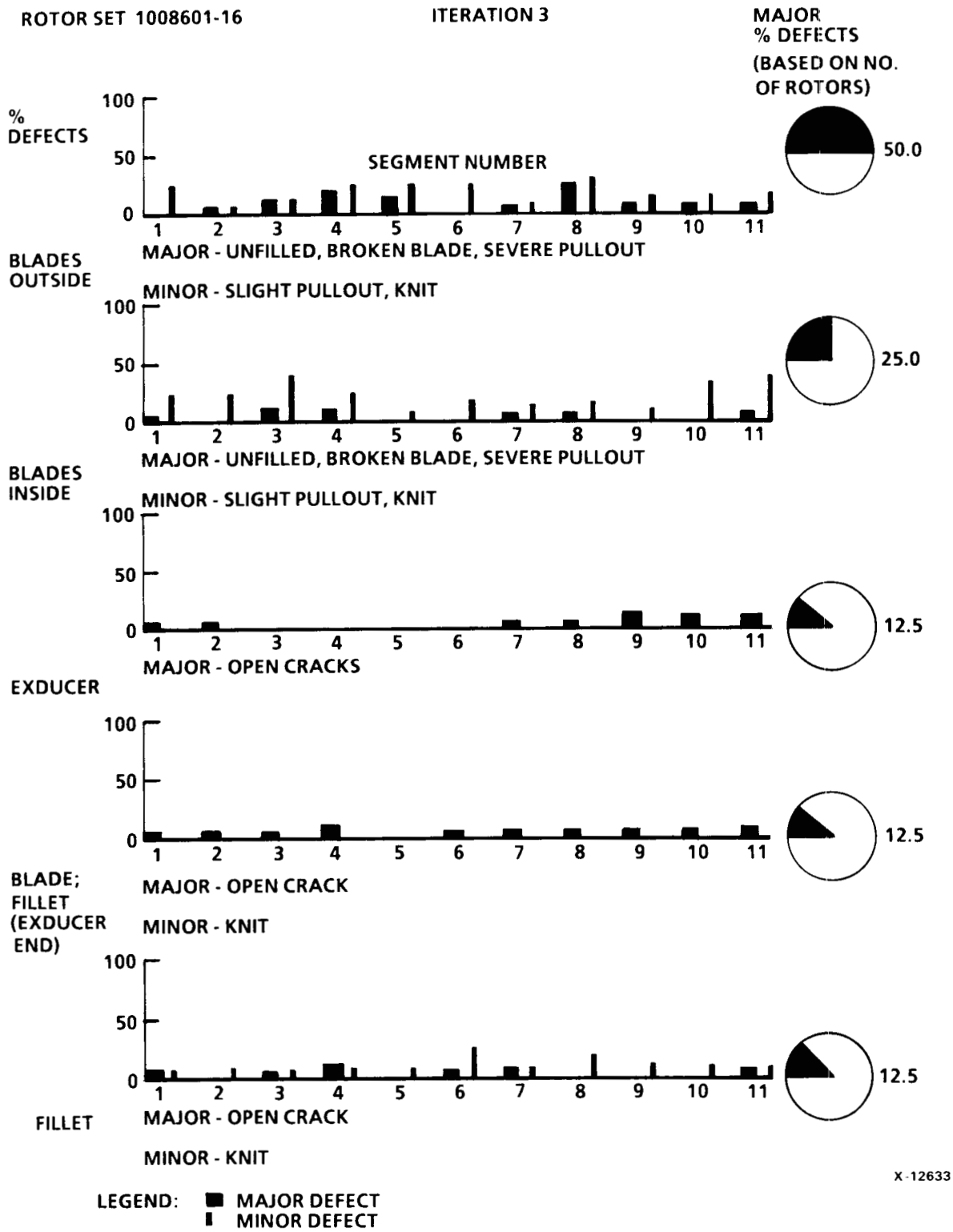

Figure 24.--Summary of Visual Inspection of 16 As-Injected Rotors in Iteration 3.

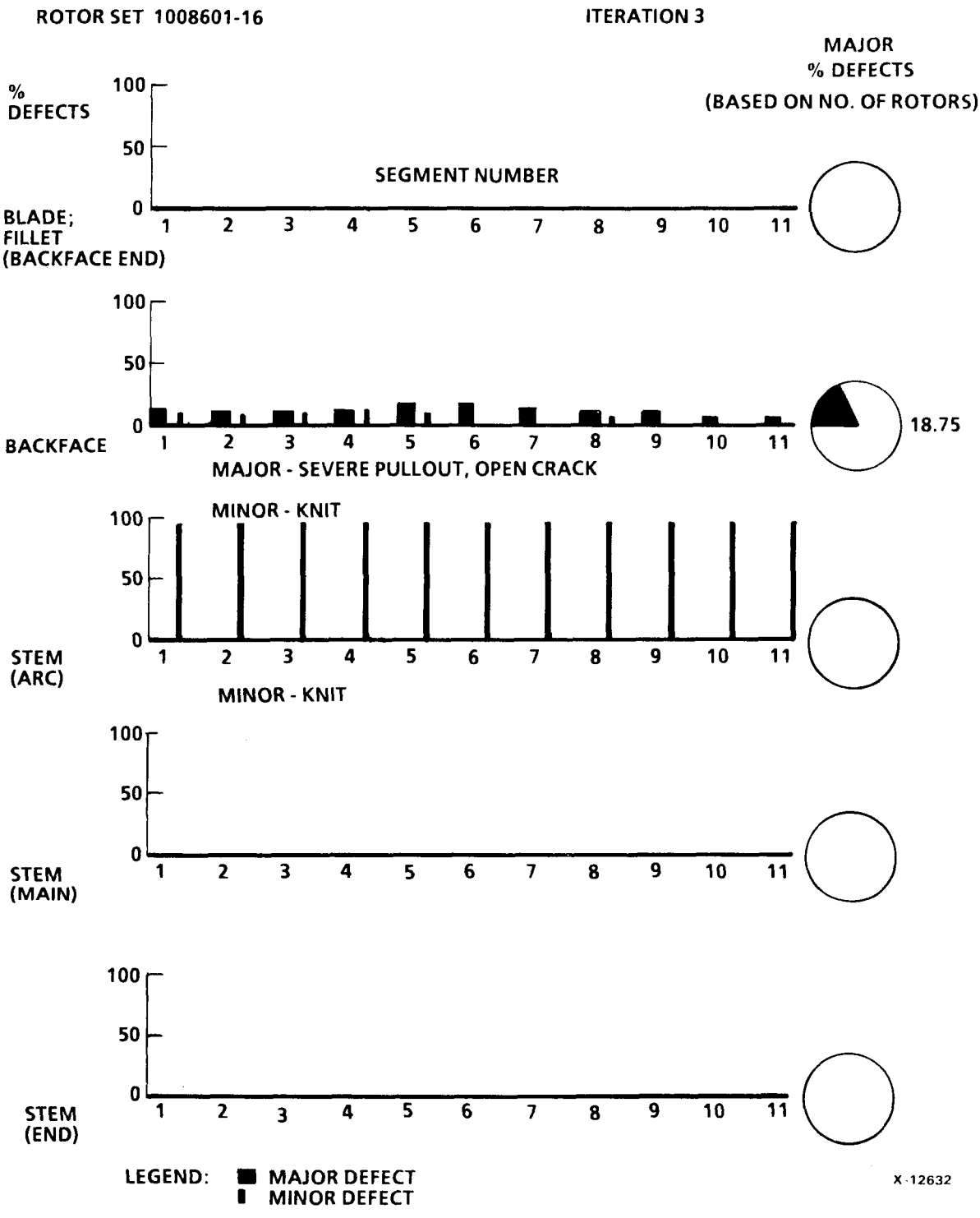

Figure 24.--Continued

Task VII - Advanced Materials and Processing

The purpose of this task is to explore new concepts in processing, to investigate the impact of major processing parameters on material properties, and to study the interactions between processing parameters. This task is cost shared by ACC. The following major parameters were selected for evaluation: alternate raw materials (Si_3N_4), alternate binder systems, binder extraction cycles, injection molding parameters, alternate powder preparation, additive compositions (sintering aids), and sintering cycles.

The evaluations were conducted iteratively. Two or more processing parameters were investigated in an experimental matrix to determine possible interactions between those parameters. Prior experience was used to guide the selections of parameters included in a particular matrix. Additional investigations were also conducted to provide data to guide process improvements.

Table 29 shows the parameters chosen for evaluation and the combinations of these parameters in Matrixes 1 through 11. The results of Matrixes 1 through 5 and 7 were reported in the last annual report. The analysis of the results of Matrixes 6, 8, 9, 10, and 11 are reported in the following text.

TABLE 29

RELATIONSHIP BETWEEN PROCESS EVALUATION SUBTASKS AND EXPERIMENTAL MATRIXES

	Experimental Matrix Number										
	1	2	3	4	5	6	7	8	9	10	11
Raw material	X				X	X					
Binder (chemistry and content)		X			X	X	X			X	X
Binder extraction			X			X	X				
Injection molding			X			X			X		
Powder preparation			X		X				X		X
Composition				X					X		
Sintering cycle	X			X		X		X			

Matrix 6 - raw materials, molding, and thermal processing.--Matrix 6 was designed to provide a range of processing conditions in order to evaluate Si_3N_4 raw material (M1, M4, M5, and M6)* and milling aids (MA1 and MA2). A statistically designed experiment was planned to include five variables: Si_3N_4 powder, milling aid, molding temperature, binder removal cycle, and sintering cycle. The original form of Matrix 6 is shown in figure 25.

Modifications were required after recognizing the sintering temperature required for densification was similar for M1 and M6 and similar for M4 and M5 but very different for the two pairs; therefore, the matrix was divided into two submatrixes. The configuration of the submatrixes was reduced by the elimination of M5/MA2 and M6/MA2, and the revised matrix is shown in figure 26.

Characterization: The MOR results are summarized in tables 30 and 31. Due to the difference in treatment conditions of groups M1 and M6, and M4 and M5, the fractography results will be discussed separately. For specimens from the M1 and M6 sections of Matrix 6, optical fractography showed that the higher strength specimens generally failed from the tensile surface without any observable flaws at the fracture origins. Most of the low-strength test specimen failures originated from distinct existing flaws. The majority of the flaws observed were cracks, both surface and internal, inclusions, and voids.

Dark inclusions were found at the fracture origins of some low-strength specimens in treatment combination groups M1MA1 and M6MA0, which have high average MOR. SEM and EDX analysis were carried out on specimens from these two groups and found that the inclusions contained Fe and a trace of Cr. Large grains (10 to 20 microns) were also readily observed on the fracture surfaces on M6 specimens, probably due to exaggerated grain growth. SEM micrographs of such inclusions in two specimens and their respective EDX plots are shown in figures 27 through 29.

In section M4, a higher proportion of specimens failed from internal flaws, mainly voids and cracks. Most of the fractured specimens showed a dark internal core or a lighter colored skin, depending on the extent of the core. Specimens from the M4 section with MA0 and MA1 milling aid/time parameters did not show dark cores. No correlation between MOR and core presence was found. The average MOR of all the M4 specimens was 64.6 ksi, but ranged from 20.8 to 89.3 ksi. The majority of the internal flaws were voids and the SEM micrographs of two low MOR (20.8 and 39.0 ksi) specimens are shown in figures 30a through 30d and 31a through 31d.

The average MOR of the M5 specimens was higher and less specimens (23 percent) failed from internal flaws. Less voids were observed, in agreement with the higher density.

*M1 = GTE SN 502 Si_3N_4 + 6% Y_2O_3 + 2% Al_2O_3; M4 = Starck H-1 Si_3N_4 + 6% Y_2O_3 + 2% Al_2O_3; M5 = Starck LC -1 Si_3N_4 + 6% Y_2O_3 + 2% Al_2O_3; M6 = KemaNord P95M Si_3N_4 + 6% Y_2O_3 + 2% Al_2O_3.

1/2 REPLICA OF A 3 x 2 x 2 x 2 x 4 DESIGN
TEST THE BLOCKS WITH SHADING ONLY

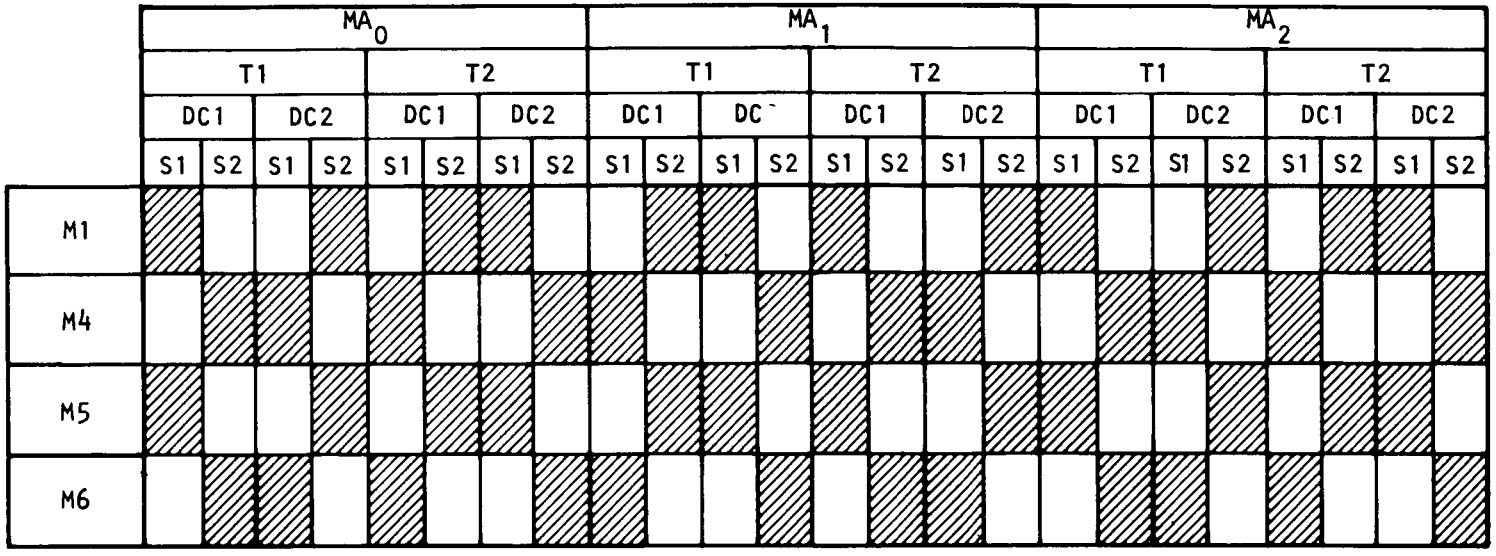

M: RAW MATERIAL (VARIABLE A)
MA: MILLING AID (VARIABLE B)
T: MATERIAL TEMPERATURE (VARIABLE C)
DC: DEWAX CYCLE (VARIABLE D)
S: SINTERING CYCLE (VARIABLE E)

EVALUATE: { MAIN EFFECTS: A, B, C, D, E
INTERACTIONS: AB, AC, BC, AD, BD, AE, BE, ABE, ABC

OTHER INTERACTIONS ASSUMED TO BE NEGLECTABLE

A-79491

Figure 25.--Matrix 6 (Material, Molding Temperature, Dewax Cycle, Milling Aid, and Sintering Cycle).

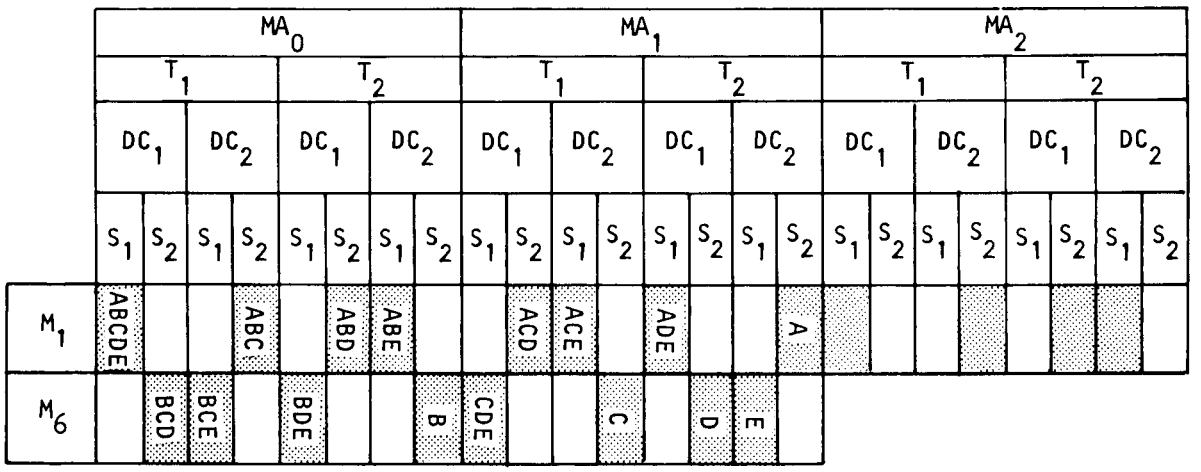

a. M1 AND M6

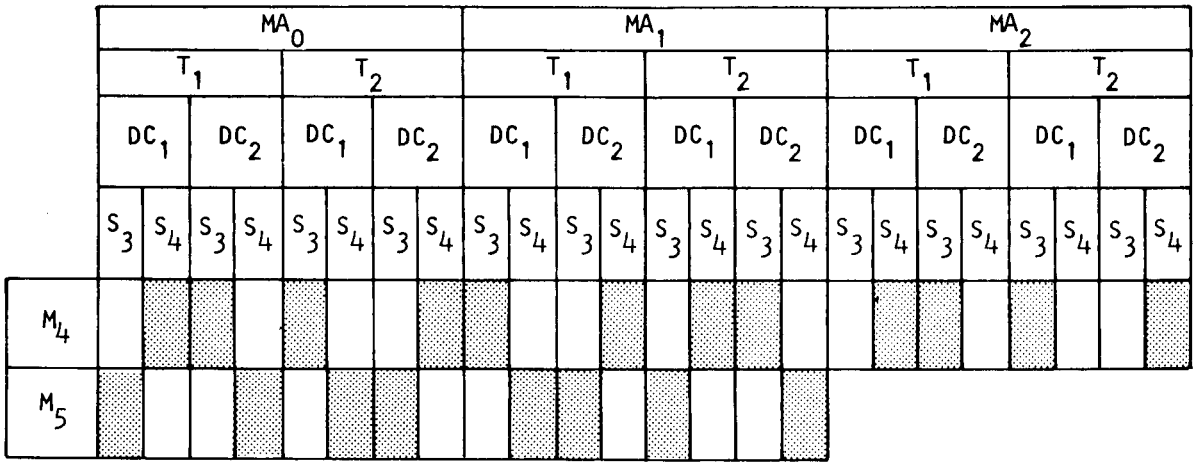

b. M4 AND M5

NOTES:

1. M = Si_3N_4
2. MA = MILLING AID
3. T = MOLDING TEMPERATURE
4. DC = DEWAX CYCLE
5. S = SINTERING CYCLE

A-87181

Figure 26.--Matrix 6 Submatrixes; Shaded Areas to be Performed.

TABLE 30

MATRIX 6-1 (MOR ksi)

	MA_0								MA_1								MA_2							
	T1				T2				T1				T2				T1				T2			
	DC1		DC2		DC1		DC2		DC1		DC2		DC1		DC2		DC1		DC2		DC1		DC2	
	S1	S2	S1	S2	S1	S2	S1	S2	S1	S2	S1	S2	S1	S2	S1	S2	S1	S2	S1	S2	S1	S2	S1	S2
M1	86.3			84.7		72.6	85.6			85.0	64.4		84.4			92.6				86.3		83.7	81.6	
	85.1			75.0		77.1	88.3			94.0	84.5		89.8			87.0	83.1			73.7		79.1	85.4	
	64.1			89.4		78.1	81.9			78.4	86.3		85.5			92.8	73.5			85.6		86.2	63.7	
	84.7			91.3		61.2	90.0			80.1	84.0		94.0			90.4	79.6			77.0		85.6	79.8	
	83.6			78.6		79.0	79.8				63.1		94.8			97.4	80.2			86.4		75.3	88.0	
	83.3			78.9		81.8	87.6									96.4	86.9			86.1		80.5	91.4	
																	85.2			81.5				
																	81.6			78.9				
																	82.4							
	$\bar{x}$ =			$\bar{x}$ =		$\bar{x}$ =	$\bar{x}$ =			$\bar{x}$ =	$\bar{x}$ =		$\bar{x}$ =			$\bar{x}$ =	$\bar{x}$ =			$\bar{x}$ =		$\bar{x}$ =	$\bar{x}$ =	
	81.18			82.65		74.96	85.53			84.37	76.46		89.7			92.76	81.56			81.94		81.73	81.65	
M6		*32.7	66.6		82.1			96.3	81.6			85.7		81.5	33.4									
		86.7	84.3		102.0			93.9	79.5			78.5		69.3	35.2									
		61.5	95.6		87.3			84.5	62.7			90.7		91.7	36.5									
		97.8	99.1		97.2			92.3	88.9			85.2		*57.2	32.8									
		91.7	89.7		95.6			94.1	79.6			88.1		83.6	30.2									
		65.1	92.2		77.8			96.9	82.2			73.2		76.2	30.6									
		65.4	87.1		96.1			90.0	81.7			82.7		86.4	29.8									
		80.1	60.1					88.3	80.9			*46.7		69.4	29.6									
		$\bar{x}$ =	$\bar{x}$ =		$\bar{x}$ =			$\bar{x}$ =	$\bar{x}$ =			$\bar{x}$ =		$\bar{x}$ =	$\bar{x}$ =									
		78.33	84.34		91.15			92.0	79.64			83.44		79.73	32.26									

*Test bar not included in the analysis.

TABLE 31

MATRIX 6-2, POWDERS M4, M5 (MOR)

	MA_0								MA_1								MA_2							
	T1				T2				T1				T2				T1				T2			
	DC1		DC2		DC1		DC2		DC1		DC2		DC1		DC2		DC1		DC2		DC1		DC2	
	S3	S4	S3	S4	S3	S4	S3	S4	S3	S4	S3	S4	S3	S4	S3	S4	S3	S4	S3	S4	S3	S4	S3	S4
M4		49.7 51.1 62.5 52.1 75.1 66.7 50.2 66.4 66.2 $\bar{x}$ = 60.0	67.3 58.7 62.4 56.9 66.9 58.3 51.8 51.3 49.2 $\bar{x}$ = 54.9		79.3 64.3 82.8 61.7 $\bar{x}$ = 72.0			65.3 73.6 89.3 70.9 $\bar{x}$ = 74.8	55.7 62.1 79.0 82.6 20.8 $\bar{x}$ = 60.0			57.5 71.1 74.8 68.2 89.3 61.0 $\bar{x}$ = 70.3		48.4 60.8 82.9 61.0 $\bar{x}$ = 63.3	39.0 61.1 74.5 69.2 $\bar{x}$ = 60.9			48.4 62.3 45.9 $\bar{x}$ = 52.2	60.9 60.7 71.7 $\bar{x}$ = 64.4		61.0 69.0 82.2 72.0 73.7 70.6 61.2 $\bar{x}$ = 69.9			83.4 85.7 82.2 70.9 71.8 73.1 $\bar{x}$ = 77.8
M5	68.1 61.4 92.7 68.1 63.9 77.6 80.7 77.5 $\bar{x}$ = 73.7			48.1 88.6 85.5 81.2 75.7 79.6 85.9 81.7 $\bar{x}$ = 78.3		74.3 83.9 70.1 84.0 81.4 84.5 77.4 84.1 $\bar{x}$ = 79.9	59.5 66.1 80.5 87.0 75.1 63.3 68.7 73.5 $\bar{x}$ = 71.7			74.1 81.5 81.4 83.6 35.7 81.8 88.9 85.4 $\bar{x}$ = 76.5	78.3 70.3 74.7 90.5 94.0 75.8 83.1 72.1 $\bar{x}$ = 79.8		75.1 68.3 86.9 57.6 69.5 91.2 85.4 66.2 $\bar{x}$ = 75.0			70.5 95.1 64.5 74.4 89.3 77.9 51.3 70.1 $\bar{x}$ = 74.1								

a. INCLUSIONS SHOWN AT ARROWS A AND B

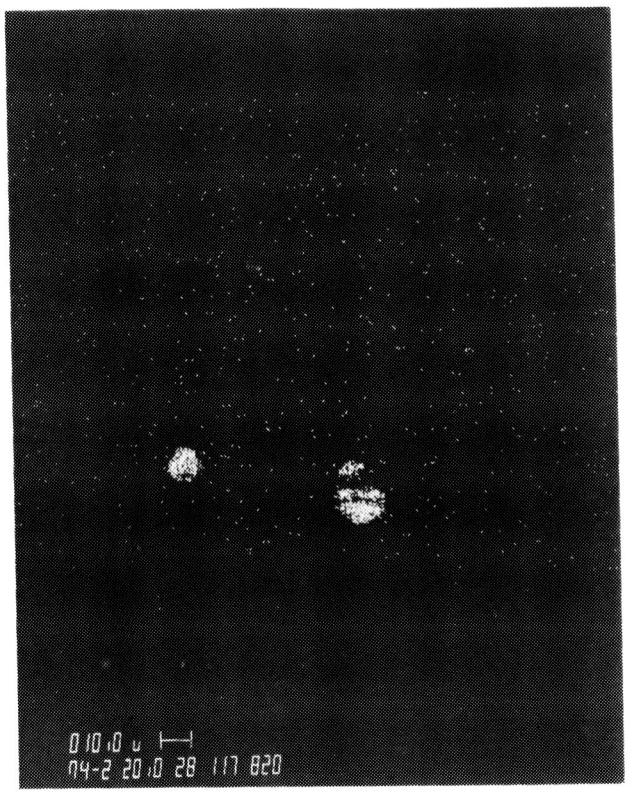

b. X-RAY MAP OF FRACTURE SURFACE WITH INCLUSIONS

K-10926

Figure 27.--Two Inclusions at the Tensile Fracture Surface of an M6 Specimen.

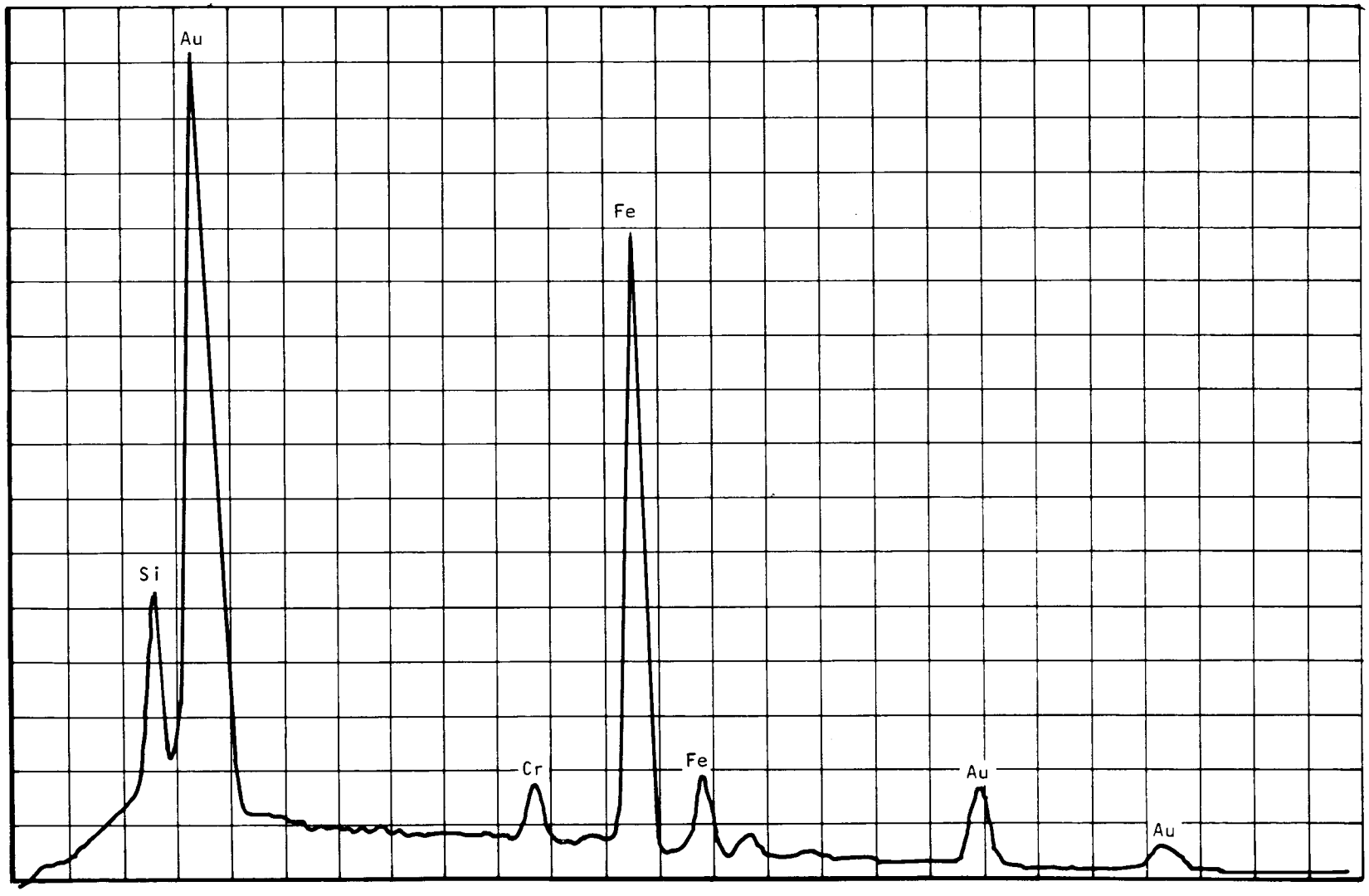

X-12577

Figure 28.--EDX Plot of M6 Specimen (a).

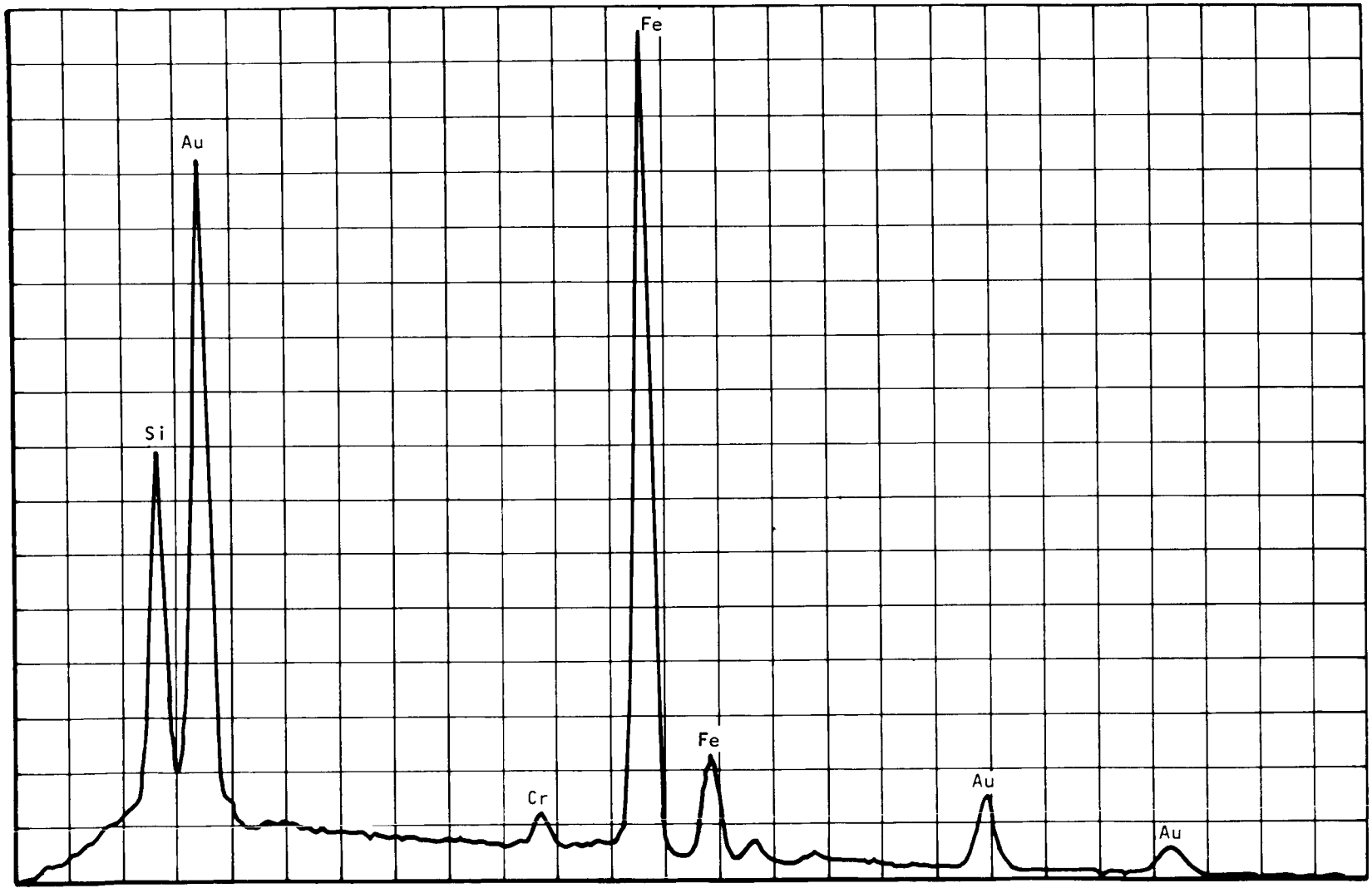

X-12578

Figure 29.--EDX Plot of M6 Specimen (b).

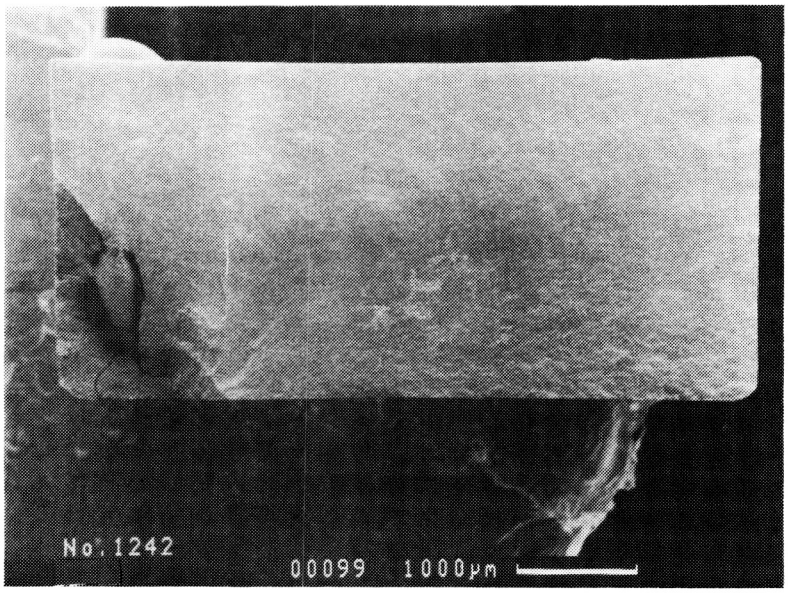

a. VIEW 1

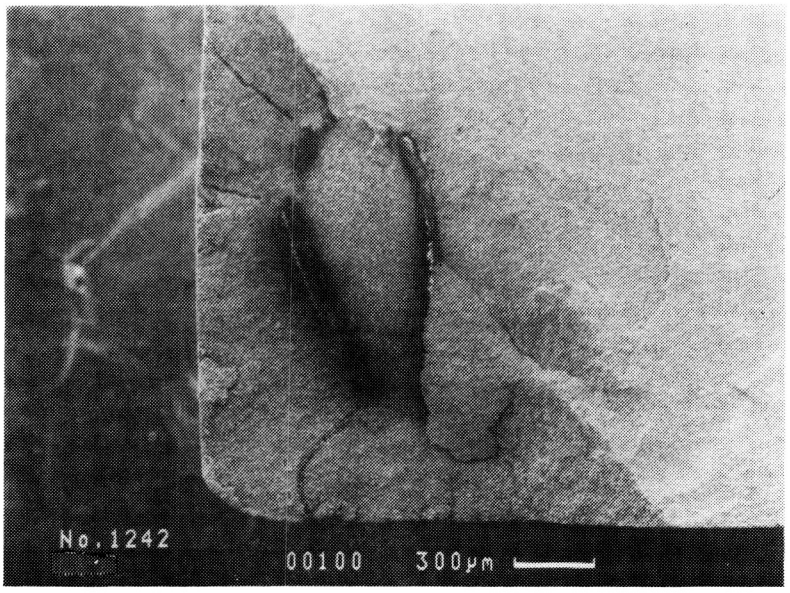

b. VIEW 2

K-10915

Figure 30.--Large Agglomerate and Void.

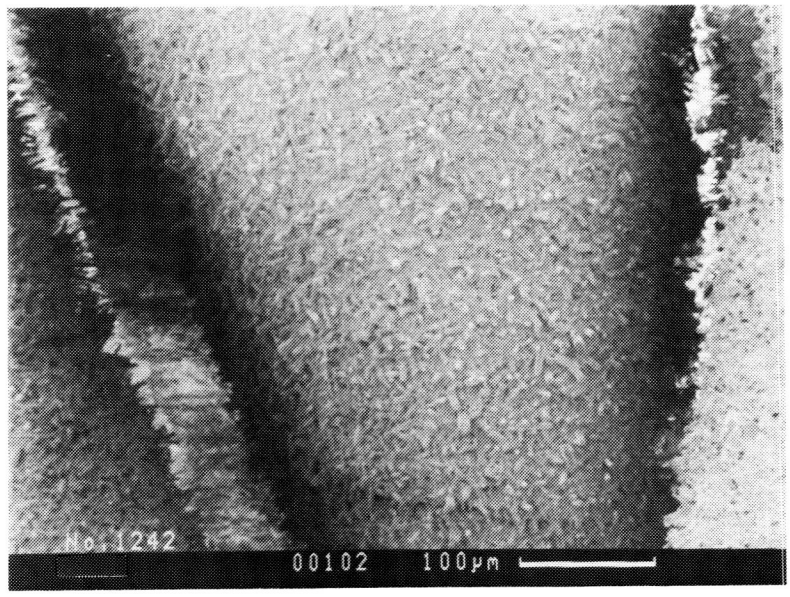

c. VIEW 3

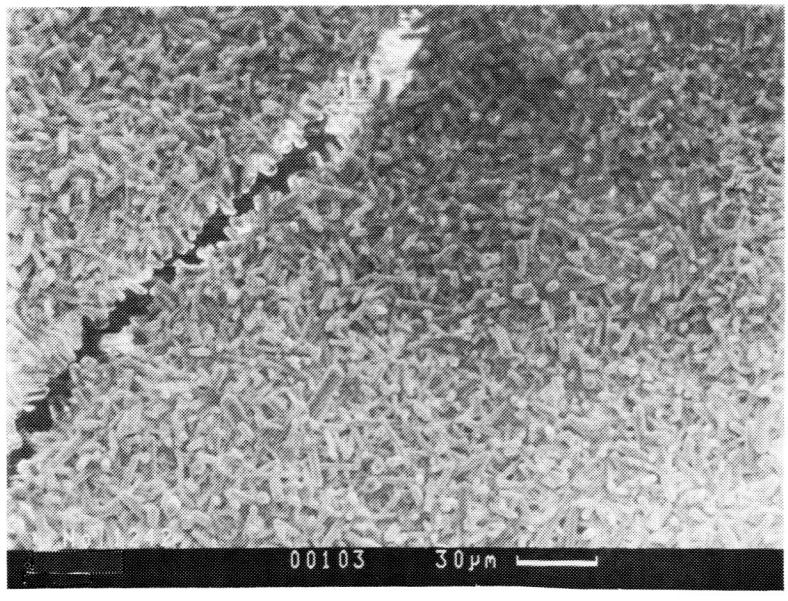

d. VIEW 4

K-10916

Figure 30.--Continued.

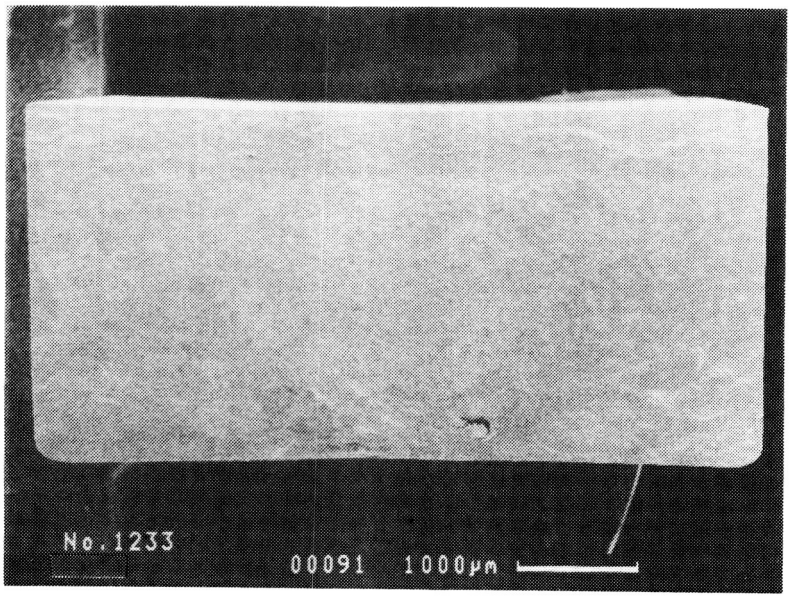

a. VIEW 1

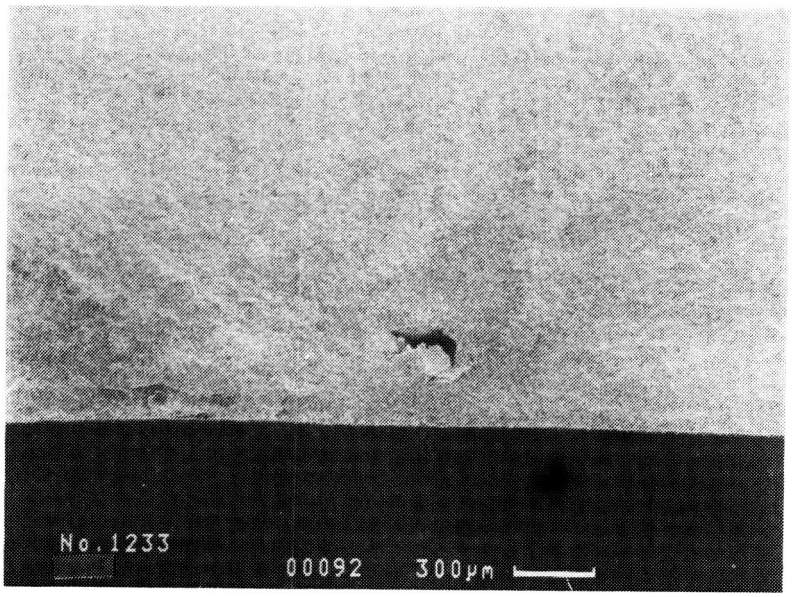

K-10918

b. VIEW 2

Figure 31.--Agglomerate in Void.

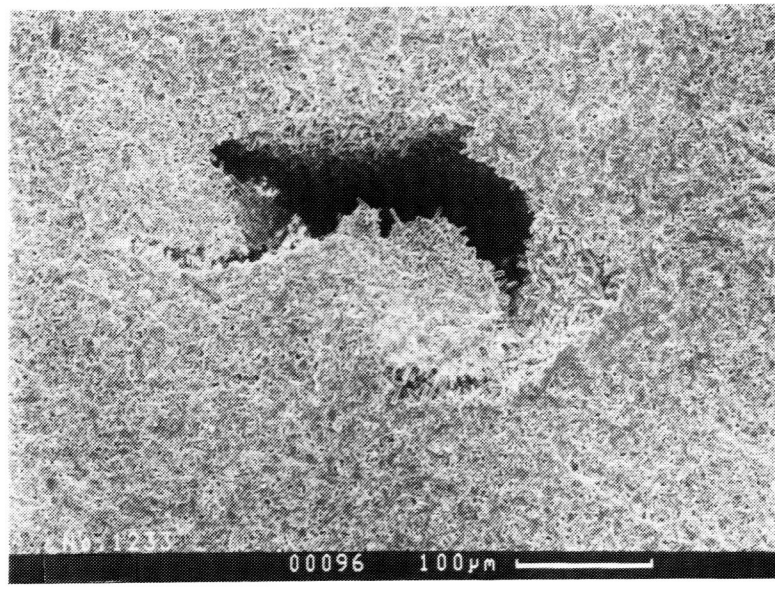

c. VIEW 3

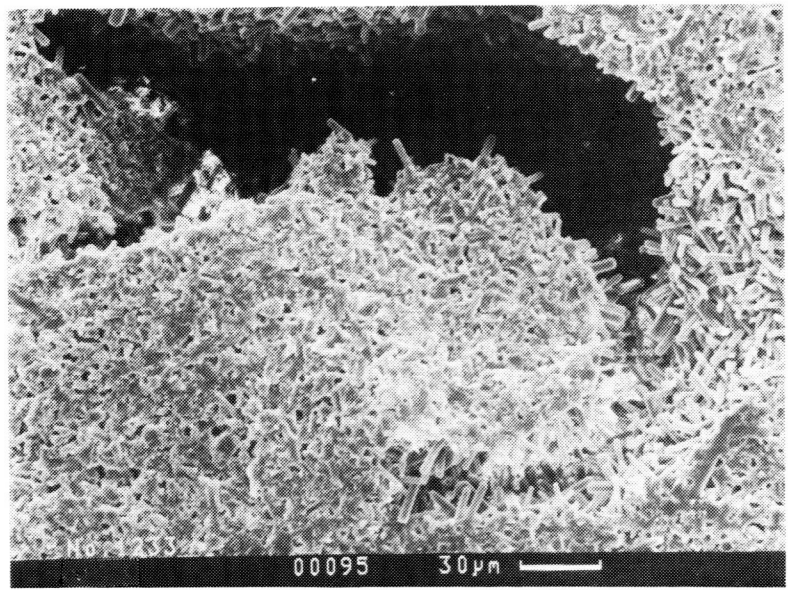

K-10917

d. VIEW 4

Figure 31.--Continued.

Correlating the fractograph data with the processing parameters revealed certain trends. In material section M4, more than 80 percent of the specimens that failed from internal flaws or surface inclusions were processed at the injection molding temperature T1. The data also showed that all specimens that failed from internal agglomerates and inclusions were processed under condition MAOT1DC2S3. The trends are less obvious in specimens from the M5 section. The only indication is that 80 percent of the specimens failing from internal flaws were processed with the DC2 dewax cycle.

Statistical analysis: The MOR and density data of 264 bars were used in this analysis. Of the 264 bars, there are 72 M1 bars, 65 M4 bars, 64 M5 bars, and 63 M6 bars. The correlation between MOR, density, sintering weight loss (SWT), and dewax weight loss (DWT) was evaluated for materials M1 and M6. The effect of processing factors on strength and density was also evaluated for all four materials.

Under the experimental conditions of Matrix 6, it was found that a major cause of differences in strength and density between bars was the starting Si_3N_4 material used in processing. Among the four grades of Si_3N_4 material, M1 was found to be superior to the others in both strength and density. Material M1 had high measurements of both MOR and density values, and also had a very low variation in both measurements. Material M4 resulted in the lowest density and strength. Material M6 had the largest variation in both MOR and density. The strength of material M5 was unaffected by any of the processing factors. The mean values of MOR and density along with the number of test bars used in the calculation are given in table 32.

TABLE 32

LIST OF MEAN VALUES OF MOR AND DENSITY
OF FOUR GRADES OF Si_3N_4 - M1, M4, M5, AND M6

Parameter	M1	M4	M5	M6
Number of test bars	72	65	64	63
MOR, ksi	82.77	64.64	76.16	75.74
Density, g/cc	3.23	2.97	3.18	3.04

Material M1 is a high-density material with values ranging from 3.21 to 3.25 g/cc. Material M5 can also be considered a high-density material. The density values of M5 bars ranged from 3.06 to 3.25. Both M4 and M6 are low-density materials. The density of M4 and M6 bars ranged from 2.87 to 3.13 g/cc and 2.78 to 3.22 g/cc, respectively.

Bars made of material M1 had higher strength when compared with bars made of materials M4, M5, and M6. Under all treatment combinations, the average MOR for M1 ranged from 75 to 93 ksi, and the average MOR for M4 and M5 ranged from 52 to 78 ksi and 73 to 83 ksi, respectively. In all treatment combinations except one, the average MOR for M6 ranged from 78 to 92 ksi, which is comparable with the range of average MOR values of M1. However, for the one exception (MA1, T2, DC2, S1) the average MOR dropped to 32 ksi.

Correlation coefficients between MOR, density, SWT, and DWT were computed and tested for significance separately for each material. No consistent pattern was found. The correlation coefficients are listed in table 33. For material M1, none of the correlations was found to be significant. However, for material M6, all of the correlations were significant. The correlation coefficients between density, SWT, and DWT even reached 0.9 in absolute value. Such a high correlation could be the result of the extremely low values obtained under the treatment combination MA1, T2, DC2, and S1.

TABLE 33

CORRELATION COEFFICIENTS BETWEEN MOR, DENSITY, SWT, AND DWT FOR MATERIALS M1 AND M6

Variables/ Material	MOR and Density	MOR and SWT	MOR and DWT	Density and SWT	Density and DWT	SWT and DWT
M1	-0.062	0.018	-0.033	-0.248	-0.135	0.006
M6	0.500[1]	-0.378[1]	0.429[1]	-0.881[1]	0.923[1]	-0.897[1]

[1]With 99 percent confidence, the correlation between two variables is statistically significant.

For each of the materials, the MOR and density values were analyzed to identify significant factors and interactions. These varied from material to material. Table 34 provides a list of factors and interactions that had a significant effect on strength and density. The interaction between milling aid (MA) and molding temperature (T) was found to have a significant effect on strength for M1, M4, and M6. None of the

factors or interactions was significant for M6. The sintering cycle was found to have a significant effect on density for materials M4, M5, and M6; and MA was significant for materials M1, M4, and M6. The mean values of MOR at different levels of MA and T are listed in table 35. The mean values of density at different levels of MA and S are presented in table 36.

TABLE 34

SUMMARY OF ANALYSIS OF VARIANCE,
LIST OF SIGNIFICANT PROCESSING FACTORS FOR M1, M4, M5, AND M6

Response Variable	M1	M4	M5	M6
MOR	MA T MA*T	T MA*T	None[1]	MA,MA*T DC, MA*DC S,T*DC
Density	MA	MA S	S	MA S MA*S T*DC

[1]None of the processing factors was significant on M5 MOR values.

TABLE 35

MEAN VALUES OF MOR AT DIFFERENT LEVELS OF MA AND T

MA	T	M1	M4	M5	M6
0	1	81.92	57.30	76.01	78.48
	2	80.25	73.40	75.83	91.63
1	1	79.97	56.64	78.20	79.24
	2	91.37	62.11	74.58	54.58
2	1	81.75	58.31		
	2	81.69	73.60		

TABLE 36

MEAN VALUES OF DENSITY AT DIFFERENT LEVELS OF MA AND S

MA	S	M1	M4	M5	M6
0	S1	3.237			3.204
	S3		2.890	3.156	
	S2	3.236			3.201
	S4		2.961	3.199	
1	S1	3.232			2.825
	S3		2.930	3.172	
	S2	3.229			2.939
	S4		3.001	3.195	
2	S1	3.239			
	S3		3.031		
	S2	3.236			
	S4		3.067		

In conclusion, material M1, under the experimental conditions of Matrix 6, results in a high-density, high-MOR material with an exceptionally low variation in density. Most M1 bars had a MOR value of 80 to 90 ksi and a density of 3.2. The other Si_3N_4 powders were found to be inferior to M1 for various reasons. The two-factor interaction of milling aid and injection temperature was found to have a significant effect on MOR values; the milling aid and sintering cycle were found to be significant to density.

No correlation was found between MOR and density for material M1; in contrast, for material M6, the correlation was found to be significant.

Matrix 8 - sintering.--Matrix 8 was an iterative series of sintering runs. Test bars included extra bars that were molded in parallel with Task II efforts specifically for the purpose of optimization experiments. Sintering runs included use of the baseline 0.7 MPa (100-psi) furnace, the 207 MPa (30,000-psi) sinter/HIP furnace, and the newly installed 10.3 MPa (1500-psi) furnace. The experiment included a survey of time, temperature, and pressure conditions. Data from these experiments were then used to establish appropriate sintering conditions for M_4 and M_5 in Matrix 6 and for Starck H-1 and Denka 9FW in Task II Matrixes II-1 and II-2.

Results and discussion: Significant parameters relating to densification were identified. The 1900°C cycle in the 0.7-MPa (100-psi) furnace included test bars using Si_3N_4 powder from GTE, Starck, and Denka. Table 37 provides powder properties after milling each powder with 6% Y_2O_3 and 2% Al_2O_3. Oxygen content and particle size both appear to play a major role in obtaining high density. The resulting density for each material is also given. The full PSD curve is shown for each powder in figure 32.

TABLE 37

COMPARISON OF MILLED POWDERS, 6+2 COMPOSITION

Si_3N_4 Powder Used	Oxygen Content, percent	Surface Area m^2/g	Particle Size at 50%, µm	Sintered* Density, g/cc
Baseline GTE 502	4.66	7.2	0.90	3.25
Matrix II-1 - Starck	3.86	11.8	0.97	2.87
Matrix II-2 - Denka	3.67	12.0	0.64	3.23

*Sintering Run U-585 1900°C/100 psi

The density spread for these materials is significant. The use of GTE and Denka powders resulted in 99.7 percent and 99.1 percent of theoretical density (3.26 g/cc), respectively. The Starck powder used resulted in 88 percent of theoretical density. It would appear that high oxygen content in the GTE powder significantly enhances densification. The fine particle size of the Denka powder also appears to enhance densification. Surface area does not appear to be directly related to the densification behavior for this group of test bars.

MOR testing and fractographic analysis of Matrix 8 test specimen results are presented in table 38. Table 39 lists the sintering cycles used. This matrix was a survey of sintering conditions and environments using test specimens molded in parallel with the Task II specimens. Thirty Denka 9FW and 20 Starck H-1 test specimens were used to investigate over 20 processing combinations in support of Matrix II-1 and Matrix II-2. In general, the Denka specimens showed higher sintered density than the Starck H-1 specimens. Test specimens that failed from internal flaws have lower MOR than those that failed from surface flaws. These

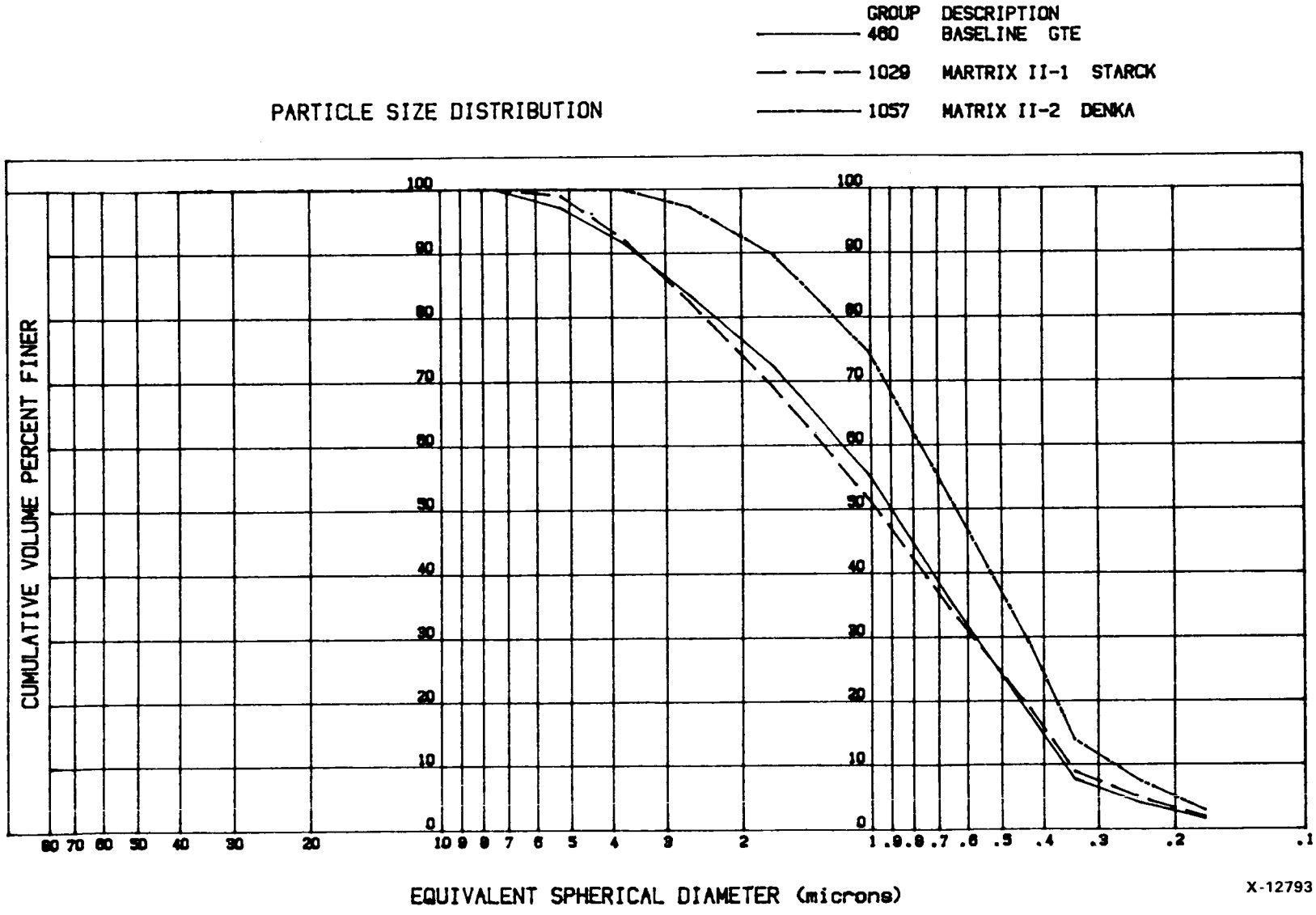

Figure 32.--Particle Size Distribution of Milled Powders Sintered in Matrix 8.

TABLE 38

SINTER/HIP SUMMARY - DENKA 9FW BARS*

Binder Content	15.5%			14.5%		
Run No.	9	468	11	9	468	11
Bar No.	3157	3158	3159	3557	3558	3560
Density	3.13	3.25	3.25	3.14	3.26	3.26
MOR MPa	464	576	550	393	747	629
(ksi)	67.3	83.6	79.8	57	108.4	91.2

*All six bars with 6% Y_2O_3 + 2% Al_2O_3 and not extruded.

TABLE 39

SINTERING CYCLES

Run No.	100 psi N_2	Other Pressure, psi N_2
9	1750°C - 1 hr	2 hr at 1900°C/1500 psi
11	1900°C - 1 hr	2 hr at 1900°C/1500 psi
468	1900°C - 30 min	1900° to 1850°C/10,000 psi

data are summarized in table 40 where the average MOR for each type of failure is listed. The difference in MOR between the two types of failures in the Denka 9FW specimens was not as large as in the Starck H-1 test bars. For the Denka specimens, all but one of the internal defects were dark inclusions. This is not surprising since all of the specimens were extruded and Matrix II-2 results with Denka bars showed that the dark colored inclusions are related to extrusion. In the Starck specimens, fracture also originated from other internal flaws such as voids and agglomerates in addition to the dark inclusions.

The fracture surfaces of four specimens from Matrix 8 runs were examined under SEM and analyzed by EDX. Figures 33a and 33b show a

TABLE 40

MATERIAL PROPERTIES AND FAILURE FLAW TYPES

Flaw Type	Material	
	Denka 9FW	Starck H-1
Internal Flaws	MOR, ksi Avg. = 76.7 S.D. = 10.38 N = 10	MOR, ksi Avg. = 58.3 S.D. = 15.01 N = 10
	Density, g/cc Avg. = 3.18 S.D. = 0.157	 Avg. = 2.96 S.D. = 0.123
Surface Flaws	MOR, ksi Avg. = 78.8 S.D. = 11.73 N = 10	MOR, ksi Avg. = 64.9 S.D. = 7.367 N = 10
	Density, g/cc Avg. = 2.99 S.D. = 0.212	 Avg. = 2.93 S.D. = 0.139

subsurface void in Specimen 1783 (Starck, B-C-D-E+). The material for this specimen was not extruded and no inclusions were found. Figures 34a and 34b show an inclusion near the tensile surface of Specimen 3397 (Denka 9FW, B-C+D-E-). The inclusion contains Fe and a small amount of Cr. The iron containing inclusion appeared to have prompted grain growth. The fracture surface of Specimen 3398 (Denka B+C+D-E-) is shown in figures 35a through 35f. A large (approximately 0.025 in. x 0.012 in.) shiny inclusion and some dark areas can be seen. The EDX plot (figure 36) shows that the inclusion contains Fe and traces of Cr and Ni. The iron X-ray map (figure 35d) shows the distribution of iron. It should be noted that due to the position of the X-ray energy detector, X-ray from the left part of the particle was obstructed and appeared dark. The Cu, Ag, and Zn probably came from the specimen mount. No other element besides silicon was detected in the dark area in figures 35e and 35f. A magnified view of the boundary between the dark zone and the matrix in figure 35f shows that the fracture mode in the

Figure 33.--Subsurface Void in Starck H-1 Test Bar (No. 1783).

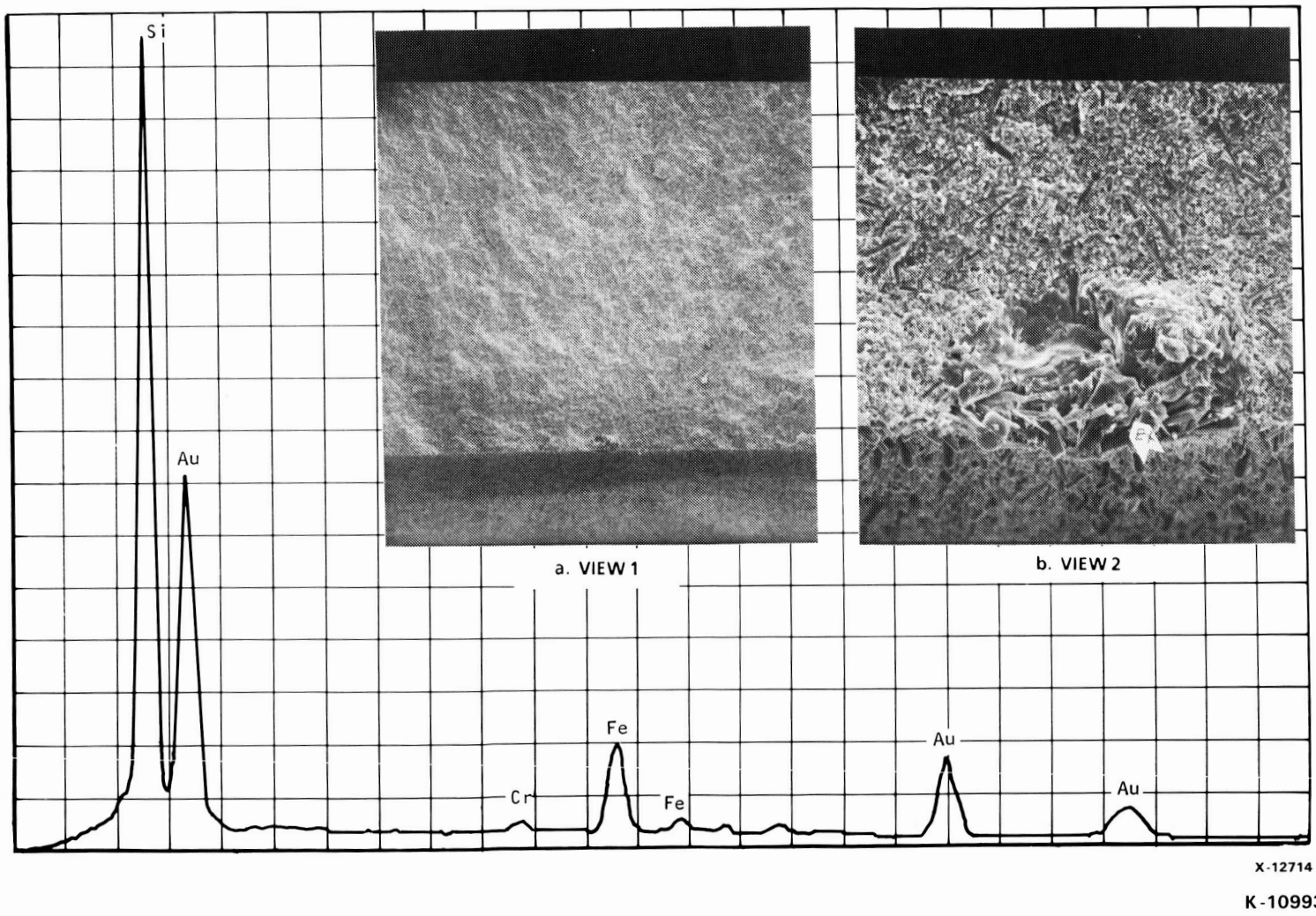

Figure 34.--Inclusion or Grain Cluster in Denka Test Bar Containing Fe and a Small Amount of CR.

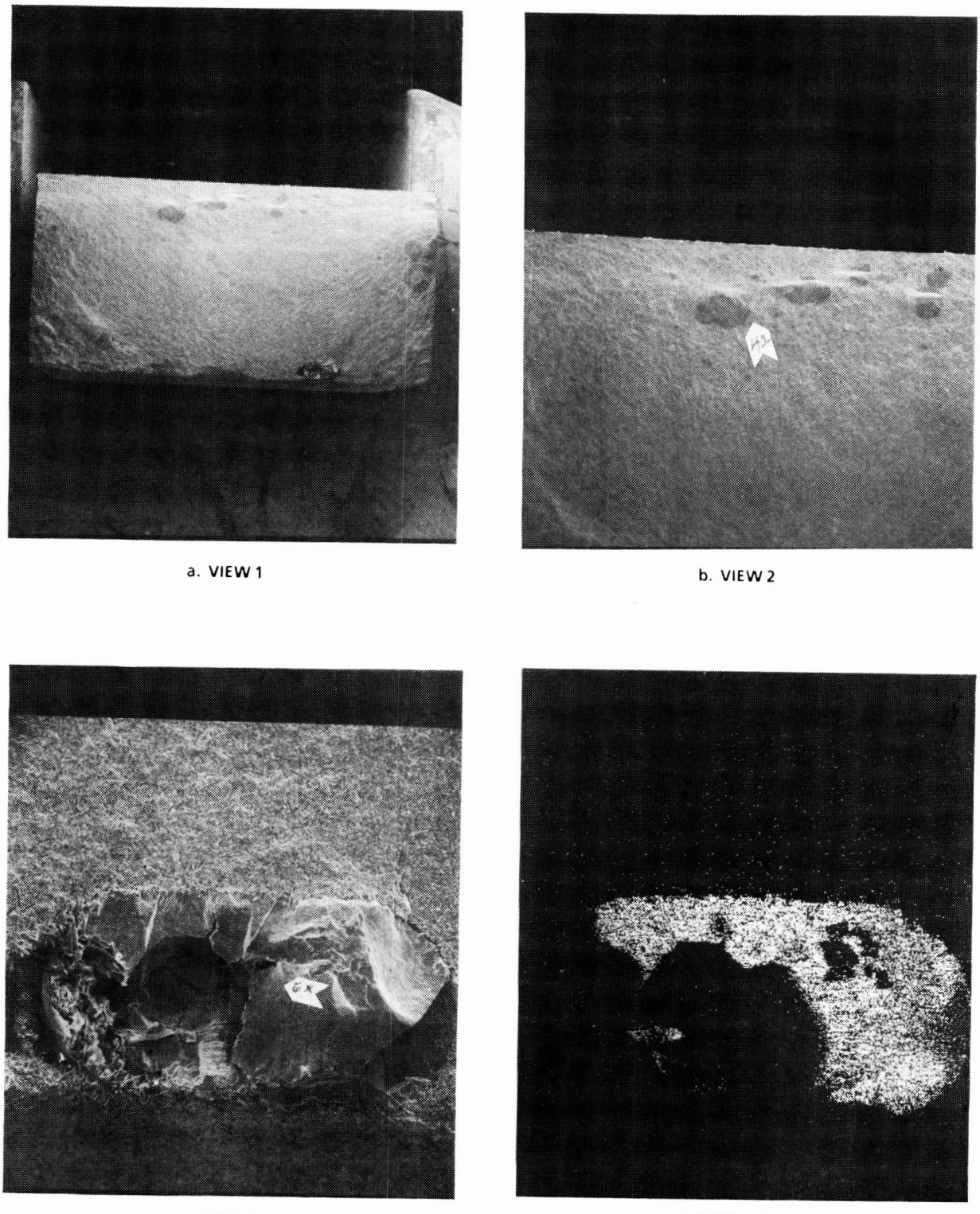

a. VIEW 1

b. VIEW 2

c. VIEW3

d. VIEW 4 (Fe X-RAY) K-10991

Figure 35.--Large Inclusion and Dark Patches in Test Bar No. 3398

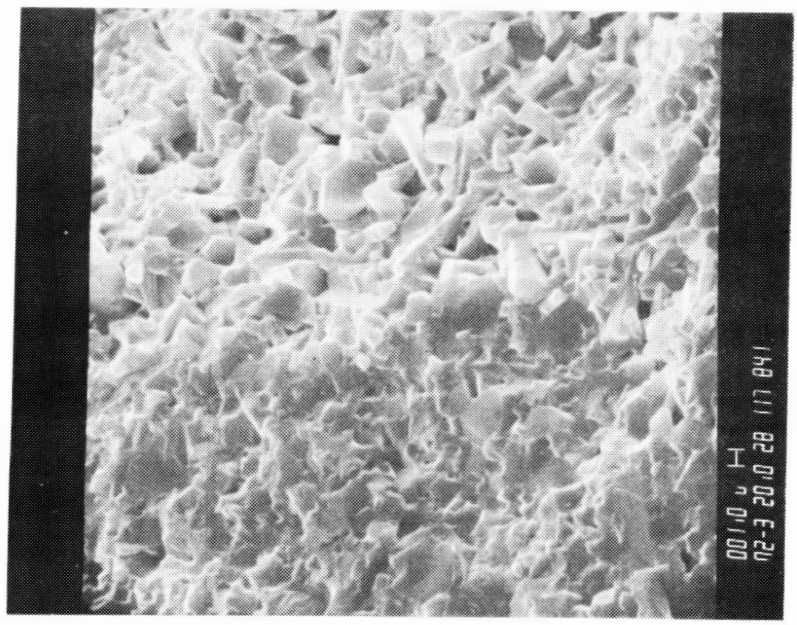

f. VIEW 6

K-10922

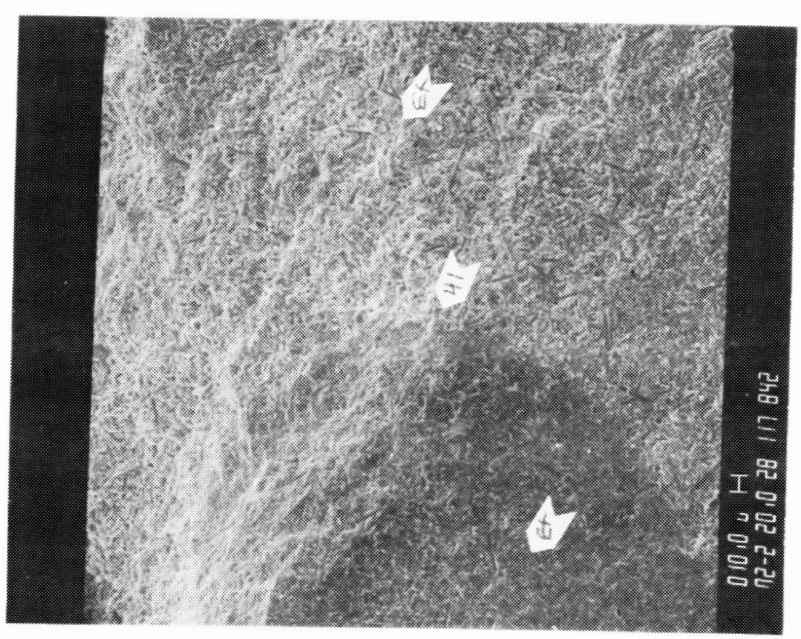

e. VIEW 5

Figure 35.--Continued.

Figure 36.--EDX Plot of Inclusion Containing Fe and Traces of Cr and Ni.

dark area was transgranular. This area of smoother surface emitted less electrons into the detector and therefore appeared darker due to surface morphology effects. The change in fracture mode for the dark zones may be due to higher iron concentration which changed the grain boundary phase. Dark areas similar to these were also observed in Matrix II-2 specimens. Figures 37a and 37b show a subsurface inclusion on the fracture surface of Specimen 3824 (Denka, B-C+D-E+). EDX indicated that the inclusion was probably stainless steel, judging from the Fe, Ni, and Cr content (figure 38). There was also an inclusion containing vanadium, probably tool steel, as seen in the X-ray map in figure 37f. The Fe, Cr, and Ni X-ray maps are also included in figures 37c, 37d, and 37e to show the respective element distribution.

These results indicate that the inclusions in the Denka specimens were quite similar in nature and probably came from the same source. The fact that specimens with inclusions were extruded is in agreement with separate Task II findings that the extruder was introducing steel particles.

Matrix 9 - iron contamination from processing.--Wet chemical analysis was conducted to determine possible iron pickup at various stages of processing prior to binder removal. Table 41 shows the preliminary data.

TABLE 41

WET CHEMICAL IRON CONTENT ANALYSIS (WEIGHT PERCENT)

Process Step	Task I GTE Baseline	Batch IM 94-57A[1]	Extruded IM 94-57A
Milled powder	0.03	0.03	0.03[3]
Pelletized After sigma (binder removed)	Not available	0.01	N/A
Pelletized After extruder (binder removed)	N/A[2]	N/A	0.03
Molded (binder removed)	0.03	0.04	0.05

NOTES:
1. An injection mix batch number
2. Not applicable
3. Same sample as the one used for IM 94-57A because the material was not extruded at this step.

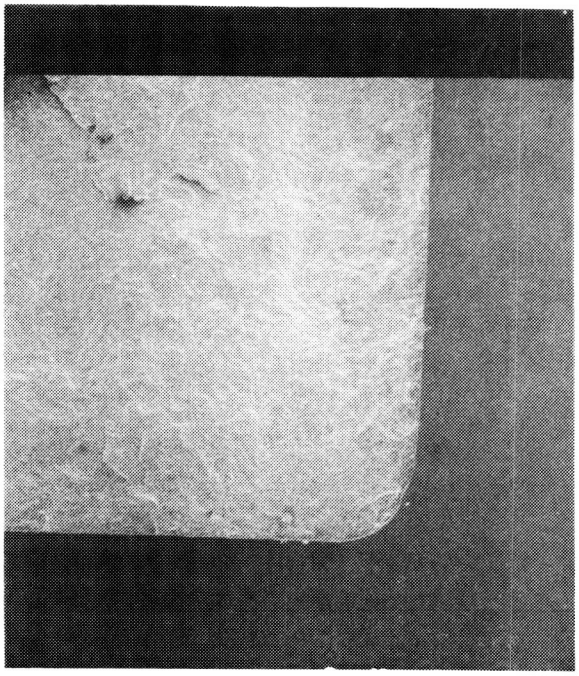

a. VIEW 1

b. VIEW 2

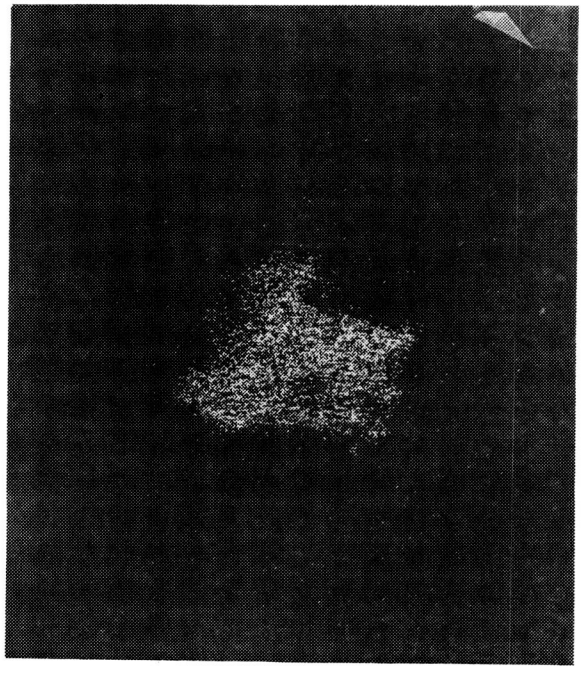

c. VIEW 3 (Fe X-RAY)

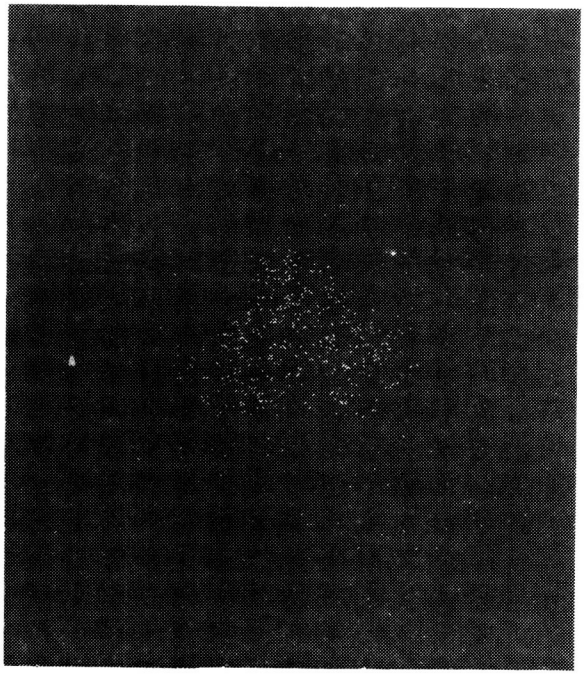

d. VIEW 4 (Cr X-RAY)

K-10990

Figure 37.--Subsurface Inclusion in Denka Bar Containing Fe, Ni, Cr, and V.

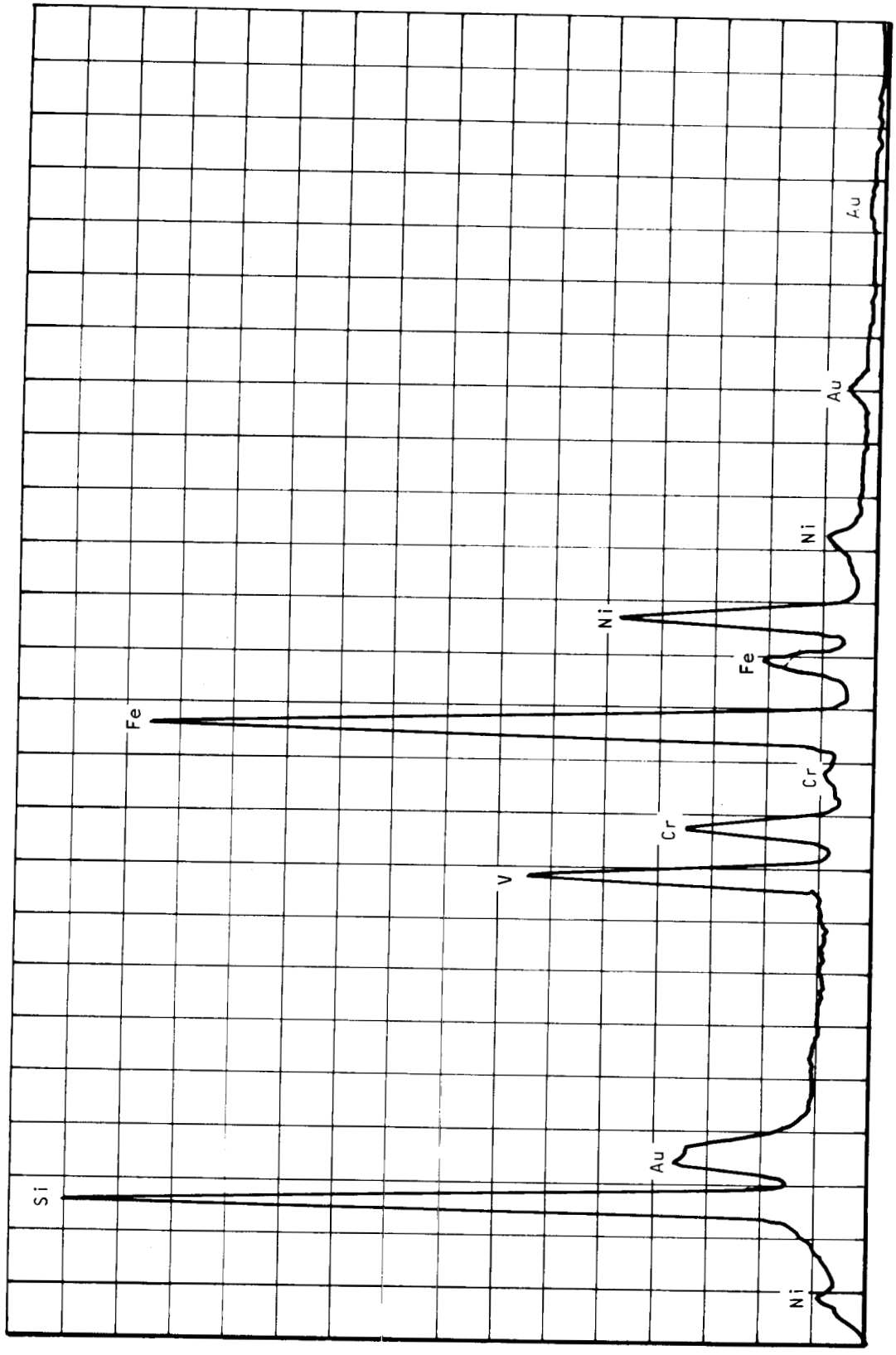

Figure 38.--EDX Plot of Inclusion Containing Fe, Ni, and Cr.

The result is not conclusive regarding the Fe pickup at the two intermediate steps; however, it does show that the molded materials have an either equal or higher Fe content than the as-milled materials. Additional analysis will be continued.

Matrix 10 - binder composition.--This matrix was to conduct a binder survey in which modifications of the existing binder are being evaluated along with changes in the generic type of polymers used. TGA and TMA were used in the screening evaluation. This investigation is to be continued. Some of the initial data are presented in the following text.

Sufficient powder was milled to provide a uniform lot of powder for mixing with a variety of binders. The new binders represent modifications of the existing binder and also totally new binder materials. Six binders have been mixed with powders and temperature-vs-torque relationships determined. Samples from mixing experiments were dewaxed. Promising compositions were evaluated in test bar fabrication. Additional compositions were prepared based on the dewax results. TMA data were completed for the same six compositions. Noticeable differences were identified for binders based on different polymers. Thermal expansion coefficients range from 100 to 500 x $10^{-6}/^{o}C$ at room temperature.

Three compositions were selected for test bar processing. Powder milling was initiated to provide for three batches of sufficient size to assure that proper molding and binder removal parameters are attained. Binder densities were measured and mixing was completed. The binder volume fraction was calculated for each material so that it would equal the E + (14.5 wt%) condition used in Matrix II-2. The powder used was equivalent to the D- (6 + 2) composition used in Matrix II-2. Injection was completed on 64 test bars, using 2 of the selected compositions. The injection molded bars were evaluated by X-ray analysis, and initial results indicated that these binders caused more injection voids than the present binder. This observation suggested that additional efforts beyond the current scope of the program are needed.

Matrix 11 - sinter/HIP, additive, binder, and milling time.--Matrix 11 was a screening experiment to determine whether there was a significant effect upon density and MOR of specific changes in sinter/HIP parameters, post-sinter cooling, and binder content (see tables 42 and 43). Twenty bars were tested and the results are discussed below.

Characterization: Results of room temperature MOR and fractographic analysis of the 20 test specimens are listed in table 44. Nineteen of the specimens fractured from the tensile surface and one specimen had a damaged fracture origin. No dark internal inclusions were observed on any of the fracture surfaces and no visible cracks were detected on the tensile surface to account for any specimens with lower than average MOR.

TABLE 42

MOR MEASUREMENTS - TASK VII, MATRIX 11

Milling Time		16 Hours				64 Hours			
Sinter/HIP* Parameter		Parameter Set A		Parameter Set B		Parameter Set A		Parameter Set B	
Post-sinter Cooling		Unit On	Unit Off	Unit On	Unit Off	Unit On	Unit Off	Unit On	Unit Off
Binder content at 6+1% Additive:	13.5	69.2 63.1 $\bar{x}$=66.15				61.3 62.0 $\bar{x}$=61.65		72.4 71.7 98.2 x=80.76	76.4 96.3 99.7 $\bar{x}$=90.80
	14.5	61.5 68.2 $\bar{x}$=64.85				68.2 55.5 $\bar{x}$=61.85		103.1 76.2 62.8 x=80.63	88.4 70.1 91.4 $\bar{x}$=83.30

*Sinter/HIP parameter definitions:

Parameter Set A: 1750°C presinter T_p, 1900°C sinter T_s, 2 hr time at T_s, 2700 psi, BN powder bed.

Parameter Set B: 1830°C presinter T_p, 1900°C sinter T_s, 6 hr time at T_s, 1500 psi, PB-2 powder bed.

TABLE 43

DENSITY MEASUREMENTS - TASK VII, MATRIX 11

Milling Time		16 Hours				64 Hours			
Sinter/HIP* Parameter		Parameter Set A		Parameter Set B		Parameter Set A		Parameter Set B	
Post-sinter Cooling		Unit On	Unit Off	Unit On	Unit Off	Unit On	Unit Off	Unit On	Unit Off
Binder content at 6+1 Additive:	13.5	2.92 2.78 $\bar{x}$=2.85		Crack 3.16 3.13 3.12 $\bar{x}$=3.14	Crack 3.16 3.14 3.21 3.14 $\bar{x}$=3.16	2.80 2.83 $\bar{x}$=2.815		3.24 3.23 3.26 $\bar{x}$=3.243	3.26 3.25 3.27 $\bar{x}$=3.26
	14.5	2.77 2.77 $\bar{x}$=2.77		Crack 3.05 3.10 3.10 $\bar{x}$=3.08	Crack 3.09 3.10 3.08 3.13 $\bar{x}$=3.10	2.79 2.80 $\bar{x}$=2.795		3.24 3.25 3.23 $\bar{x}$=3.24	3.26 3.26 3.26 $\bar{x}$=3.26

*Sinter/HIP parameter definitions:

Parameter Set A: 1750°C presinter T_p, 1900°C sinter T_s, 2 hr time at T_s, 2700 psi, BN powder bed.

Parameter Set B: 1830°C presinter T_p, 1900°C sinter T_s, 6 hr time at T_s, 1500 psi, PB-2 powder bed.

TABLE 44

TASK VII, MATRIX 11

Bar No.	MOR	Density	S/I	Type	Location	Fracture Observations	Add. %	Binder wt %	Mill Time	Run	Powder Bed
4569	69.2	2.92	S	TF*	TF	Intergran. frac.	6+1	13.5	16	512	BN
4571	63.1	2.78	S	TF	TF	Intergran. frac.	6+1	13.5	16	512	BN
4668	68.2	2.77	S	TF	TF	Intergran. frac.	6+1	14.5	16	512	BN
4665	61.5	2.77	S	TF	Chamfer	Intergran. frac.	6+1	14.5	16	512	BN
4753	62.0	2.83	S	TF	Cham. corner		6+1	13.5	64	512	BN
4750	61.3	2.80	S	TF	Cham. corner	Intergran. frac.	6+1	13.5	64	512	BN
4847	55.5	2.80	S	TF	TF	Intergran. frac.	6+1	14.5	64	512	BN
4845	68.2	2.79	S	TF	TF	Intergran frac.	6+1	14.5	64	512	BN
4760	98.2	3.26	S	TF	Cham. corner		6+1	13.5	64	42-3	PB2
4854	62.8	3.24	S	TF	Cham. corner		6+1	14.5	64	42-3	PB2
4754	72.4	3.24	S	TF	Cham. corner		6+1	13.5	64	42-3	PB2
4850	76.0	3.25	S	TF	TF		6+1	14.5	64	42-3	PB2
4849	103.1	3.24	S	TF	TF		6+1	14.5	64	42-3	PB2
4759	71.7	3.23	S	TF	TF		6+1	13.5	64	42-3	PB2
4761	99.7	3.27	S	TF	TF		6+1	13.5	64	44-5	PB2
4856	91.4	3.26	S	TF	TF		6+1	14.5	64	44-5	PB2
4758	96.3	3.25	S	TF	Chamfer		6+1	13.5	64	44-5	PB2
4851	88.4	3.26	S	TF	Chamfer	Outside knife edge	6+1	14.5	64	44-5	PB2
4855	70.1	3.26	S	TF	TF	White mat. patch	6+1	14.5	64	44-5	PB2
4756	76.4	3.26	DM		Origin damaged		6+1	13.5	64	44-5	PB2

*TF = tensile face

Most of the specimens sintered in run 512 showed a predominantly intergranular fracture mode, which may be due to the low density and low strength of the material, and was reflected in the low MOR of the specimens.

The absence of observable defects at the fracture origins supported that the MOR of these specimens may be a function of their density. A plot of MOR against density is shown in figure 39. The data show that the group of low-density specimens from run 512 has a lower average MOR but there was no correlation between MOR and density for individual specimens. The same conclusion applies to the group of higher density specimens from sintering runs 42-3 and 44-5.

Statistical analysis: The density and MOR of 20 test specimens processed under 8 different treatment combinations were analyzed to study the effect of processing factors. The t-test and analysis of variance were used to determine whether the effects were statistically significant. The processing factors and the corresponding levels are summarized in table 45. Note that for analysis purposes, each of the three sintering runs was represented by two factors--the sinter/HIP parameter set and the post-sinter cooling cycle. For clarification, this arrangement is presented as a simple diagram in figure 40.

Table 42 presents Matrix 11 and the MOR values of the specimens processed under the corresponding treatment combinations. Both individual and mean MOR values are listed. In table 43, the density values are listed in the same manner. The four groups of cracked specimens processed with 16-hr milling time were not included in the analysis due to lack of MOR data.

Results of the analysis showed that only the sinter/HIP parameter set had a statistically significant effect on either the MOR or the density of the specimens. The rest of the factors, including the binder content, milling time, and post-sinter cooling cycle, did not have a significant effect.

The sinter/HIP parameter Set A produced specimens with low density (mean = 2.81 g/cc) and low MOR (mean = 63.6 ksi). Specimens processed with sinter/HIP parameter Set B have high density (mean = 3.25 g/cc) and high MOR (mean = 83.9 ksi).

The limited number of specimens used to represent each treatment combination introduces uncertainties in the analysis and may produce misleading results. A statistically designed screening test is recommended to be used in the future for this type of study.

Additional investigations on binders.

Gas analysis of vacuum dewaxing: Langan Engineering in Santa Barbara, California, has conducted a vacuum dewaxing process study on one of ACC's as-injection-molded rotors and an as-injection-molded test bar in a vacuum furnace equipped with a magnetic sector mass spectrometer.

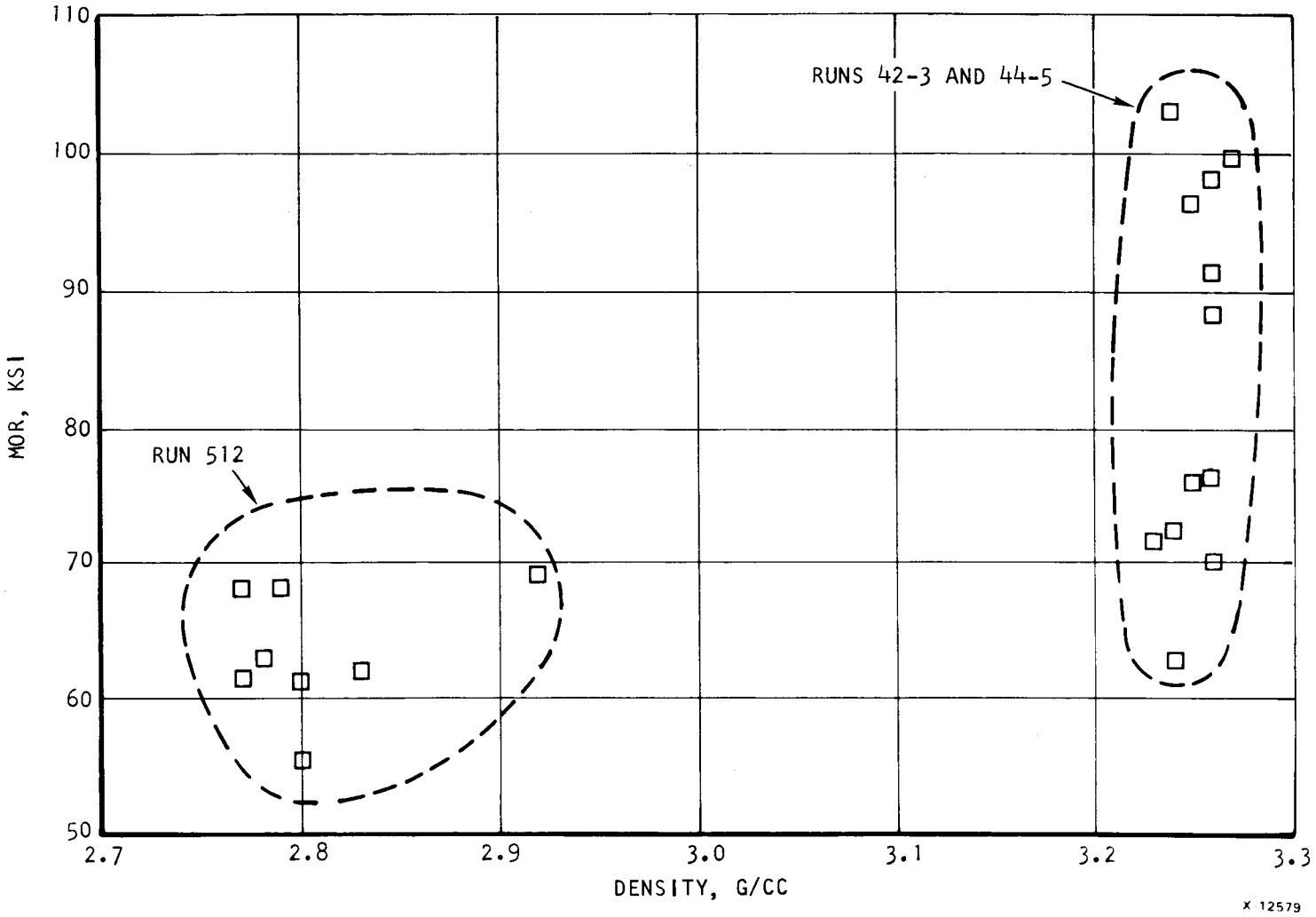

Figure 39.--Task VII Matrix 11 Specimens.

TABLE 45

PROCESSING FACTOR AND CORRESPONDING LEVEL

Factor	Level
Binder content	13.5% 14.5%
Milling time	16 hr 64 hr
Sinter/HIP parameters	Parameter Set A: (Run 512) 1750°C presinter temperature, 1900°C sinter temperature, 2-hr sintering time, 27,000 psi pressure Boron nitride powder bed Parameter Set B: (Run 42-3 and 44-5) 1830°C presinter temperature, 1900°C sinter temperature, 6-hr sintering time, 1500 psi pressure, PB-2 powder bed
Post-sinter	Unit off (Run 512 and 42-3)
Cooling cycle	Unit on (Run 44-5)

C-2

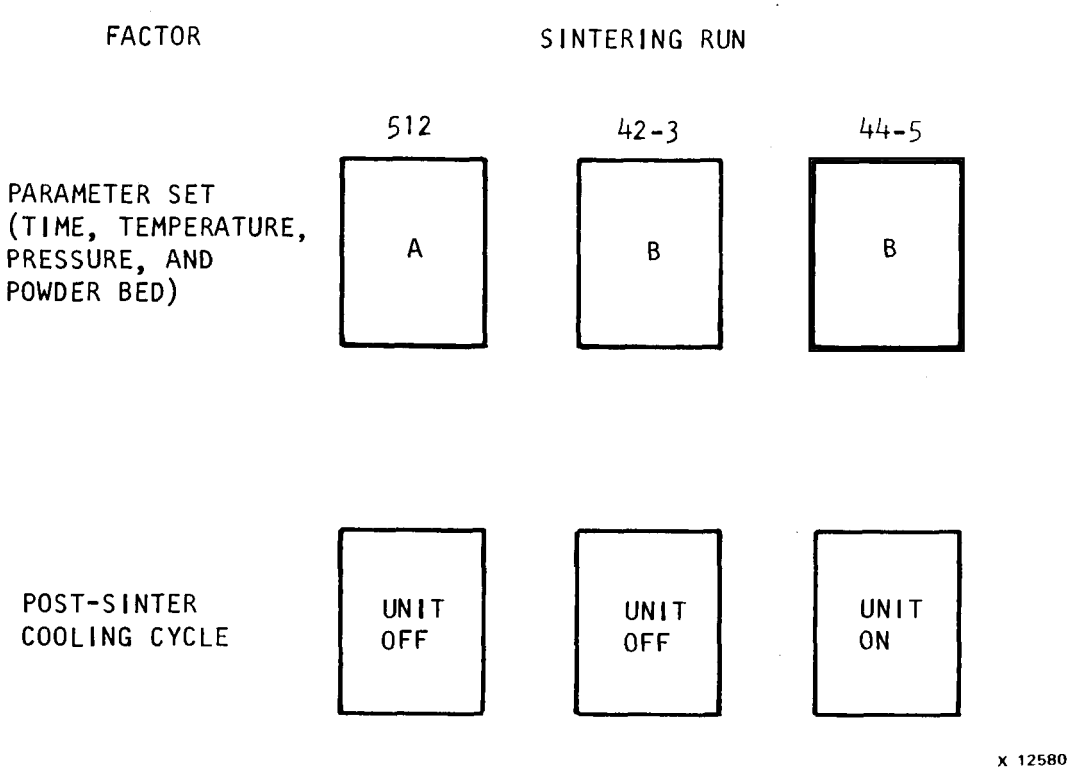

Figure 40.--Three Sintering Runs by Two Factors.

This investigation will provide useful information for designing an alternate dewax cycle for thick net shape parts. The critical temperature ranges in which rapid binder decomposition and gas evolution can be detected by the mass spectrometer have been determined. The major findings of this study are listed below:

(1) Water and residual air, primarily nitrogen (see figures 41 and 42), were major gases at low temperatures. This result suggested that a vacuum degas/bakeout was required before dewaxing.

(2) Hydrocarbon and methane were tracked with total pressure at temperatures above 615°F (see figure 43).

(3) Hydrogen, methane, mass 28 (light hydrocarbon, nitrogen, and carbon monoxide) and hydrocarbon (masses 41, 42, and 43), which all related to binder decomposition, were detected at various dewaxing temperatures.

Further study will concentrate on the correlation of dewaxing temperature, total pressure, and hydrocarbon partial pressure. If the critical temperature ranges can be clearly identified and controlled well, the rotor cracking problem during dewaxing can be reduced.

Binder removal study by TGA-FTIR: Allied-Signal Engineered Materials Research Center conducted a study of binder removal mechanism of the ACC baseline injection molding wax by using the technique of thermogravimetric analysis - Fourier transfer infrared spectroscopy (TGA-FTIR).

TGA-FTIR is an instrument that couples thermogravimetric analysis (TGA) with evolved gas analysis (EGA) performed with a Fourier Transform Infrared (FTIR) spectrometer. This technique can continuously monitor infrared spectra of evolving species, quantitatively analyze the gases during pyrolyis or other reactions, and related the gas concentrations to the measured weight loss from TGA. Therefore, the TGA-FTIR technique is very useful in elucidating the source and kinetics of the binder removal process used in ceramics fabrication.

During the experiment, the weight change of the wax sample was monitored continuously. The absorbance spectra of the gases in the collection cell shows that the dominant feature is the C-H stretching and the C-H bending vibration in the 2830-2960 cm^{-1} regions, respectively. This indicates that the major constituents from the binder removal process appear to be long chain hydrocarbons. No other gas species were detected by the FTIR. The peak area under the paraffin C-H stretching region was integrated by using computer data-reduction routine and was plotted against temperature. Two distinct paraffinic evolution peaks at 420° and 510°C were evident from the area plot. The findings agree with the derivative TGA results and confirm the two evolution regimes during binder removal.

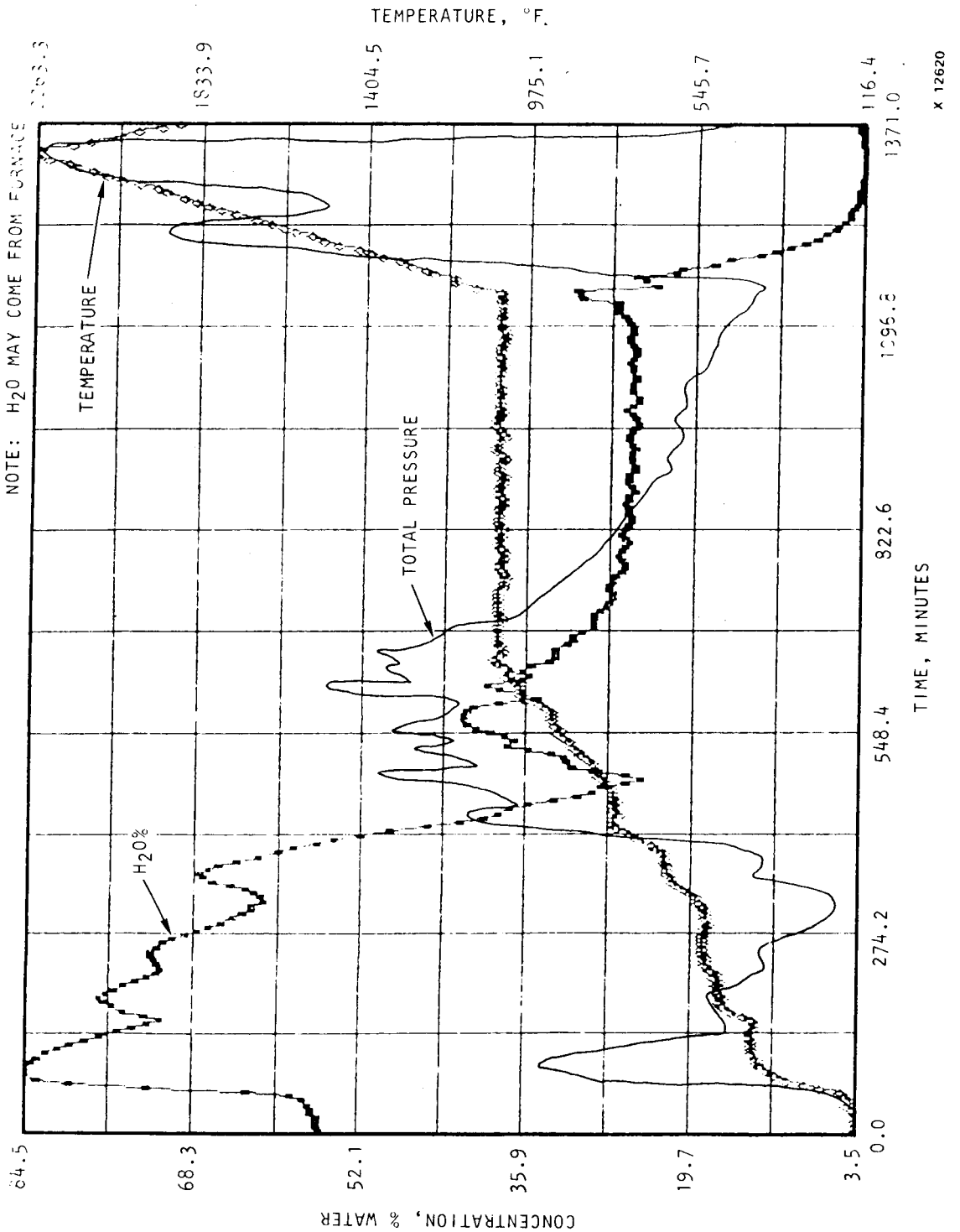

Figure 41.--Partial Pressure of Water and Total Pressure (Different Scale, for Reference Only) vs Dewaxing Temperature.

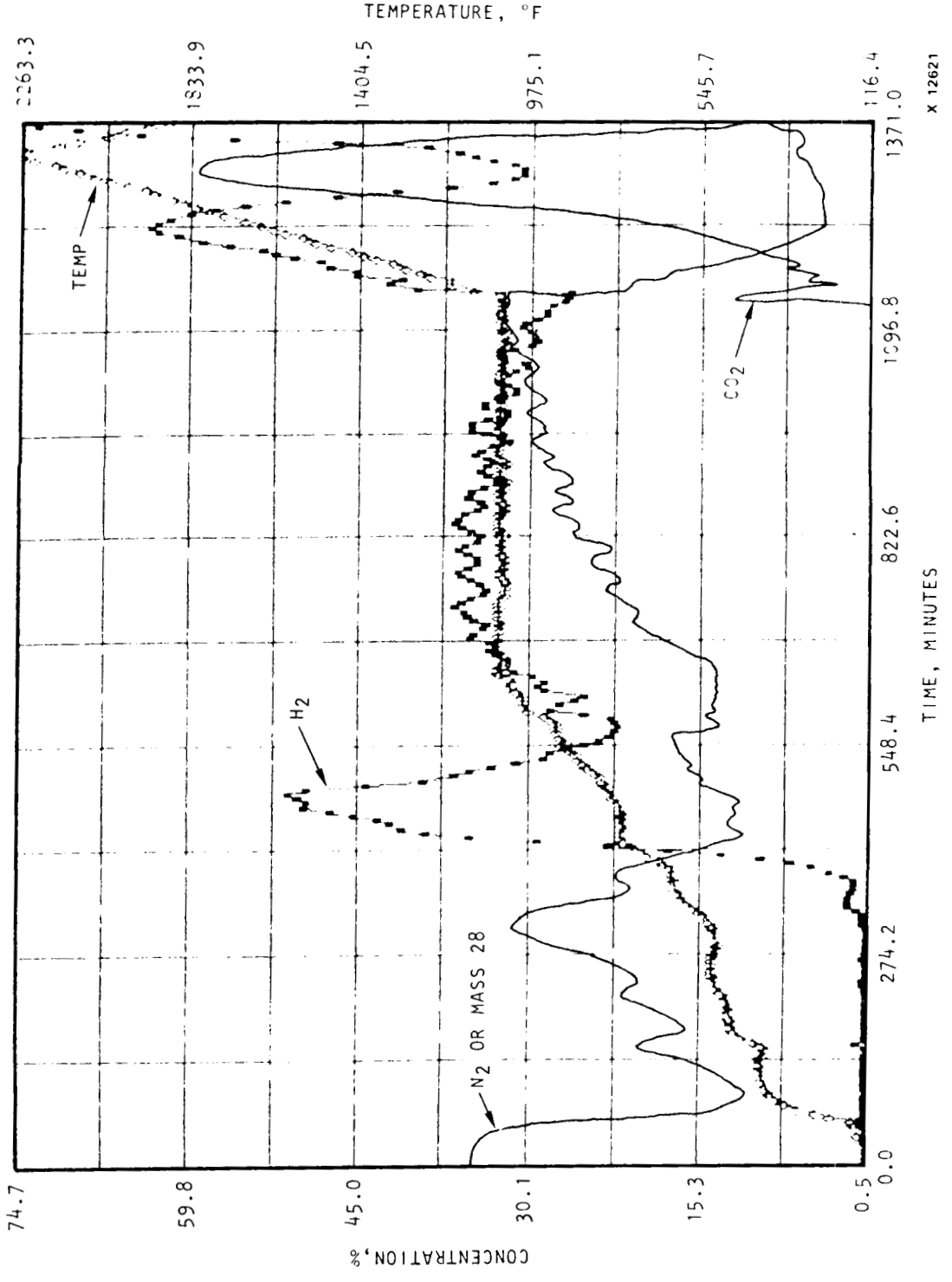

Figure 42.--Partial Pressure of Nitrogen, Hydrogen, and Carbon Monoxide vs Dewaxing Temperature.

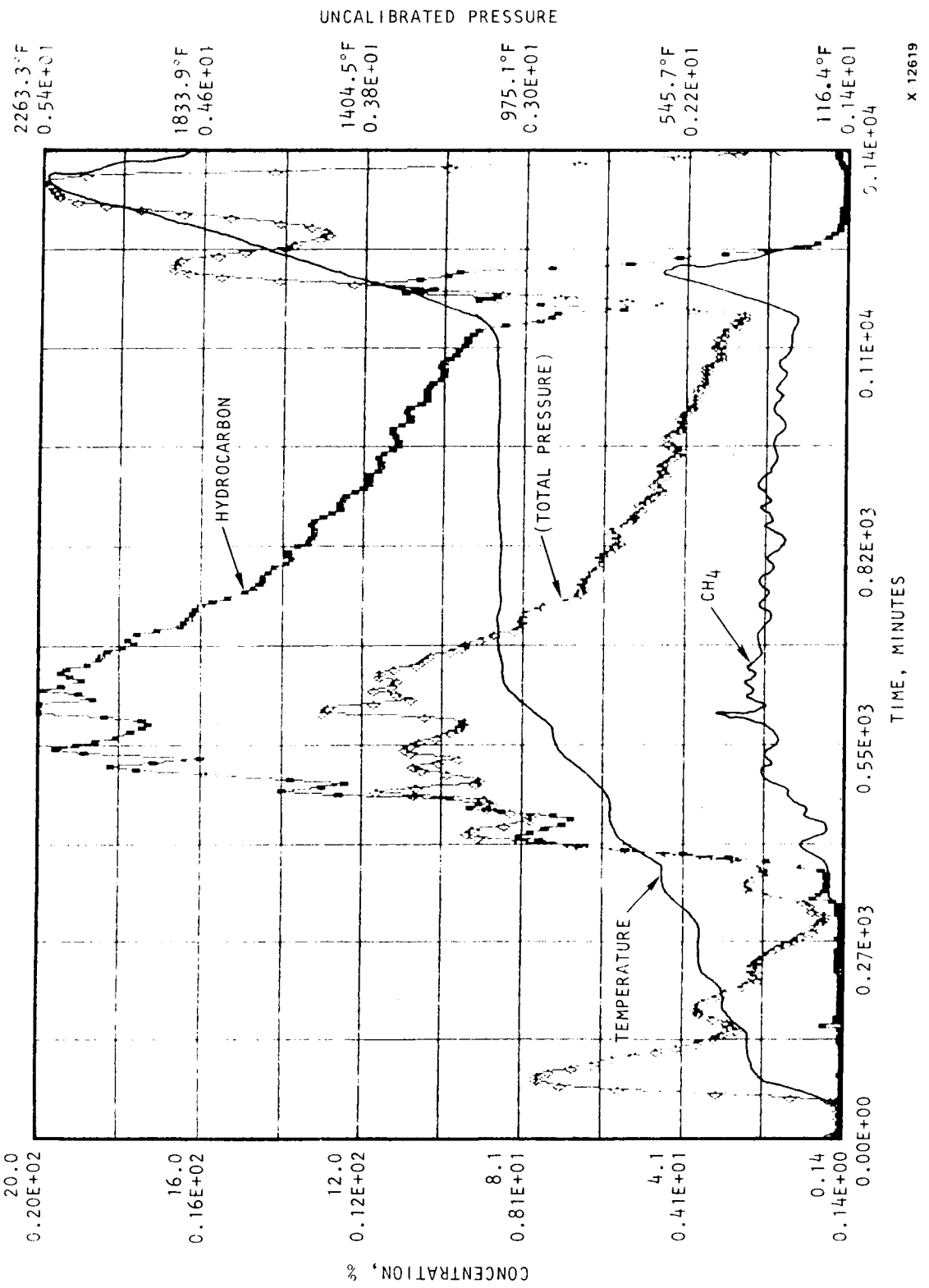

Figure 43.--Partial Pressure of Hydrocarbon, Methane, and Total Pressure (Different Scale, for Reference Only) vs Dewaxing Temperature.

Furthermore, the IR spectra show that the evolving gases are paraffins having the same chemical structure as the starting materials. The IR spectrum of the wax showed that the major binder removal mechanism operating at atmospheric pressure was volatilization of the paraffin wax near their boiling points. However, since volatilization is affected very much by external pressure, binder extraction at the above atmospheric pressure may have a mechanism different from that observed at one atmospheric pressure. High pressure operation may increase the boiling points of the binder systems and therefore suppress the devolatilization process. If the binder does not evaporate away at high temperature above a threshold pressure, pyrolysis may take place during or before the evaporization of the binders. In this situation, pyrolysis would be the major binder removal mechanism, rather than the devolatilization process.

Water-based binder: An evaluation on using Dow Chemical water-based binder (Methocel 20-231) for injection molding of Si_3N_4 was initiated, with technical inputs from Dow Chemical. Initial data indicated that injection mixes made from this binder could not be transported easily by the screw mechanism of the Arburg injection molder. A modified injection procedure, which provides a piston-like material transport mechanism, was tried. Test bars were able to be injection-molded with this modified procedure. The resulting bars from the initial experiments were mostly cracked. More comprehensive investigation will be conducted.

CONCLUSION

Statistically designed experiments aimed at optimizing processing parameters produced test bars with a 20 percent increase in room temperature flexural strength and an 86 percent increase in Weibull slope over the baseline material, GTE 502. The program goal was a 20 percent increase in strength to 96 ksi and a 100 percent increase in Weibull slope to 16 ksi.

Longer sintering time and sintering in a powder bed were found to be the statistically significant beneficial factors for strength. The binder content exhibited no effect within the range studied. There were also statistically significant effects due to the interactions between sintering in powder bed and extrusion of the injection molding mixture (B*C), powder bed and sintering aid content (B*D), and extrusion and sintering aid (C*D).

With the processing parameters used in this program, the Denka 9FW Si_3N_4 powder was found to be superior to the Starck H-1 and the baseline (GTE SN 502) powder. Additional experiments also showed that higher sintered density can be achieved at a 50°C lower maximum sintering temperature by increasing the sintering time by 2 hr and modifying the presintering parameters.

It has been demonstrated that a statistically designed half-replicate fractional factorial matrix experiment is a useful method in defining the processing direction for improved ceramic material property.

Significant progress was made in the initial net-shape scale-up evaluation using a turbocharger die (T-25). It was found that the as-injected rotor quality strongly depends on injection-molding parameters.

APPENDIX A

TASK II NEW GOAL PLAN

I. Introduction

In the last quarterly program review meeting held at ACC on February 20, 1986, it became apparent that the encouraging results from Task II 1st Iteration suggested that the original goals could be met at a much earlier date than originally projected. Marc Freedman, NASA Project Manager, expressed his desire to change the program to aim at a set of more ambitious goals. This document is a response to the official NASA request via a letter dated March 4, 1986. The new goals are to be accomplished "without changing either the scope or budget."

A brief discussion of the goals, in order of priority, will be presented. Following the discussion of goals is a proposed plan and schedule for the remaining period of Task II, April-December 1986. Task VII work during the same period will concentrate on small scale experiments directly beneficial to the new goals. The existing Tasks III through VI plans remain the same.

II. Discussions

1. High Weibull Slope

This goal is to retain the original goal of attaining an 100 percent improvement in Weibull slope over baseline (i.e., m $\geq$16). The results from Matrix II-2 (Denka 9FW) showed that 8 out of 16 processing combinations (treatments) have already attained Weibull modulus more than 20 percent higher than the baseline (i.e., m $\geq$10). The treatment which yielded the best combination between average strength and Weibull slope is treatment "ab"*, which has an average strength of 97 ksi with a Weibull of 14.

The improvement in Weibull accomplished has to be repeated under the exact same conditions to be sure this is the typical Weibull for these conditions, because an in-depth review of Matrix II-2 work has identified deviations from the desired process parameters. It is believed that a repeat of one of the Matrix II-2 treatments with improved process control can significantly improve the Weibull. Treatment "ab," mentioned earlier, is a reasonable choice for this purpose.

*Denka 9FW Si_3N_4, 6% Y_2O_3 + 2% Al_2O_3, 15.5% binder, Sigma mixer only, powder bed, A+ sinter/HIP cycle.

2. High Temperature Materials

The goal is to develop a material with a room-temperature strength of at least 95 ksi and a high-temperature strength (up to 2550°F) of no less than 85 ksi for "as-sintered" specimens. The key to improved high temperature strength lies in the grain boundary chemistry. Therefore, the experimental approach is focused on modifying the chemistry and amount of the sintering additives. This includes the investigation of alternate sintering aids as well as the optimization of the baseline Y_2O_3/Al_2O_3 system. As the sintering aids are changed, the sintering cycle must also be modified to optimize densification and control grain boundary phases. Full densification may require sinter/HIP to high pressures. In addition, post-sinter heat treatments may be beneficial if glassy grain boundary phases can be crystallized without experiencing an overall weakening of the material due to grain boundary volume changes during crystallization.

3. Net Shape Component Fabrication

It is reasonable to question whether the optimized processing parameters developed on test bars will be directly transferable to a much larger complex shaped component. It is beneficial to evaluate the scale-up processing problems using a component such as the T-25 turbocharger rotor (diameter≈2.5 in.). The emphasis of this goal is to assess the correlation in process parameters between test bars and T-25 rotor. The T-25 size rotor tooling for injection molding purchased by ACC would be made available to this program.

4. Toughened Si_3N_4

After having given it a serious consideration, the Garrett team (ACC and GTEC) has concluded that under the constraints of the program scope and budget, this goal cannot be addressed adequately at this time. This goal could be more effectively addressed in a future date when the ongoing ORNL composite program at ACC has demonstrated the feasibility of the SiC_w/Si_3N_4 system.

III. Plans

Figure A-1 shows the overall schedule and the percentages of efforts on each goal. The major steps proposed in achieving the goals are described in the following paragraphs.

1. High-Weibull Modulus

The processing condition (treatment) "ab" is chosen for this subtask. All processing steps and environment will be identical to the ones designed for treatment "ab" in Matrix II-2 (Denka 9FW).

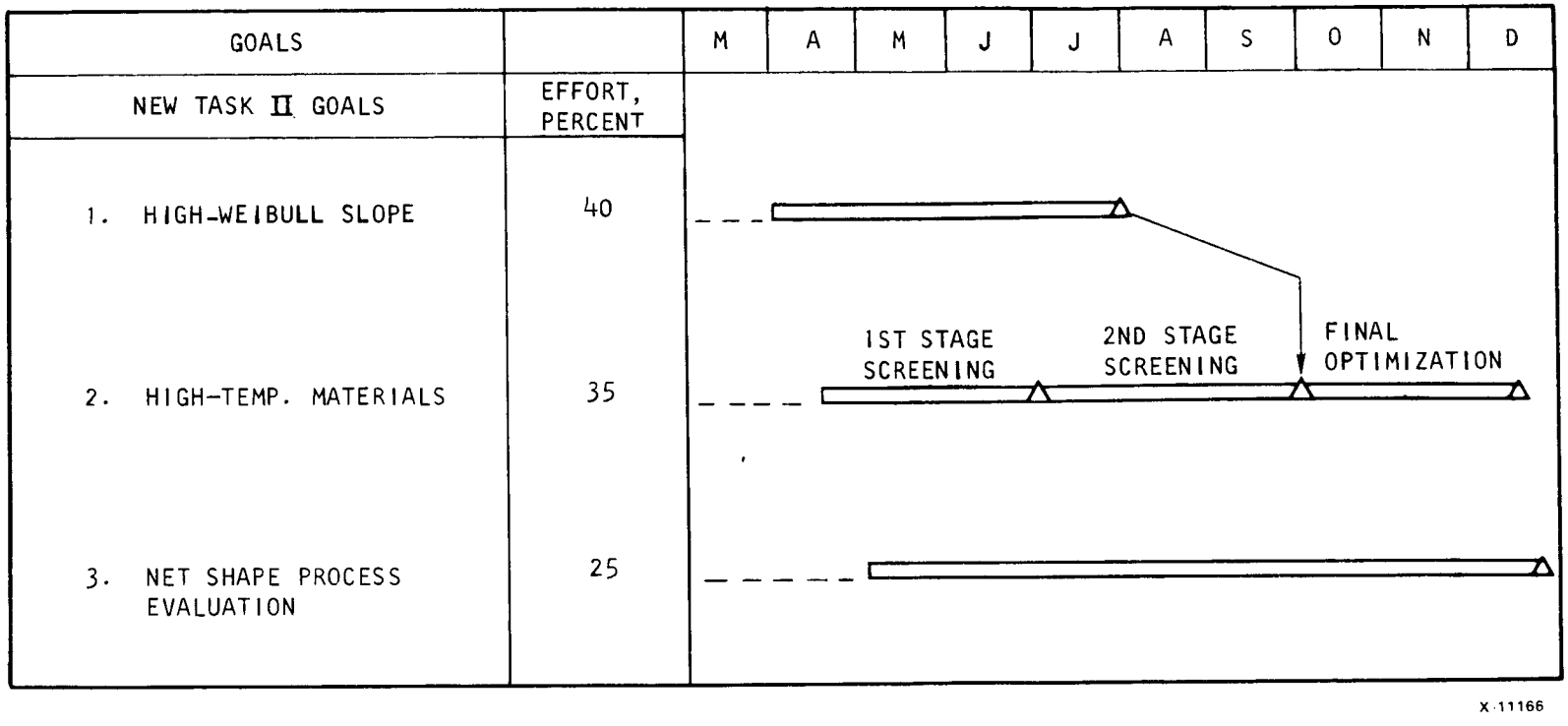

Figure A-1.--Proposed New Task II Program Schedule.

Upon the completion of this subtask, the information learned on improving Weibull modulus will be applied to the High-Temperature Material subtask.

Two injection mix batches are to be prepared on separate days. One-half of each batch will be injected on the old Arburg molder, the other half on the new Battenfeld. After dewaxing, each batch will be divided into two sinter/HIP runs. In each run, the total number of test bars and powder bed arrangements will be the same as used in Matrix II-2.

A statistically meaningful group of test bars will be evaluated for density and room temperature strength. It is anticipated that the strength and Weibull of the test bars will meet the original program goal of 95 ksi and 16 Weibull at room temperature. A detailed analysis of this experiment and a comparison with earlier results should generate a better understanding on process factors influencing the Weibull modulus of sintered Si_3N_4. The high temperature properties will also be assessed.

2. High-Temperature Materials

A. Alternate Sintering Aids

Based on literature data and Garrett IR&D research results, Y_2O_3 is beneficial for high temperature strength. Al_2O_3 has been shown to be a limiting factor in obtaining optimum high temperature strength properties. Therefore, we propose to retain Y_2O_3 but replace Al_2O_3 with alternate sintering aids. The following sintering aids have been selected for initial study: Y_2O_3, ZrO_2, SrO, CeO_2, and MgO. This selection is based on an ACC-funded patent and literature survey as well as informal communications with foreign materials suppliers.

Ten sintering aid compositions (five binary compositions and five ternary compositions) will be formulated using the above five oxides. A three-stage screening evaluation will be conducted (Figure A-2). In the first stage, cold isostatically pressed (CIP) samples will be encapsulated in niobium cans, then hot isostatically pressed to high density. This is the most effective method to produce high density samples. Samples with high densities (densities >95% theoretical) will be evaluated for high-temperature properties by four-point bending tests. The focus of the second stage is to develop sinter HIP cycles without encapsulation for those compositions passing the first stage screening. Finally, in the third stage, the most promising compositions will be fabricated into test bars for the standard room- and high-temperature MOR characterization.

B. Optimization of Y_2O_3/Al_2O_3 System

Several compositions of the Y_2O_3/Al_2O_3 binary system will be evaluated by the same three stages as described in the above paragraph (see Figure A-2). The emphasis here is to minimize the concentration of Al_2O_3, and/or the sum of Y_2O_3 and Al_2O_3.

C. Heat Treatment

Initially, the 6 + 2 composition has been selected for this evaluation. Test bars produced in subtask 1 (High-Weibull Modulus) will be used here. An ongoing EMRC*/Garrett STEM grain boundary program will provide support to this subtask. ACC has already provided heat treated samples to EMRC for analysis.

The 100-psi N_2 furnace will be used for this purpose. The room and 2550°F MOR will be the major property evaluation method. Additional heat treated specimens generated in this new program will also be sent to SRC for STEM and XRD analysis.

3. Net Shape Component Fabrication

Again, the 6 + 2 composition is selected for this evaluation. The Arburg molder used for all the test bar work up to now is marginal for molding T-25 rotor. The new Battenfeld molder has a much larger capacity and is equipped with microprocess controls. This new molder will be used in this scale-up study.

Standard batches of material ("ab" treatment) will be prepared through mixing. It is necessary to establish an optimized test bar injection molding parameter on the new molder. This set of parameters most likely will be different than the one developed on the Arburg molder. Once the optimized test bar molding parameters have been determined, an attempt will be made to apply them to molding T-25 rotors. If defective T-25 rotors result, a systematic variation of molding parameters will be conducted to improve the rotor quality.

The next evaluation is dewax scale up. Test bars and T-25 rotors will be dewaxed side by side in the same run. Weight loss and defects developed during dewax will be used to correlate the dewax behavior between test bars and rotors. Several different dewax cycles will be carried out. The defect-free rotors will then be processed through sinter/HIP.

*Engineered Material Research Center, Des Plains, Illinois.

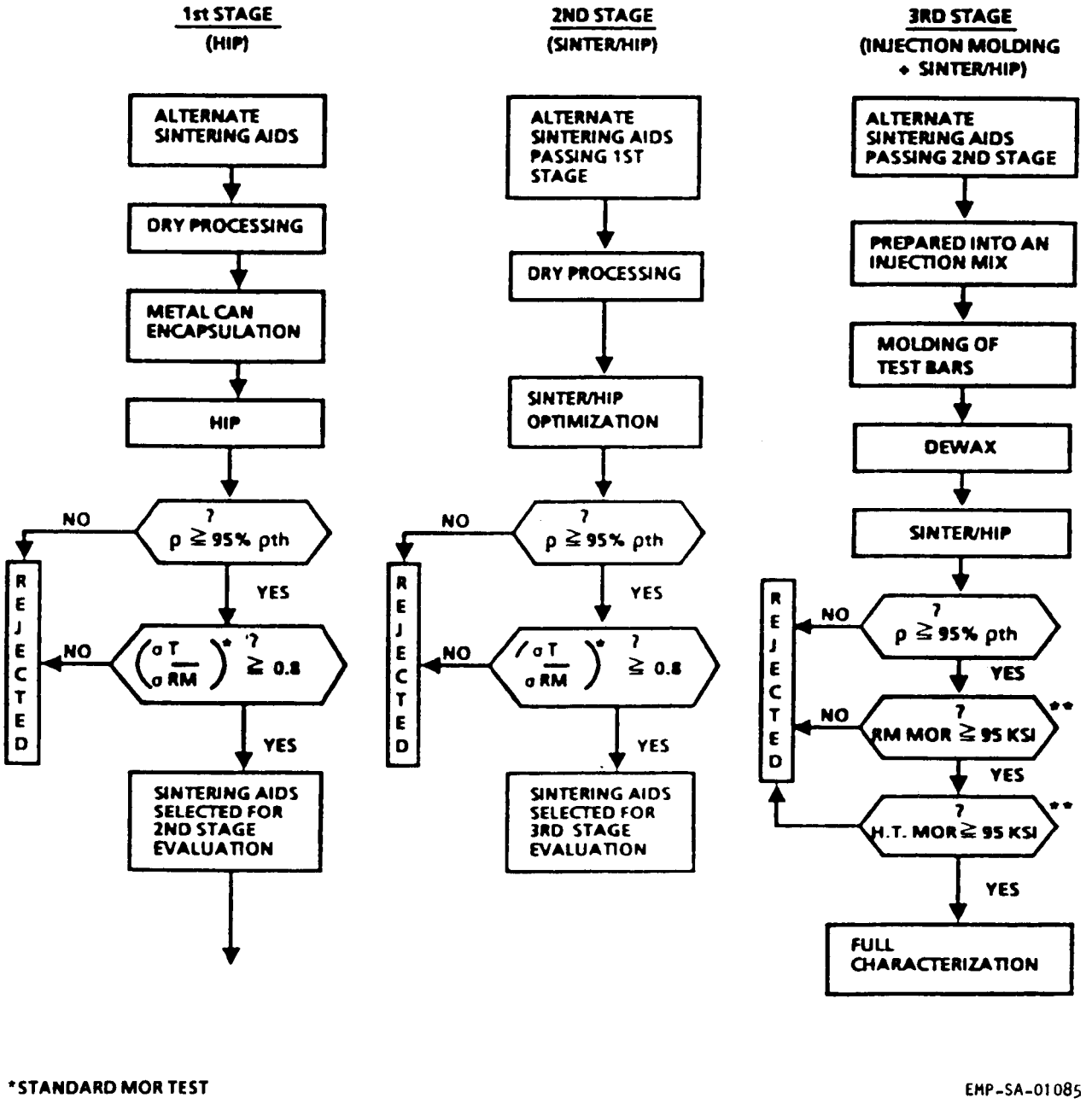

Figure A-2.--Flow Chart Showing the Three-Stage Screening Procedure for High-Temperature Material Development.

APPENDIX B

GLOSSARY

ACC	AiResearch Casting Company
A/C	Air classified
AR	As-received
BET	Brunauer-Emmett-Teller Surface Area Measurement Method
BSE	Back scatter electron imaging in SEM
CIP	Cold isostatic pressing
EDX	Energy dispersive X-ray
GTE	General Telephone and Electronics, Inc.
GTEC	Garrett Turbine Engine Company
HIP	Hot isostatic pressing
IRT	IRT Corporation, San Diego, CA
ksi	Thousand pounds per square inch
L/N	Leeds and Northrup
MOR	Modulus of rupture
MPa	MegaPascals
NASA	National Aeronautics and Space Administration
NDE	Nondestructive evaluation
PSD	Particle size distribution
RBSN	Reaction-bonded silicon nitride
RPM	Revolutions per minute
SEM	Scanning electron microscope
STEM	Scanning transmission electron microscope
TGA	Thermogravimetric analysis
TMA	Thermomechanical analysis
USP	Ultrasonic probe dispersion time
XRD	X-ray diffraction analysis

1. Report No.	2. Government Accession No.	3. Recipient's Catalog No.
NASA CR-179525		

4. Title and Subtitle	5. Report Date
Improved Silicon Nitride for Advanced Heat Engines	February 1987
	6. Performing Organization Code

7. Author(s)	8. Performing Organization Report No.
Hun C. Yeh and Ho T. Fang	AiResearch 86-60365
	10. Work Unit No. 533-05-01

9. Performing Organization Name and Address	11. Contract or Grant No.
AiResearch Casting Company A Division of The Garrett Corporation 19800 Van Ness Avenue Torrance, California 90509	NAS3-24385
	13. Type of Report and Period Covered Contractor Report Annual
12. Sponsoring Agency Name and Address National Aeronautics and Space Administration Lewis Research Center Cleveland, Ohio 44135	14. Sponsoring Agency Code

15. Supplementary Notes

Project Manager, Marc R. Freedman, Materials Division, NASA Lewis Research Center. Hun C. Yeh, AiResearch Casting Company; Ho T. Fang, Garrett Turbine Engine Company, Phoenix, Arizona.

16. Abstract

The objective of the program is to establish the technology base required to fabricate silicon nitride components that have the strength, reliability, and reproducibility necessary for actual heat engine applications. Task II was set up to develop test bars with high Weibull slope and greater high temperature strength, and to conduct an initial net shape component fabrication evaluation. Screening experiments were performed in Task VII on advanced materials and processing for input to Task II. This report covers the technical efforts performed in the second year of this five-year program. The first iteration of Task II was completed as planned. Two half-replicated, fractional factorial (2^5), statistically designed matrix experiments were conducted. These experiments have identified Denka 9FW Si_3N_4 as an alternate raw material to GTE SN_5O_2 Si_3N_4 for subsequent process evaluation. A detailed statistical analysis was conducted to correlate processing conditions with as-processed test bar properties. One processing condition produced a material with 97 ksi average room temperature MOR (100 percent of goal) with 13.2 Weibull slope (83 percent of goal); another condition produced 85 ksi (6 percent over baseline) room temperature strength with a Weibull slope of 20 (125 percent of goal). Because of these promising results, the program was redirected to focus on more agressive goals, including improved high temperature strength and net-shape fabrication evaluation. Additional experiments were continued in Task VII to explore advanced processing concepts. Analyses of Matrixes 6 through 11 were completed. In-depth analysis of the baseline binder system was performed. Experiments on a water-based binder system were initiated.

17. Key Words (Suggested by Author(s))	18. Distribution Statement
Ceramics; Statistics; Injection molding; Properties; Silicon nitride; Sinter/HIP	[redacted] STAR Category 27

19. Security Classif. (of this report)	20. Security Classif. (of this page)	21. No. of pages	22. Price*
Unclassified	Unclassified	113	